Membrane proteins
in the outer membrane of plastids and mitochondria

vorgelegt von
Iryna Ilkavets

Dissertation der Fakultät für Biologie
der Ludwig-Maximilians-Universität München

München
19.12.2005

Gutachter:

1. Prof. Dr. J. Soll
2. PD Dr. J. Meurer

Date of the exam: 13.02.2006

Contents

Summary 4

Zusammenfassung 5

Abbreviations 6

1. Introduction 7

2. Materials and methods 9

2.1 Bacterial strains 9

2.2 Plant material 9

2.3 DNA methods 9

2.3.1 Isolation of genomic DNA from *Arabidopsis thaliana* 10
2.3.2 Polymerase Chain Reaction 10
2.3.3 Southern hybridisation 10

2.4 Cloning 11

2.4.1 Conventional cloning 11
2.4.2 Site directed mutagenesis 11
2.4.3 GATEWAY cloning 11

2.5 RNA methods 12

2.5.1 RNA isolation from plant material 12
2.5.2 cDNA synthesis 12
2.5.3 Semi-quantitative RT-PCR 12
2.5.4 cDNA macroarray analysis of wild type and *Atoep16.1-p* knockout mutant 12
2.5.5 Affymetrix genechip analysis 13

2.6 **Overexpression of recombinant proteins and antibody purification** 13

2.6.1 Heterologous expression of proteins in *E.coli* 14
2.6.2 Inclusion bodies preparation 15
2.6.3 Purification of overexpressed protein 15
2.6.4 Antibody production 15

2.7 GFP, RFP-fusion protein analysis 16

2.7.1 Cloning of constructs with the C-terminal reporter protein fusions 16
2.7.2 Biolistic bombardment 16
2.7.2.1 DNA coating on the gold particles 16
2.7.2.2 DNA bombardment 17
2.7.3 *Arabidopsis* protoplasts isolation and PEG-mediated DNA transformation 17
2.7.4 Fluorescent microscopy 17

2.8 Promoter-GUS analysis 18

2.8.1 Construction of plasmids 18
2.8.2 Transformation of *Agrobacterium tumefaciens* 18

2.8.3 Stable transformation of *Arabidopsis* with floral dip method 19
2.8.4 GUS – staining 19
2.8.5 *In vitro* pollen tube germination 19

2.9 Isolation of organelles and suborganellar fractions 20

2.9.1 Isolation of intact chloroplasts from *Arabidopsis* 20
2.9.2 Isolation of mitochondria from *Arabidopsis* 20
2.9.3 Isolation of chloroplastic fractions from pea 21
2.9.4 Isolation of membrane fraction proteins from pea and *Arabidopsis* 21

2.10 PAGE and Immunoblotting 22

2.11 T-DNA knockout mutants 22

2.11.1 Screening of the *Atoep16.1-p* knockout mutant 22
2.11.2 Conventional screening of the *Arabidopsis* knockout mutants 24
2.11.3 Abs *Arabidopsis* double knockout mutant generation 25

2.12 *In silico* analysis 25

3. Results 26

3.1 Characterisation of the OEP16 protein family 27

3.1.1 The OEP16 protein from *Pisum sativum* 27

3.1.1.1 Decomposition of fluorescence spectra of the PsOEP16 protein 27
3.1.1.2 Topology model of PsOEP16 protein 28

3.1.2 The OEP16 protein family from *Arabidopsis thaliana* 28

3.1.2.1 *In silico* protein sequence analysis of the Arabidopsis OEP16 orthologs 29

3.1.2.2 Isolation of AtOEP16.1, AtOEP16.2, AtOEP16.3 and AtOEP16.4 31

3.1.2.3 Intracellular distribution of the AtOEP16 proteins 34
A) Intracellular localization via GFP-protein fusion 34
B) Immunoblot analysis of subcellular localization of the AtOEP16 family 39

3.1.2.4 Gene expression patterns of the *AtOEP16* family 41
A) Affymetrix analysis of the *AtOEP16* family 41
B) RT-PCR analysis of the *AtOEP16.1*, *AtOEP16.2* and *AtOEP16.4* distribution in *Arabidopsis* 42
C) Promoter-GUS analysis of *AtOEP16.1*, *AtOEP16.2* and *AtOEP16.4* 43

3.1.2.5 Mutants of the *AtOEP16* gene family 47
A) Isolation and characterisation of *Arabidopsis OEP16.1* knockout mutants 47
B) cDNA macroarray analysis of the *Atoep16.1-p* knockout mutant 50
B) Isolation and characterisation of *Arabidopsis OEP16.2* knockout mutant 52
C) Isolation and characterisation of *Arabidopsis OEP16.4* knockout mutants 54
E) Double knockout mutants 57

3.1.2.6 Electrophysiological analysis of the recombinant AtOEP16.2 protein 57

3.2 OEP37 in *Pisum sativum* and in *Arabidopsis thaliana* **58**
3.2.1 Isolation of *OEP37* from *Arabidopsis* **58**
3.2.2 Subcellular and suborganellar localisation of the AtOEP37 and PsOEP37 proteins **60**
3.2.3 OEP37 expression analysis **62**
3.2.3.1 *AtOEP37* mRNA distribution within the *Arabidopsis* plant 62
3.2.3.2 The *AtOEP37* gene expression in leaves depending on plant age 63
3.2.3.3 AtOEP37 promoter::GUS analysis 63
3.2.3.4 Tissue-specific expression of the PsOEP37 protein 64
3.2.4 Isolation and characterization of an *AtOEP37* knock out mutant **67**
3.2.5 Electrophysiological analysis of the recombinant PsOEP37 protein **66**
3.3 VDAC in *Pisum sativum* and *Arabidopsis thaliana* **68**
3.3.1 Pea and *Arabidopsis* VDAC orthologous proteins 68
3.3.2 Subcellular localization of the VDAC proteins 70
3.3.3 The VDACs mRNA levels in leaves and roots of *Arabidopsis* 71

4. Discussion **73**
4.1 The OEP16 family in pea and *Arabidopsis thaliana* **73**
4.1.1 Structure and topology of the OEP16 proteins 73
4.1.2 Subcellular localization of the AtOEP16.1-4 proteins 75
4.1.3 *AtOEP16.1-4* gene expression 75
4.1.4 *Arabidopsis OEP16* knockout mutants 80
4.1.5 Proposed function of proteins from the *Arabidopsis* OEP16 family 81
4.2 OEP37 proteins in pea and *Arabidopsis* **83**
4.3 VDAC proteins in pea and *Arabidopsis* **84**
5 References **85**
6 Appendix **92**
Curriculum vitae **95**
Publications **96**
Acknowledgements **97**
Ehrenwörtliche Versicherung **98**

Summary

Channels of the plastid and mitochondrial outer membranes facilitate the turnover of molecules and ions via these membranes. Although channels have been studied many questions pertaining to the whole diversity of plastid and mitochondrial channels in *Arabidopsis thaliana* and *Pisum sativum* remain unanswered. In this thesis I studied OEP16, OEP37 and VDAC families in two model plants, in *Arabidopsis* and pea.

The *Arabidopsis* OEP16 family represents four channels of α-helical structure, similar to the pea OEP16 protein. These channels are suggested to transport amino acids and compounds with primary amino groups. Immunoblot analysis, GFP/RFP protein fusion expression, as well as proteomic analysis showed that AtOEP16.1, AtOEP16.2 and AtOEP16.4 are located in the outer envelope membrane of plastids, while AtOEP16.3 is in mitochondria. The gene expression and immunoblot analyses revealed that AtOEP16.1 and AtOEP16.3 proteins are highly abundant and ubiquitous; expression of *AtOEP16.1* is regulated by light and cold. AtOEP16.2 is highly expressed in pollen, seeds and seedlings. AtOEP16.4 is a low expressed housekeeping protein. Single knockout mutants of *AtOEP16.1, AtOEP16.2* and *AtOEP16.4,* and double mutants of *AtOEP16* gene family did not show any remarkable phenotype. However, macroarray analysis of *Atoep16.1-p* T-DNA mutant revealed 10 down-regulated and 6 up-regulated genes.

In contrast to the α-helical OEP16 proteins, the OEP37 and VDAC proteins are of β-barrel structure. The PsOEP37 and AtOEP37 channel proteins form a selective barrier in the outer envelope of chloroplasts. Electrophysiological studies in lipid bilayer membranes showed that the PsOEP37 channel is permeable for cations. Specific expression profiles showed that AtOEP37 and PsOEP37 are highly expressed in the entire plant.

The isolated PsVDAC gene encodes a protein, which is located in mitochondria. In *Arabidopsis* gene database, five *Arabidopsis* genes, which code for VDAC-like proteins were announced. One gene was not detected, whereas four of these genes expressed in leaves, roots, flower buds and pollen.

Zusammenfassung

Kanäle in den äußeren Hülmembranen von Chloroplasten und Mitochondrien ermöglichen den Transport von Molekülen und Ionen über diese Membranen. Trotz intensiver Forschung an vielen Kanälen bleiben einige Fragen, die plastidäre und mitochondriale Kanäle betreffen, offen. In dieser Arbeit habe ich Kanäle der OEP16, OEP37 and VDAC-Familien in zwei Modellpflanzen *Arabidopsis* und Erbse untersucht.

Die OEP16 Familie aus *Arabidopsis* umfasst vier Kanäle mit vorwiegend α-helikaler Struktur. Auch die Struktur von OEP16 aus Erbse ist vorwiegend α-helikal. Putative Substrate dieser Kanäle sind Aminosäuren und andere Stoffe mit primären Aminogruppen. Immunoblot Analysen, GFP/RFP-Fusionen sowie Proteom-Analysen zeigen, dass AtOEP16.1, AtOEP16.2 und AtOEP16.4 in dir äußeren Membran von Plastiden lokalisiert ist, während AtOEP16.3 in der äußeren Membran von Mitochondrien zu finden ist. Geneexpressionstudien und Immunoblot Analysen machen deutlich, dass AtOEP16.1 und AtOEP16.3 stark exprimiert werden und in allen Geweben vorhanden sind. Die Expression von *AtOEP16.1* wird durch Licht und Kälte reguliert. AtOEP16.2 wird stark in Pollen, Samen und Keimlingen exprimiert. AtOEP16.4 ist überall nur schwachexprimiert. Knock-out Mutanten von *AtOEP16.1*, *AtOEP16.2* und *AtOEP16.4* und Doppelmutanten der *AtOEP16*-Familie zeigen keinen Phänotyp. Macroarray-Analysen von *AtOEP16.1* T-DNA-Insertionsmutanten ergaben 10 Gene, deren Expression herunterreguliert war und 6 Gene, deren Expression hochreguliert war.

Im Gegensatz zu den α-helikalen OEP16 Kanälen, bestehen die OEP37 und VDAC Kanäle vorwiegend aus β-Faltblättern. OEP37 Proteine aus *Pisum sativum* und *Arabidopsis thaliana* bilden eine selektive Barriere in der äußeren Membran von Chloroplasten. Elektrophysiologische Messungen von PsOEP37 zeigen, dass OEP37 einen Kation-selectiven Kanal bildet. Expressionstudien ergaben, dass AtOEP37 und PsOEP37 in allen pflanzlichen Organen stark exprimiert werden.

Das isolierte PsVDAC Gen kodiert für ein Protein, das in der äußeren Hüllmembran von Mitochondrien lokalisiert ist. In der *Arabidopsis* Gendatenbank gibt es fünf Gene, die für VDAC-ähnliche Proteine kodieren. Wärend bei einem Gen der Ort der Expression bis jetzt nicht nachgewiesen werden konnte, wurde für die vier anderen die Expression in Blättern, Wurzeln, Blütenknospen und Pollen nachgewiesen.

Abbreviations

35S	35S promoter from Cauliflower Mosaic Virus
DLD	dihydrolipoamide dehydrogenase
mSSU	mature form of SSU
No RT	no reverse transcription
OEP	outer envelope protein
ON	over night
ORF	open reading frame
PCR	Polymerase Chain Reaction
PEG	polyethylene glycol
RT	room temperature
SSU	small subunit of ribulose 1,5 biphosphate carboxylase-oxygenase (RuBisCo)
VDAC	voltage-dependent anion channel

Plant yeast and bacterial species:

At	*Arabidopsis thaliana*
Bi	*Bromus intermis*
Col-0	Columbia-0 ecotype of *Arabidopsis*
E. coli	*Escherichia coli*
Hv	*Hordeum vulgaris*
Os	*Oryza sativa*
Ps	*Pisum sativum*
Sc	*Saccharomices cerevisae*
WS	Wasilevskiya ecotype of *Arabidopsis*

1. Introduction

Biological membranes are built as lipid bilayers. Lipid bilayers show little permeability for hydrophilic solutes. Therefore, membranes contain channel-forming proteins, which allow transmembrane passage of molecules. Among the outer membrane proteins of Gram-negative bacteria are channels, which transport molecules up to 600 Da of size (Delcour, 2002, 2003; Robertson and Tieleman, 2002; Philippsen et al., 2002; Nikaido 2003; Nestorovich et al., 2003). A nonspecific channel forming protein, porin from the outer membrane of *Salmonella typhimurium*, was discovered in 1976 (Nakae, 1976) and the word "porin" was proposed for this class of proteins forming nonspecific diffusion channels. Now, several families of bacterial porins are known: (i) General diffusion pores (OmpF, OmpC, and PhoE from *E. coli*), which show general preferences for charge and size of the solute. While OmpF and OmpC prefer cations over anions, PhoE is anion-selective. Furthermore, OmpF allows the permeation of slightly larger solutes than OmpC (Watanabe Y et al., 2005). (ii) Slow porins (OprF from *E. coli*) which allow a much slower diffusion of small solutes, e.g. the influx of arabinose was 50 times slower via OprF than through the OmpF channel (Nestorovich et al., 2003). (iii) Ligand-gated pores, *e.g. E. coli* ferric enterobactin channels (FepA), providing energy-dependent uptake of iron into bacteria (Jiang et al., 1997).

Many outer membrane proteins in Gram-negative bacteria are known to form β-barrels. As shown by X-ray crystallography, these β-barrels are oligomeric, often trimeric structures. (Hancock et a., 1990; Jeanteur et al., 1991). In contrast to proteins located in outer envelope membranes, those of inner membrane are mostly α-helical (Sukharev at al., 1997; Bhattacharjee et al., 2000; Gier 2005).

The ancestral relation between mitochondria and plastids with Gram-negative bacteria (Osteryoung, 1998) suggests the presence of multiple channel proteins in the chloroplast and mitochondria outer membranes. Chloroplasts and mitochondria as well as Gram-negative bacteria, are both surrounded by two membranes, which separate the organelles from the cytosol and which allow solute translocation between these compartments and the import of nuclear-encoded proteins.

The outer envelope membrane of chloroplasts has been assumed earlier to be freely permeable for molecules with a weight up to 10 kDa, whereas the inner envelope membrane of chloroplasts has been shown to be a main selective barrier for exchange of metabolites (Flugge et al., 1998). This idea was based on the identification of specific carriers in the inner envelope membrane, whereas an unselective large conductance allowing the diffusion of

molecules was measured in the outer envelope membrane. However, recently, several channels of the outer envelope of chloroplasts have been characterized at the molecular level. These channels were named according to their location and their molecular weight. The outer envelope protein of 16 kDa (OEP16), isolated from pea, is a cation-selective high conductance channel with permeability to amino acids and compounds with primary amino groups (Pohlmeyer et al., 1997). OEP21 forms an anion-selective channel with permeability to triosephostates (Bölter et al., 1999). The OEP24 protein is a non-selective channel, similar to the general diffusion pores of Gram-negative bacteria (Pohlmeyer et al., 1998). Although slightly cation-selective, the channel allows the passage of triosephosphates, ATP, PPi, dicarboxylate, and positively or negatively charged amino acids in a reconstituted system. OEP37 is a newly identified β-barrel protein from pea of still unknown function (Schleiff et al., 2003). All chloroplastic channels are encoded in the nucleus.

Porins in the mitochondrial outer membrane show permeability for hydrophilic molecules up to a molecular mass of 4-5 kDa. They are called voltage-dependent anion-selective channels (VDAC; Schein et al., 1976; Schein et al., 1976; Colombini, 1979; Benz, 1985). Isolation and reconstitution of the mitochondrial porins from protist *Paramecium* (Schein et al., 1976), yeast (Forte et al., 1987; Ludwig et al., 1988), rice (Colombini et al., 1980), and pea (Schmid et al., 1992) led to a detailed analysis of their biochemical and biophysical properties. At low membrane potentials, VDACs are weakly anion-selective in the "open" state. At voltages higher than 20 mV, the pore switches to the cation-selective "closed" state. The large, water-filled pore is probably built up by 16 membrane-spanning antiparallel β-strands. The N terminus of the protein and the large extramembrane loops are located at the cytosolic side of the membrane (De Pinto et al., 1991). The mitochondrial porins are encoded in the nucleus without any cleavable N-terminal extensions, similar to chloroplastic outer envelope channels. Surprisingly to that postulate that VDACs are mitochondrial porins, Fischer et al., (1994) showed the presence of a VDAC-like porin of 30 kDa in pea root plastids. *In vitro* synthesized protein was analyzed in import studies into different plastids and found to be specifically imported into non-green plastids but not into chloroplasts.

Despite isolation of some genes and proteins of the outer envelope of pea chloroplasts, the question, whether outer envelope of chloroplasts is a selectivity barrier or not, is still under doubt. Therefore, the goal of this work was to study the proteins localized in the outer envelope of chloroplasts, OEP16, OEP37 and VDAC.

2 Materials and Methods

2.1 Bacterial strains

For general cloning techniques, the *E. coli* strains DH5α, TOP10 and TOP10F' (Novagen) and for overexpression of recombinant proteins *E.coli* BL21 (DE3) (Novagen) strain were used. E. *coli* strains were transformed with use of a heat shock method according to Hanahan (1988). For stable transformation of *Arabidopsis* plants, *Agrobacterium tumefaciens* strain GV3101 containing the binary vector pMP90 (Clough and Bent, 1998) was used.

2.2 Plant material

Two different plants *Arabidopsis thaliana* and *Pisum sativum* were used to study the function or regulation of gene promoters or genes coding for proteins in the outer envelope of chloroplasts and mitochondria. Growth chambers were supplied with artificial light at a long day cycle (16-h light / 8-h dark regime) for *Arabidopsis thaliana* and a 14-h light / 10-h dark cycle for *Pisum sativum*. The temperature was maintained at 21°C (day), 16°C (night), unless stated otherwise. The *Arabidopsis* ecotypes Columbia (Col-0) and Wasilevskiya (WS) were used as wild-type (Lehle seeds, USA). Seeds of *Arabidopsis* were sterilized by rinsing them in 70% (v/v) ethanol for 1 min followed by a rinse in 0.05% (v/v) Triton X-100 for 5 min and 100% ethanol for 10 min. Before plating the seeds on 1 x Murashige Skoog medium (Sigma) containing 0.5% (w/v) sucrose, 1 x vitamins (Sigma) and 0.8% agar, seeds were washed 5 times with autoclaved ddH_2O. Then seed dormancy was broken at 4°C for 3 days. Germinating seedlings were grown for two weeks on medium before transferring them to soil. The pea (*Pisum sativum* L.) cultivar “Golf” (Raiffeisen Nord AG, Kiel) was grown in vermiculite.

2.3 DNA methods

PCR fragment isolations were made by the NucleoSpin Extract Kit (Qiagen GmbH, Hilden) according to the manual. Plasmid DNA isolations were made by the Plasmid Mini Kit or Plasmid Midi Kit (Qiagen GmbH, Hilden) following the manufacturers instructions. DNA was sequenced using the automated *ABI377* sequencing equipment in the lab of Prof. Dr. Hermann (Botanik I, Botanisches Institut, LMU, München).

2.3.1 Isolation of genomic DNA from *Arabidopsis thaliana*

The rapid plant DNA extraction was carried out according to Edwards et al (1991). One leaf (~100 mg) was ground in 450 µl extraction buffer containing 200 mM Tris, pH 7.5, 250 mM NaCl, 25 mM EDTA and 5% SDS and was incubated at 37°C for 5 min. Cell debris was pelleted by centrifugation for 10 min in a table centrifuge at maximum speed. Then 300 µl isopropanol was added to 300 µl of the supernatant, transferred to a fresh tube, and DNA was precipitated for 5 min at room temperature. The DNA precipitate was then sedimented by centrifugation for 10 min at full speed in a table centrifuge, once washed with ice-cold ethanol, dried and resuspended in 50 µl H_2O. 5 µl were used for PCR experiments.

2.3.2 Polymerase Chain Reaction

PCR was done using *Taq* DNA polymerase (Eppendorf) with program according to the manufacturers manual instructions with an annealing temperature 5°C below melting temperature for primers. The elongation time was calculated by taking 1 min for 1000 bp. Products of PCR were resolved electrophoretically on 1% agarose gel in TAE buffer. The synthesis of the oligodesoxyribonucleotids was done in MWG Biotech AG, München.

2.3.3 Southern blotting

Southern blotting was performed for *AtOEP16.1* knockout mutant screen. For Southern hybridizations, PCR products were separated electrophoretically in a 1% agarose gel, which was after depurination in 0.25 N HCl transferred onto a Hybond-N^+ nylon membrane (Amersham-Pharmacia) using alkali capillary blots (0.4 M NaOH) for 16 hours.

Pre-hybridization was carried out (to prevent non-specific hybridization) at 68°C for 30 min in prehybridization solution (6xSSC, 10xDenhards, 0.5% SDS, 0.1 mg/ml denaturated salmon sperm DNA). A DIG-labeled probe for the AtOEP16.1 gene was generated by PCR using *Taq* DNA polymerase (Eppendorf) and DIG-11-dUTP as described in Roche Applied Science *DIG System User's Guide for Filter Hybridization*. Primers for PCR were At2gN and At2gC (see primer sequences in Appendix). The DIG-labeled probe was denaturated by boiling and added in fresh hybridization solution to the blot and hybridized at 68°C overnight. Then the membrane was washed twice with 2xSSPE/0.1% (w/v) SDS at room temperature (RT), twice with 1xSSPE/0.1% (w/v) SDS at RT, and once with 0.5xSSPE/0.1% (w/v) SDS at 68°C for 15 min each. After blocking for 30 min in buffer 1, containing 100 mM maleic acid, 150 mM NaCl, pH 7.5/NaOH, 2.5 % (w/v) milk powder, the membrane was hybridized with Anti-

DIG-AP Fab fragments in dilution 1 to 5000 in the buffer 1 at RT for 1 h. After washing in buffer 1 additionally containing 0.3 % (v/v) Tween 20 the membrane was developed using NBT and BCIP reagents according to manufacturers instructions.

2.4 Cloning

2.4.1 Conventional cloning

The standard molecular cloning methods (restriction digestion, ligation) were performed according to Sambrook et al., (1989). All DNA fragments were separated on 1% agarose gels stained with ethidium bromide (0.5 mg/ml), electrophoresed in TAE buffer (50 x TAE buffer: 242 gm Tris base, 57.1 ml acetic acid, 100 ml 0.1 M EDTA for 1 L ddH_2O) and visualized with an UV transilluminator.

2.4.2 Site directed mutagenesis

To obtain single tryptophan mutants of PsOEP16, polymerase chain reaction (PCR)-based site directed mutagenesis was used. In the first step, two separate PCR reactions were performed for each mutant. The OEP16 cDNA inserted in the PET21b expression vector was used as a template. The primers were, for PsOEP16W77/F mutant, (i) OEP16W77/FN and T7 promoter primer and (ii) OEP16W77/FC and T7 terminator primer. For PsOEP16W100/F mutant, (i) OEP16W100/FN and T7 promoter primer and (ii) OEP16W100/FC and T7 terminator primer. The fragments for the W77F and W100F mutants were then annealed together in a second PCR step to amplify the complete mutated gene using T7 promoter and terminator primers. The resulting PCR products were digested with *Nde*I and *Xho*I restriction enzymes and ligated into the corresponding sites of the pET21b expression vector. They were named W77F-pET21b and W100F-pET21b, respectively. The correct mutations were confirmed by sequencing.

2.4.3 GATEWAY cloning

For GATEWAY (Invitrogen) cloning attB-PCR products were generated by a two-step adaptor PCR. The first-step PCR was performed with 10 cycles using primers designed to have flanking regions with the part of *attB* recombination sequences, a ribosome-binding site, the Kozak sequence and the gene-specific open reading frame or promoter region for gene of interest. Second-step PCR was done for 15 cycles using short attB1adapter and attB2adapter

primers containing *attB* recombination sequences. The *attB* recombination sequences conferred directionality to the PCR product. The resulting *attB*-PCR product was recombinated with pDONR201 vector (Invitrogen) using BP Clonase (Invitrogen) according to the instructions of manufacturers. After selection, purification and sequencing, the resulting clone was then recombinated with a desired binary destination vector with LR Clonase (Invitrogen). The expression clones were used (i) for the transient expression of the fluorescent reporter GFP protein fused to the C-terminal part of investigated proteins directed by *35S CaMV* promoter and (ii) for *Agrobacterium*-mediated stable transformation of plants for promoter-GUS analysis (see in Appendix list of clones).

2.5 RNA methods

2.5.1 RNA isolation from plant material

Total RNA isolation was performed using RNeasy Plant Mini Kit (Qiagen GmbH, Hilden) according to the manual's instructions.

2.5.2 cDNA synthesis

cDNA was synthesized using MMLV reverse transcriptase (Promega) and SMART RACE 5'CDS primer for 1,5 h at 42°C with 2 μg total RNA (secondary structure was denaturated for 2 min at 70°C) as a template.

2.5.3 Semi-quantitative RT-PCR

For quantification of all transcripts, RT-PCR was performed with gene-specific primers with SuperScript One-Step RT-PCR kit (Invitrogen). Total RNA or mRNA was used as a template. Transcript levels were normalized using *actin 2* (At3g18780), *actin2/7* (At5g09810) or *18S rRNA* (At2g01010) genes as internal control.

2.5.4 cDNA macroarray analysis of wild-type and *Atoep16.1-p* knockout mutant

Experiments were done during my stay in the lab of Dr. Schäffner (GFS Forschungszentrum, München) within the DFG SPP 1108 project. The macroarray filters containing 600 ESTs clones of *Arabidopsis* membrane proteins were supplied by Dr. Schäffner.

The cDNA was synthesized using Superscript II RTase (Invitrogen) and mRNA from leaves of 4-week-old *Arabidopsis,* isolated using Oligo (dT)25 Dynabeads (Invitrogen), followed by conventional random primed labelling using DNA labelling kit (Fermentas) with [α-^{33}P]dATP (50 μCi) according manufacturers protocols. After pre-hybridisation of the cDNA filters for 2,5 hours at 42° C in buffer containing 20x SSC, 100x Denhardt, 20% SDS, 10 mg/ml Salmon Sperm DNA, the hybridisation of the labeled cDNA to cDNA filters was carried out in the same buffer at 42 °C over night. Then filters were washed shortly in 2x SSC/0,1% SDS at RT, followed by 30min in 2x SSC/0,1% SDS at 42°C, shortly in 0,2x SSC/0,1% SDS, 30 min in 0,2x SSC/0,1% SDS at 42°C. Then filters were exposed to an imaging plate ON (Fuji Film). The radioactive images were obtained with a high-resolution Storm scanner. The mean pixel intensity within a defined area around each spot was collected using ArrayVision (Amersham Biosciences). Enhanced or repressed genes in *Atoep16.1-p* leaves compared with wt leaves were detected by the Aida program (Tusher et al., 2001).

2.5.5 Affymetrix gene chip analysis

Affymetrix gene chip analysis was done by Dr. Rowena Thomson within DFG "Schwerpunktprogramm" SPP-1108 "Dynamik und Regulation des pflanzlichen Membrantransport bei der Ausprägung zell- und orhanspezifischer Eigenschaften". mRNA was extracted from leaves and roots of 4-week-old wild-type *Arabidopsis* plants.

2.6 Overexpression and purification of recombinant proteins

To obtain antisera against the respective OEP16 and OEP37 proteins, recombinant proteins were overexpressed in *E. coli* and purified by affinity chromatography.

A 363 bp region of the *AtOEP16.1* gene, corresponding to the N-terminal 131 amino acid residue part of the protein, was amplified by PCR with flanking restriction sites for *Eco*RI (5') and *Xho*I (3') and ligated into the pET21b plasmid vector (Novagen). pET21b possesses a C-terminal tag, consisting of six consecutive histidine residues to facilitate protein purification. After overexpression in BL21(DE3) *E. coli* cells (Novagen, see 2.6.2), the AtOEP16.1 protein was recovered in the form of inclusion bodies (see 2.6.3). It was then denaturalised in a buffer containing 8 M Urea and the pure protein was isolated using affinity chromatography (see 2.6.4).

The coding sequence of the full-length *AtOEP16.2* in pET21d was heterologously overexpressed in BL21(DH3E) *E. coli* cells and the protein was purified as described for

AtOEP16.1. This purified protein was used for antisera generation as well as for electrophysiological studies in lipid-bilayers.

The overexpression of the full length coding sequence of *AtOEP16.3* and *AtOEP16.4* (in pET21b) in BL21 (DE3) *E. coli* cells could not be obtained. Therefore, different strains of *E. coli* cells and different conditions were tested to get the overexpressed proteins. The *E. coli* strains, BL21 Star, BL21 Rosetta and BL21 pMICO (Novagen) were grown at 37°C and induced at 12°C, 20°C, 37°C with 1mM IPTG. These conditions also failed to overexpress the proteins. Then the synthesis of proteins in a cell free system using the rapid translation system RTS 100 *E. coli* HV kit (Roche) was tested without any success. Therefore, antibodies directed against peptide of AtOEP16.3 and AtOEP16.4 proteins were raised. The protein sequences of synthesized peptides (Pineda, Antikörper Service, Berlin) were as follows, (i) PRVERNVALPGLIRT and (ii) TRVDNGREYYPYTVEKRAE for AtOEP16.3; and for AtOEP16.4, (i) 15 amino acid residues from the N-terminus starting methionine, (MEEELLSAVPCSSLT), (ii) 15 amino acid residues from the C-terminus (VLANCTRTENPNNTN) and (iii) a mixture of both.

For subcloning of *PsOEP37,* which was originally cloned in *pBluescript* vector (Schleiff et al., 2003), a PCR using the forward primer 37peaNdeIf incorporating a *Nde*I restriction site at the N terminus and the reverse primer 37peaBamHIr incorporating a *Bam*HI restriction site at the C-terminus was performed. The resulting fragment was digested with *Nde*I and *Bam*HI and ligated into the *Nde*I-*BamHI*-digested plasmid vector *pET14b* (Novagen) containing N-terminal tag consisting of six consecutive histidine residues (6-His) to facilitate purification. The plasmid was named *PsOEP37/pET14b*. The cDNA of *AtOEP37* was cloned using the forward O37araXhoIs and reverse O37araNcoIr primers into pRSETA vector with an N-terminal 6-His-tag between *Xho*I (5') and *Nco*I (3') sites for restriction enzymes. The coding sequence of full-length *PsOEP37* in pET14b (Novagen) with a N-terminal 6-His-tag and of AtOEP37 in pET21b (Novagen) were heterologously overexpressed in BL21(DH3E) *E. coli* cells. The proteins were purified as described for AtOEP16.1.

2.6.1 Heterologous expression of proteins in *E. coli*

The liquid LB broth (3ml, appropriate antibiotic) was inoculated with a single colony of *E. coli* BL21(DE3) cells, harbouring the respective plasmid construct and incubated at 37°C with shaking at 250 rpm for about 3h. Then 1 ml of the culture was inoculated into 500 ml LB media and shaken at 37°C at 250 rpm for about 3 h to reach an OD_{600} of 0.8. The expression of recombinant proteins was induced with 1 mM isopropyl-1-thio-β-D-galactoside (IPTG) for

3 hours. Afterwards, bacteria were placed on ice for 5min and harvested by centrifugation at 10000 rpm for 10 min at 4 °C.

2.6.2 Inclusion bodies preparation

Lysis buffer (50 mM TRIS/HCl pH 8.0, 25% (w/v) sucrose, 1 mM EDTA) was added to the bacterial pellet and resuspended cells were passed through a French Press and three times for 20 sec sonificated. The inclusion bodies were separated from bacterial debris by centrifugation for 15 min at 20,000 rpm at 4°C and washed once in buffer, containing 20 mM NaCl, 20 mM TRIS/HCl pH 7.5, 2 mM EDTA, 0.07% (v/v) β-mercaptoethanol, 25 mM MEGA 9 and twice in buffer, containing 1 mM EDTA, 20 mM TRIS/HCl pH 7.5, 0.07% (v/v) β-mercaptoethanol, 25 mM MEGA 9. Washing was performed by vortexing for 5 min and centrifugation at 10,000 rpm for 5 min at 4°C. The detergent was removed by washing of the inclusion bodies for four times in buffer containing 50 mM TRIS/HCl pH 8.0, 1 mM EDTA, 10 mM DTT.

2.6.3 Purification of overexpressed protein

The inclusion bodies of a protein having a 6-His-tag on its C- or N-terminal end were solubilised in the loading/washing buffer containing 20 mM TRIS pH 8.0, 100 mM NaCl, 8 M Urea. After 5 min centrifugation in a table centrifuge at maximum speed, the supernatant was loaded onto a TALON column (Clohtech), pre-equilibrated with the same buffer. The bound protein was washed with 10 ml of loading/washing buffer and eluted with a buffer containing 20 mM TRIS pH 8.0, 100 mM NaCl, 6 M Urea and 100 mM Imidazole. Purified proteins were tested by SDS PAGE gel analysis.

2.6.4 Antibody production

Antibodies against all purified proteins or peptides were produced in rabbit by Pineda, Antikörper Service, Berlin. Antibodies were obtained as polyclonal serum of 61-220 days after immunization and tested by western blotting on the respective antigen or plant tissue.

2.7 GFP, RFP-fusion protein analysis

2.7.1 Cloning of constructs with the C-terminal reporter protein fusions

The full length *AtOEP16.1* was cloned in two plasmid vectors, pOL-GFP and pOL-RFP (Asseeva et al., 2004) with a conventional cloning procedure. For PCR, two primers with (i) 5'-introduced site for SpeI restriction (oep16araSpeI) and (ii) 3'-containing site for SalI (oep16araSalIr) and AtOEP16.1/pCRII as a template were used.

The full length *AtOEP16.2* was cloned in pK7FWG2 plasmid vector (Karimi et al., 2005), which contains C-terminal GFP fusion. It was performed a GATEWAY cloning (see 2.4.3). As a template for the first round of adaptor PCR, the *AtOEP16.2/pET21d* plasmid and 16seedGATf and 16seedGAT-stopR were used.

The full length *AtOEP16.3* was conventionally cloned into pOL-GFP vector using PCR with cDNA from *Arabidopsis* as a template and forward 42210SpeIf primer with restriction sites for SpeI on 5' end of PCR product and reverse 42210SalIr primer with sites for SalI restriction.

The full length *AtOEP16.4* was cloned in *pK7FWG2* plasmid vector using GATEWAY cloning procedure. For first round of adaptor PCR, an *AtOEP16.4/pET21b* template and 62880GATf and 62880GAT-stopR primers were used.

The full length VDAC from pea was cloned into the pOL vector by conventional cloning. For PCR, a *VDAC-GFP2* plasmid (Clausen et al., 2004) as a template and primers introducing (i) SpeI restriction site on 5'-terminal (VDACSpeIf) of the PCR product and (ii) SalI restriction site on 3'-terminal (VDACsalIr) were used. See sequences of primers in Appendix.

2.7.2 Biolistic bombardment

2.7.2.1 DNA coating on the gold particles

Gold particles (Biorad) with a diameter of 0.6 micron were suspended at 60 mg/ml in 100% ethanol and vortexed for 1 min to resuspend and disrupt agglomerated particles. A 35 µl aliquot of the gold particles was then pelleted at 14,000 rpm for 10 sec in a microcentrifuge, was washed 2 times in distilled water (with centrifugation steps 14 000 rpm for 1 min) and mixed with 245 µl DNA of a total concentration of 25-50 µg, 50 µl spermidin (0.1 M) and 250µl $CaCl_2$ (2.5 M). Afterwards, the DNA mixture was continuously vortexed for 30 min at 4°C. The gold with coated DNA was washed two times in 70% ethanol by vortexing for 1 min and centrifugation for 1 min at full speed in a microfuge and finally resuspended in 72 µl of 100% ethanol. 7 µl aliquots were used for biolistic DNA bombardment. An aliquot of gold

coated with DNA was pipetted in the centre of a macrocarrier (Biorad) and left until the ethanol evaporated.

2.7.2.2 DNA bombardment

The roots of 5-day-old *P. sativum* plants cut into pieces of 2 cm length and placed on pre-wetted 1 MM Whatmann paper were bombarded with DNA-gold particles using the Biorad Biolistic PDS-1000yHE Particle Delivery System. Optimised biolistic parameters were with a target distance of 6 cm and 1100-psi particle acceleration pressure. After the bombardment the roots were incubated in the dark at 21°C for 24 hours. Before fluorescent microscopy roots were fixed in 4% glutaraldehyde (Serva) for 15 min.

2.7.3 *Arabidopsis* protoplasts isolation and PEG-mediated DNA transformation

Mesophyll protoplast isolation and transient transformation with plasmid DNA were performed from leaves of 4-6-week-old *Arabidopsis* as described in Koop et al., (1996). The intactness of the protoplasts was controlled by fluorescence microscopy using the chlorophyll fluorescence as an indicator.

2.7.4 Fluorescent microscopy

The epi-fluorescence microscope (Polychrome IV System, Photonics GmbH) was used for detection of the GFP fluorescence observed at excitation with the monochromatic laser light at 470 nm and GFP TILL filter set. Fluorescence of the RFP having constructs and Mitotracker Orange signals were measured with the monochromatic laser light at 554 nm or 551 nm, respectively, and Phodamine TILL filter set. Pictures were taken using an IR CCD Camera (Polychrome IV System, Photonics GmbH) mounted on the microscope and operated by the TILLvisION 4.0 software (Photonics GmbH).

2.8 Promoter-GUS analysis

2.8.1 Construction of plasmids

1.5 kb promoter fragments of the *AtOEP16.1, AtOEP16.4, AtOEP37* genes and a 0.728 kb promoter fragment of the *AtOEP16.2* gene were amplified by adaptor PCR (see 2.4.3). For first round of PCR, next primers were used: (i) 16GUSgateF and 16GUSgateR for the *AtOEP16.1* promoter region, (ii) SeedGUSgateF and SeedGUSgateR for the *AtOEP16.2* promoter region, (iii) 62GUSgateF and 62GUSgateR for the *AtOEP16.4* gene 5' upstream region, and (iv) 37GUSgateF and 37GUSgateR for the *AtOEP37* promoter region. Primers for the PCR amplification of the promoter region are listed in Appendix. PCR products cloned by GATEWAY technology with BP clonase mix into the *pDONR201* (Invitrogen) vector followed by LR clonase recombination with the *pKGWFS7* binary destination vector (Karimi et al., 2005). The resulting *AtOEP16.1/pKGWFS7, AtOEP16.2/pKGWFS7, AtOEP16.4/pKGWFS7 and AtOEP37/pKGWFS7* expression clones possess C-terminal coding sequence of GUS and GFP.

2.8.2 Transformation of *Agrobacterium tumefaciens*

Chemically competent *Agrobacterium tumefaciens,* strain GV3101, possessing the disarmed Ti plasmid pMP90, were prepared according to Clough et al., (1991). Therefore, inoculated with GV3101, 5 ml of LB broth supplemented with antibiotics (0,15 mg/ml rifampycin, 15 µg/ml gentamycin) was grown to early saturation stage (1 day) at 28°C with shaking at 200 rpm. Then 2 ml of the culture was inoculated into 50 ml LB broth (0,1 mg/ml rifampycin, 15 µg/ml gentamycin). After the cell density reached OD_{600} of 1.0 (approximately 4h), the culture was harvested by centrifugation at 3,000 g for 15 min. The bacterial pellet was resuspended in 1 ml ice-cold 10 mM $CaCl_2$, aliquoted (100 µl) and frozen in liquid N_2. The cells were stored at – 80°C.

For transformation 1 µg plasmid DNA was pipetted on top of 100 µl frozen agrobacteria and after 5 min incubation at 37°C, 1 ml LB medium supplemented with rifampycin was added and the cells were placed on shaker for 3-4 hours at 28°C. Then the *Agrobacteria* were pelleted for 2 min at 12,000 g, resuspended in 100 µl LB, plated on LB-rifampicin-gentamycin-spectinomycin media and grown at 28°C for 3 days. To verify the intactness of the insert in the binary vector, plasmid mini-prep on the Agrobacterium clone was done and DNA was then transformed into *E. coli* DH5α cells. Mini-prep of plasmid from *E. coli* was

used for a control PCR by taking the plasmid specific primers. The prepared glycerol stocks from the positive clones were used for the transformation of *Arabidopsis* plants.

2.8.3 Stable transformation of *Arabidopsis* with floral dip method

The respective transformed *Agrobacteria* cells were grown at 28°C with 200 rpm shaking in YEB-rifampycin-kanamycin-spectinomycin media. 25 ml of media was inoculated with 50 µl glycerol stock culture and was grown overnight. 5 ml overnight culture was transferred into 500 ml broth and was shaken till an OD_{600} value of 1,2 –1,5 was reached. Then bacteria were centrifuged for 10 min at 14,000 rpm and the pellet was resuspended in 100 ml inoculation medium containing 5.0% sucrose and 0.05% (i.e. 500 µl/L) surfactant Silwet L-77 (OSi Specialties, Inc., Danbury, CT, USA). After growth of *Arabidopsis* plants for three weeks, the emerging bolts were cut to induce the growth of secondary bolts. One week after the clipping, the plants possessing numerous unopened floral buds were submerged into inoculation medium of *Agrobacterium tumefaciens*, containing a vector with a promoter of interest. The plants were then placed on their side and kept at high humidity under plastic wrap. After 24h, they were uncovered and set upright. Harvested seeds were grown on kanamycin (100 µg/ml) containing media to select transformants. The presence of transformed T-DNA insertion in selected transgenic plants was confirmed by PCR. For the GUS-analysis plants of T-2 and T-3 generations were used.

2.8.4 GUS - staining

Plant material was prefixed for 15 minutes in 0.3% paraformaldehyde in X-gluc buffer containing 100mM NaH_2PO_4 (pH 7.2), 10mM Na_2EDTA, 0.5mM K ferrocyanide, 0.5mM K ferricyanide and 0.0025% Triton X-100. Tissue was rinsed once with X-gluc buffer and then stained in 2 mg/ml 5-bromo-4-chloro-3-indoyl glucuronide (X-gluc) in X-gluc buffer. Triton X-100 for 6-18 hours until the desired intensity of staining was achieved. Stained samples were rinsed with X-gluc buffer and fixed in 4% paraformaldehyde for 15 min. After rinsing twice with X-gluc buffer, the samples were incubated in 70% ethanol to remove chlorophyll.

2.8.5 *In vitro* pollen tube germination

Freshly anther-containing flowers were dipped onto the surface of agar plates (35 mm diameter Petri dishes) with a thin layer of medium for *in vitro* pollen germination, containing 5 mM MES (pH 5.8 adjusted with TRIS), 1 mM KCl, 10 mM $CaCl_2$, 0.8 mM $MgSO_4$, 1.5 mM

boric acid, 1% (w/v) agar, 16.6% (w/v) sucrose, 3.65% (w/v) sorbitol, and 10 µg ml^{-1} myo-inositol to transfer the pollen grains (based upon Fan et al., 2001). Following pollen application, the dishes were immediately transferred to a chamber at 21 °C with 100% relative humidity in the light. Germinated pollen were stained for GUS analysis as described in 2.8.4.

2.9 Isolation of organelles and suborganellar fractions

2.9.1 Isolation of intact chloroplasts from *Arabidopsis*

During the isolation procedure, plant material was kept at 4°C according to Aronsson et al., (2002). About 10 g of leaves of *Arabidopsis* seedlings grown for 10 days on plates with MS media and 0.5% (w/v) sucrose were homogenised 5 times in a polytron in 20 ml isolation buffer (0.3 M sorbitol, 5 mM $MgCl_2$, 5 mM EGTA, 5 mM EDTA, 20 mM HEPES/KOH, pH 8.0, 10 mM $NaHCO_3$, 50 mM ascorbic acid) with a subsequent filtration of homogenate through a double layer of Miracloth. Then the homogenate was centrifuged at 1000 g for 5 min (brake on) and the resuspended chloroplasts were loaded on a two-step gradient which consisted of a bottom layer (3 ml) comprising 2.55 ml percoll solution (95% (w/v) percoll, 3% (w/v) PEG 6000, 1% (w/v) ficol, 1% (w/v) BSA) and 0,45 ml gradient mixture (25 mM HEPES-NaOH, pH 8.0, 10 mM EDTA, 5% (w/v) sorbitol) and the top layer (7 ml) comprising 2.94 ml percoll solution and 4.06 ml gradient mixture. The two-step gradients were centrifuged in a swing-out rotor at 1,500 *g* for 10 min (brake off). Intact chloroplasts (the band that appeared between the phases) were recovered using a 1-ml Gilson pipette tip, cut at the end. Then chloroplasts were washed in buffer containing 50 mM HEPES/KOH, pH 8.0, 3 mM $MgSO_4$, 0.3 M sorbitol, 50 mM ascorbic acid) and centrifuged in a swing –out rotor at 1,000 *g* for 5 min (brake on). The supernatant was decanted and discarded, and the pellet was resuspended in the residual washing buffer.

2.9.2 Isolation of mitochondria from *Arabidopsis*

Mitochondria were isolated from 50 g of leaves of 10-days-old *Arabidopsis* by grinding with mortar and pestle as outlined in Day et al., (1985).

2.9.3 Isolation of chloroplastic fractions from pea

Chloroplasts compartments from pea were purified as described in Schleiff et al., (2003). Therefore, pea leaves were harvested and minced in 15 liter of buffer A (20 mM Mops, 13

mM Tris, 0.1 mM MgCl2, 330 mM sorbitol, 0.05% BSA, 0.1 mM PMSF, 2 mM β-mercaptoethanol, pH 7.9) using a blender. The cell fragments were removed by passing the solution through four layers of cheesecloth and one layer of 25 μm gaze. The suspension was pelleted at 1,500 *g* for 5 min at 4° C. The supernatant was centrifuged again for 5 min at 1,500 *g* at 4° C, and both pellets were thoroughly resuspended in buffer A, combined and adjusted to 680 ml. The suspension was layered on top of 34 Percoll gradients formed by 12 ml of 40% and 7 ml of 80% Percoll in 330 mM sorbitol, 50 mM Mops, 0.1 mM PMSF, 2 mM β-mercaptoethanol, pH 7.9, and centrifuged for 10 min at 5,000 *g*. Chloroplasts on top of the 80% Percoll layer were combined and diluted to 1 liter using 330 mM sorbitol, 0.1 mM PMSF, 2 mM β-mercaptoethanol, pH 7.6. Chloroplasts were repelleted at 2,250 *g* for 5 min at 4° C. The pellet was resuspended again in 1 liter of buffer, and the process was repeated. Pellets were resuspended to a final volume of 240 ml in 0.65 M sucrose, 10 mM Tricine, 1 mM EDTA, 0.1 mM PMSF, 2 mM β-mercaptoethanol, pH 7.9, and kept on ice for 10 min. Chloroplasts were ruptured by 50 strokes in a Dounce homogenizer. The volume was then adjusted to 720 ml by slow addition of buffer B (10 mM Tricine, 1 mM EDTA, 0.1 mM PMSF, 2 mM β-mercaptoethanol, pH 7.9), and the suspension was centrifuged for 10 min at 4,000 *g* at 4° C. The volume of supernatant was adjusted again using buffer B to 720 ml and centrifuged for 30 min at 30,000 *g* and 60 min at 150,000 *g* at 4° C. The pellet was carefully washed to resuspend the envelopes present on top of the thylakoids. The envelope suspension was diluted to 120 ml using buffer B, and 10-ml fractions were layered on top of a sucrose step gradient (8 ml 0.465 M sucrose, 10 ml 0.8 M sucrose, and 8 ml 0.996 M sucrose in buffer C [10 mM sodium phosphate, 1 mM EDTA, 2 mM β-mercaptoethanol, pH 7.9]). The gradients were centrifuged for 3 h at 100,000 *g* at 4° C. The layer on top of the 0.8 M sucrose layer contained the outer envelope. The chloroplast fractions were collected, diluted three times using buffer C, and pelleted by centrifugation for 1 h at 100,000 *g* at 4° C. The pellet was resuspended in 3 ml of buffer C, directly frozen in liquid nitrogen, and stored at –80° C for further use. The amount of the outer envelope membranes was determined using the Bio-Rad protein assay (BioRad, Germany; Bradford 1976).

2.9.4 Isolation of membrane fraction proteins from pea and *Arabidopsis*

Plant material (100 mg) was grinded in liquid nitrogen and the proteins were extracted by vortexing for 30 s and incubation for 15 at 4°C in buffer containing 0,05 M TRIS/HCl pH 8.0, 2% LDS and 0,1 mM PMSF. The soluble membrane fraction was separated from cell debris

by centrifugation for 15 min at 15000 rpm at 4°C. Protein concentration of membrane fraction were estimated using the Biorad protein assay reagent (BioRad, Germany; Bradford, 1976), and 50 mM EDTA and 0,15% DTT (final) were added to rest of the sample which was stored at – 80°C.

2.10 PAGE and Immunoblotting

Proteins were separated on a 12.5% (w/v) SDS-polyacrylamide gel electrophoresis. Samples were visualised either by Coomassie blue staining or by Western blotting. After electrophoresis, proteins were transferred in blotting buffer (0.25 M Tris, 0.192 M glycine, 20% methanol, 0.1% SDS) to a nitrocellulose membrane (Schleier&Schuell) at 300 mA for 1 h. The membrane was blocked using 3% Milk Powder, 0.1% Tween 20 in TN buffer (10 mM Tris pH 8, 150 mM NaCl) for 1 h at RT to prevent non-specific binding of the antibody, followed by overnight incubation at 4°C in an 1:1,000 dilution of the primary antibody. After three washes with 0,1% Tween 20 in TN buffer, the membrane was incubated in TN buffer containing 3% Milk Powder, 0,1% Tween 20 with secondary antibodies (anti-mouse or anti-rabbit alkaline phosphatase conjugate, Amersham) for 1 h at RT in an 1:20,000 dilution. Then the blot was washed for three times with TN buffer, and protein/antibody complex bands were visualized by detection of alkaline phosphatase activity using 5-bromo-4-chloro-3-indolyl phosphate/nitroblue tetrasolium as a precipitating substrate (Sigma) in AP buffer (0.1 M Tris, 0.1 M NaCl, 5 mM $MgCl_2$, pH 9.5).

2.11 T-DNA knockout mutants

2.11.1 Screening of the *Atoep16.1-p* knockout mutant

An *Atoep16.1-p* knockout mutant was found in the 72960 lines T-DNA library (basta population) generated in the Rick Amasino lab (Gene Knockout Service Facility of the AFGC, Biotechnology Center of the University of Wisconsin, USA). The T-DNA library was generated by transformation of *Arabidopsis* plants (ecotype WS) with an activation-tagging vector pSKI015 (GenBank accession AF187951) containing the BAR gene conferring the basta resistance for plan selection in soil.

The screen of the T-DNA insertion library was performed in two “PCR rounds” (Sussman et al., 2000), which involved PCR and southern blot analysis of the PCR products. The PCRs were carried out in the Gene Knockout Service Facility, University of Wisconsin. For reaction, the pooled *Arabidopsis* genomic DNA isolated from mutants of the T-DNA insertion

library was used as a template. One of two *AtOEP16.1* gene-specific primers (forward, At2gN, or reverse, At2gC) and the T-DNA left border-specific primer JL202 were used to amplify junction sequence between the T-DNA left border (LB202) and the disrupted *AtOEP16.1* gene.

In the first round, the PCR was performed on genomic DNA of 30 super-pools. The PCR products, obtained from Wisconsin, were hybridisized with a digoxigenin-labeled probe, which was amplified from genomic DNA of wild-type *Arabidopsis* using the gene-specific primers At2gN and At2gC for *AtOEP16.1*. Results of the southern blot analysis of the first "PCR round" are presented in Fig. 2.1 A. Several high-size-bands, detected on the blot, represented the PCR products, which have a T-DNA insert outside of the *AtOEP16.1* gene. Only two PCR band hits were of appropriate size for the mutant of interest: 1200 and 1100 bp (24-th and 39-th super-pools, respectively). The At2gN and At2gC primers were designed to anneal near the start of the first exon and the end of the last exon of *AtOEP16.1* gene, and the size of genomic DNA between these primers is 1036 bp. Therefore, the mutant genome of the identified positive hits would have a T-DNA localized close to the ATG start codon of the *AtOEP16.1* open reading frame.

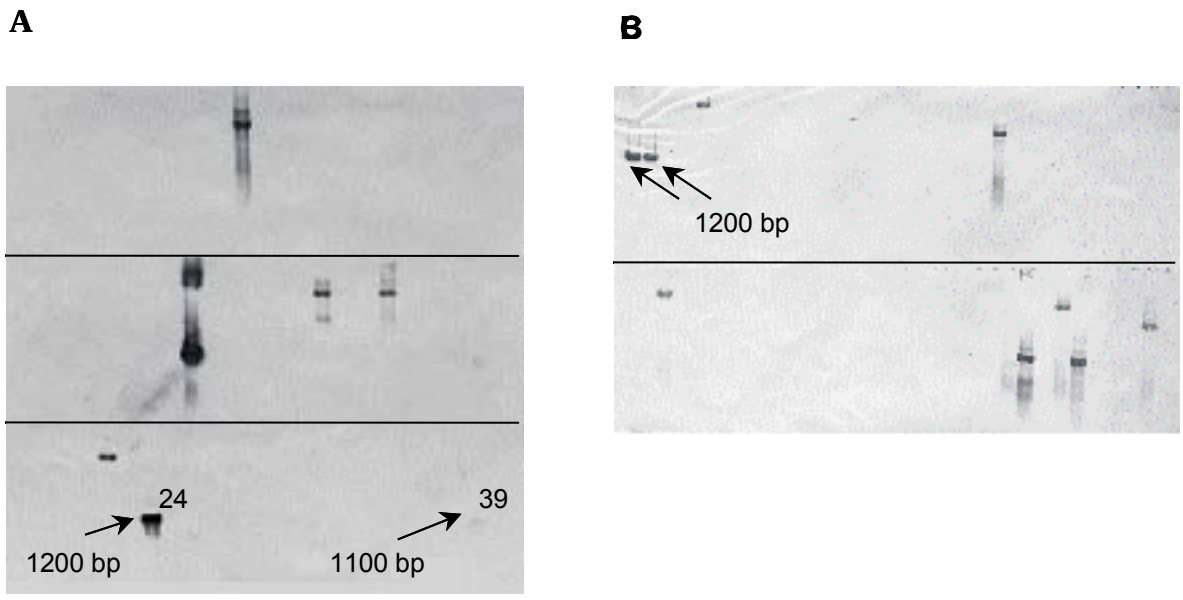

Fig. 2.1 T-DNA screen of an *AtOEP16.1* knockout mutant in the T-DNA library of Rick Amasino (Gene Knockout Service Facility, Wisconsin, USA).

A. First „PCR round": southern blot analysis of the PCR products amplified from 30 super-pools of the T-DNA library. Two positive hits (24 and 39) of the appropriate size are shown with the arrows. **B**. Second „PCR round": southern blot analysis of the PCR products amplified from 24-th and 39-th pools of 225 of the T-DNA library. The positive hits in 24 pool are shown with the arrows.

These two super pools (samples 24 and 39) were chosen for a second "PCR round" of the T-DNA screen. Subsequently, PCR products of the second "PCR round" were used for southern blot analysis, which resulted in 2 hits of about 1200 bp (Fig. 3.23 B). Unfortunately, the PCR product corresponding to pool 39 was absent on the blot. Sequencing of the two positive 1200 bp PCR products with the JL202 primer showed that these products represent one identical line with a T-DNA localized 68 bp upstream of the first ATG codon in the open reading frame of *AtOEP16.1.* Therefore, seeds of one mutant line (24-th super pool, 9-th row, G column, P_{45} plate) were ordered from the Gene Knockout Service Facility, Wisconsin and were used in further experiments. That mutant line was named *Atoep16.1-p*.

2.11.2 Conventional screening of the *Arabidopsis* knockout mutants

Arabidopsis knockout mutant database (SIGnAL with SALK, SAIL, GABI lines) were searched for lines containing T-DNA insertion in the genes of interest. Seeds of the chosen lines were ordered and plants were grown, followed by DNA analysis experiments for the determination of T-DNA presence in the gene of interest. A second knockout mutant of the *AtOEP16.1* locus was found in the T-DNA insertion mutant SALK database. This mutant line, SALK_024018, was generated by transformation of *Arabidopsis* plants with the binary T-DNA vector pROK2, harboring kanamycin resistance to allow the selection of mutants in Col-0 background. An *Atoep16.2* knockout mutant was found by the web search in the Syngenta's T-DNA insertion library, which was created by *Arabidopsis* transformation with pDAP101 vector (basta resistance) in Col-0 background. Two mutants of *AtOEP16.4* locus were screened, one in SALK database (SALK_109275), and another in Syngenta database (Garlic 769 E11). A search in the GABI T-DNA insertion library revealed a knockout mutant line GABI 722C01 (Col-0 background) in the *AtOEP37* locus (GABI-Kat, Rosso et al., 2003). Information about lines, which were used in this work, is summarized in Table 1.1.

Table 1.1 *Arabidopsis* knockout mutants.

Gene name, T-DNA knockout mutant name; source of mutant line (-[1]); plasmid, which was used for T-DNA mutant generation (-[2]) are given.

	gene	mutant name	source[1]	plasmid[2]
1	*AtOEP16.1*	*Atoep16.1-p*	Gene Knockout Service Facility	pSKI015
2	*AtOEP16.1*	*Atoep16.1-e*	SALK	pROK2
3	*AtOEP16.2*	*Atoep16.2*	Syngenta	pDAP101
4	*AtOEP16.4*	*Atoep16.4-e*	Syngenta	pDAP101
5	*AtOEP16.4*	*Atoep16.4-i*	SALK	pROK2
6	*AtOEP37*	*Atoep37*	GABI	PGABI1

2.11.3 *Arabidopsis* double knockout mutant generation

For crossing of two individual single knockout lines the female and male parent flowers were chosen. Flowers of the female parent were not yet self-fertilized, although the stigma was mature. This was achieved by choosing flowers in which the sepals are still closed, and a stigma is protruding from the end of the flower. The sepals, petals and stamens were stripped away from the chosen flowers, leaving the pistil. 4-5 flowers on the same inflorescence was castrated and crossed. Flowers of the male parent were full-blown with visible pollen on the anthers. For crossing, the removed whole male flower was dabbed at the stigma of the castrated female flower. Generated double mutants were named according to the single mutant names in the following order: female parent/ male parent. The F1 and F2 generation of the double mutants were tested with PCR for presence T-DNA in both genes, followed by screening homozygous double knockout lines.

2.12 *In silico* analysis

Arabidopsis web sites	TAIR	http://www.arabidopsis.org/
	MIPS	http://www.mips.biochem.mpg.de/proj/thal/
	NASC	http://nasc.nott.ac.uk/
Homology search	Blast P	http://searchlauncher.bcm.tmc.edu/
Secondary structure,	PROFsec	http://cubic.bioc.columbia.edu/predictprotein/
domains	THMM	http://www.CBS.dk/
	Prosite	http://au.expasy.org/prosite/
Subcellular location	Target P	http://www.cbs.dtu.dk/services/TargetP/
	Predator	http://www.inra.fr/predator/
	Aramemnon	http://www.aramemnon.botanik.uni-koeln.de/
	Cloro P	http://www.cbs.dtu.dk/services/ChloroP/
cis-elements	NSITE-PL	http://www.softberry.com/
Mutant search	SIGnAL (SALK, GABI, SAIL lines)	http://signal.salk.edu/
Expression	NASCArrays, AtGenExpress	http://affymetrix.arabidopsis.info/narrays/experimentbrowse.pl

- Smith - Gene expression and carbohydrate metabolism through the diurnal cycle.
- Nover - Stress treatments (cold stress).
- Honys - Transcriptome analysis of *Arabidopsis* microgametogenesis.
- Bergua - Functional genomics of shoot meristem dormancy.

3. Results

3.1 Characterization of the OEP16 protein family

3.1.1 The OEP16 protein from *Pisum sativum*

OEP16, the 16-kDa transmembrane outer envelope protein of chloroplasts, was first identified in *Pisum sativum* (Pohlmeyer et al., 1997). PsOEP16 represents a channel, facilitating metabolic communication between cytosol and chloroplasts, namely by the transport of amino acids and compounds with primary amino groups via the outer envelope (see Introduction). PsOEP16 is a cation-selective, high-conductance channel most likely forming dimers for its function (Pohlmeyer et al., 1997, Steinkamp et al., 2000).

3.1.1.1 Decomposition of fluorescence spectra of the PsOEP16 protein

The open reading frame of the *PsOEP16* gene contains two nucleotide triplets encoding for the aromatic amino acid tryptophan (Trp-77 and Trp-100), which contribute to the intrinsic fluorescence of the refolded protein by excitation at 280 nm. The emission spectrum of the tryptophan residues is usually highly dependent on the polarity of the surrounding microenvironment. Therefore, a study of the contribution of both tryptophan residues in the fluorescence spectrum of PsOEP16 was performed to elucidate the local tryptophan environment. For this purpose, two single mutants of PsOEP16 with substitution of the tryptophans by a phenylalanin residue, Trp-77→Phe-77 (W77F) and Trp-100→Phe-100 (W100F), were constructed by using recombinant PCR and subsequent subcloning into the pET21b expression vector (see 2.4.2). Then the wild-type PsOEP16 and mutants in pET21b were overexpressed in BL21 *E.coli* cells. After reconstitution in a buffer containing 20 mM HEPES/KOH pH 7.6, 1 mM EDTA, and 0.03% octaethyleneglycol-monododecylether ($C_{12}E_8$), the refolded proteins were used for fluorescence spectra measurements. All fluorescence spectra, circular dichroism and stopped flow measurements were done by Dirk Linke, Max Volmer Laboratorium, Institut für Chemie der Technischen Universität Berlin, Berlin.

The results show that the wild-type spectrum has its fluorescence maximum at 336 nm (Fig. 3.1). In contrast to this, the emission spectra of the mutants have shifts; W77F has a peak at 340 nm and W100F at 333 nm.

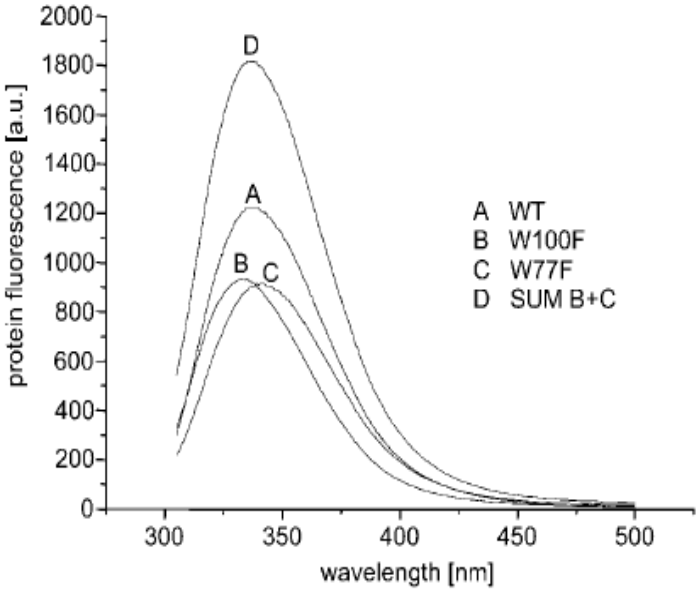

Fig. 3.1 Protein fluorescence of PsOEP16 (Linke et al., 2004).

WT (A) and tryptophan mutants W100F (B) and W77F (C), and the sum of B+C (D).

According to a classification of tryptophan fluorophores in proteins depending on their emission maxima (Burstein et al., 2001; Reshetnyak and Burstein, 2001), Trp-77 belongs to class I fluorophores, which are buried in the nonpolar lipid bilayer environment of the protein. In contrast, Trp-100 represents a fluorophore of II class and is exposed to boundary water. When summing up the two mutant spectra at equal protein concentrations, the calculated spectrum is almost identical in shape to the wild-type spectrum, even though its intensity is stronger (Fig. 3.1 (D)). Thus, two tryptophan residues contribute independently to the wild-type spectrum, and their contribution can be detected in the single-tryptophan mutants. Tryptophan fluorescence assays (Fig. 3.1) suggest that Trp-77 is embedded between hydrophobic residues in helix II, whereas Trp-100 is located adjacent to helix III in the loop region.

3.1.1.2 Topology model of PsOEP16

The determination of conformation of the refolded recombinant wild-type and tryptophan mutants of PsOEP16 (Linke at al., 2004), as well as hydrophobic cluster analysis and mutagenesis experiments (Steinkamp et al., 2000) led to the topology model of PsOEP16 (Fig. 3.2). It is suggested that the protein is purely α-helical, consisting of four transmembrane helices, which have an amphipathic character and form a water-filled pore by formation of dimers.

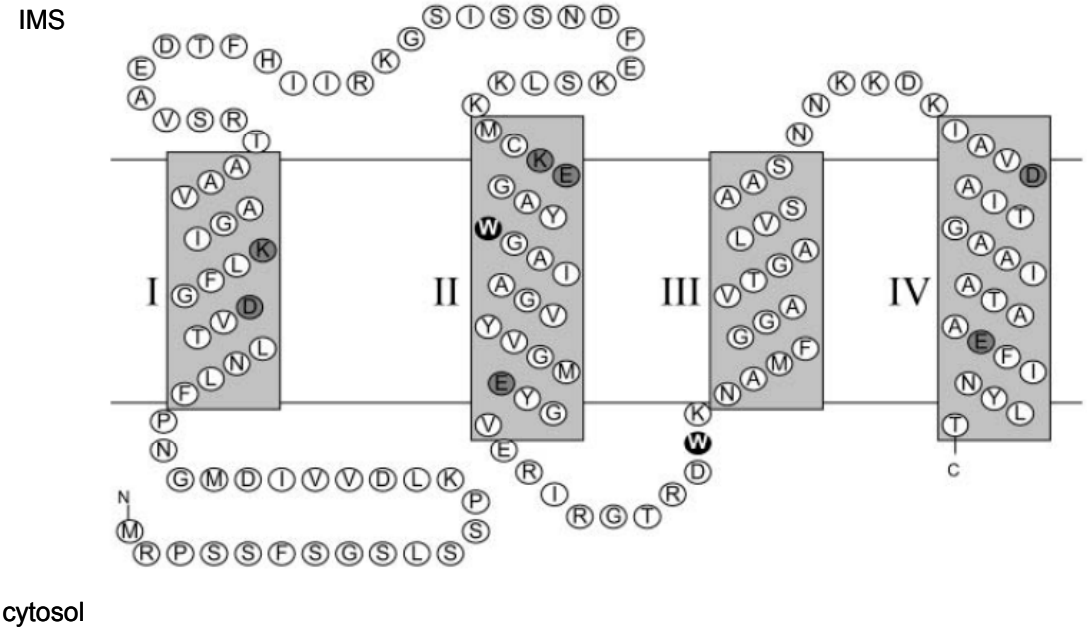

Fig. 3.2 Topology model of PsOEP16 insertion in the lipid membrane (Linke et al., 2004).

The tryptophan residues 77 and 100 (W) are highlighted, as are charged residues within predicted transmembrane α-helices. Helix I contains charged residues in a central position, helices II and IV have similar patterns of charged residues at their ends. IMS, intermembrane space, and cytosol are indicated. According to Pohlmeyer (1997), the N-terminus is located in the cytosol.

On one hand, the transmembrane domains contain stretches of hydrophobic amino acids which have contact with the lipid membrane, on the other hand the α-helices I, II and IV contain charged residues (glutamate, aspartate and lysine). In a functional channel these charged amino acids are most probably coordinated in a fashion such that positively charged sidegroups on one helix have their negatively charged counterparts on another helix. However, the proportion of the negatively charged amino acids is higher and therefore this could determine the selectivity of PsOEP16 for cations.

3.1.2 The OEP16 protein family from *Arabidopsis thaliana*

In *Pisum sativum* only one *OEP16* gene has been identified so far. In the *Arabidopsis* genome, which tends to have predominance of small multigene families, one could expect to find several genes encoding orthologous proteins with common features (Cooke et al., 1997). Indeed, a BLASTP analysis of PsOEP16 against the *Arabidopsis* genome revealed high

similarities to four proteins. On the amino acid level, PsOEP16 showed highest identity to the gene product of At2g28900 (62%), followed by At4g16160, At3g62880 and At2g42210 (27-34%). In the following these genes were named AtOEP16.1 (At2g28900), AtOEP16.2 (At4g16160), AtOEP16.3 (At2g42210) and AtOEP16.4 (At3g62880). Table 3.1 summarizes the obtained BLAST results. In the following these genes were selected for the study as possible ion channels transporting amino acids across the outer envelope of chloroplasts in *Arabidopsis*.

Table 3.1 The genes identified by BLASTP search of the PsOEP16 orthologs in *Arabidopsis*.

AGI code from the MIPS database, GenBank accession number, amino acid identity and similarity to PsOEP16 are listed for AtOEP16.1, AtOEP16.2, AtOEP16.3 and AtOEP16.4.

	AtOEP16.1	AtOEP16.2	AtOEP16.3	AtOEP16.4
AGI code	At2g28900	At4g16160	At2g42210	At3g62880
GenBank accesion number	AAM60853.1	AAM65873.1	AAM63925.1	CAB83138
Amino acid identity to PsOEP16	62%	30%	34%	27%
Amino acid similarity to PsOEP16	79%	50%	48%	46%

3.1.2.1 *In silico* protein sequence analysis of *Arabidopsis* OEP16 orthologs

To predict membrane topology and structure of the above-mentioned proteins, several approaches were used: an alignment of the protein sequences of PsOEP16 and all four orthologues from *Arabidopsis* (Fig. 3.3), the secondary structure prediction (see methods).
It is very likely that all AtOEP16 family proteins are composed of 4 α-helical transmembrane domains, which are connected by soluble loops exposed to the cytoplasm or intermembrane space of chloroplasts. Secondary structure analysis showed that the predicted alpha-helical transmembrane regions of the AtOEP16.1-4 proteins have amphiphilic nature. The N-terminal soluble regions of AtOEP16.1-4 are predicted to be located in the cytoplasm. The N-termini vary in length, e.g. 10 (AtOEP16.4), 15 (AtOEP16.3), 24 (PsOEP16 and AtOEP16.1) and 27 (AtOEP16.2) amino acid residues.

Fig. 3.3 Multiple alignment of the PsOEP16 protein sequence with its orthologs in Arabidopsis.

The α-helical transmembrane domains are numbered I- IV, the loop region I is boxed. Identical amino acids are indicated in black background, similar amino acids are shown in gray background.

The first and the second α-helical transmembrane regions of the AtOEP16s are connected by a long soluble loop I, which consists of 28 amino acid residues in AtOEP16.1 and AtOEP16.4, 29 amino acid residues in AtOEP16.3, while this region contains 36 residues in AtOEP16.2. This variety in the length of loop I could discriminate gating and selectivity of the channels, representing different family members.

A BLASTP search of PsOEP16 against GenBank revealed orthologous proteins from different plant species, e.g. barley (accession no. CAA09867.1), rice (accession no. BAB89876.1 and BAB93165.1), *Bromus intermis* (accession no. AAL23749.1).

A search for the domain structure using the SMART program showed that the OEP16 proteins from *Arabidopsis* and *Pisum sativum* contain Rassow consensus, similar to the TIM17/TIM22/TIM23 family proteins, which facilitates pre-protein translocation from the cytosol via the inner envelope of mitochondria (Rassow et al., 1999). To check whether the OEP16s and *Arabidopsis* proteins of the TIM17/TIM22/TIM23 family indeed exhibit evolutionary relations with OEP16, a phylogenetic analysis was conducted. As shown in Fig. 3.4, the analysed proteins are located in four significantly separated branches of the phylogenetic tree. TIM17, TIM22 and TIM 23 orthologs form three different clusters, and

PsOEP16, AtOEP16.1, AtOEP16.2 and AtOEP16.4 fall into fourth evolutionary group. AtOEP16.3 does not display high similarity to the tested proteins.

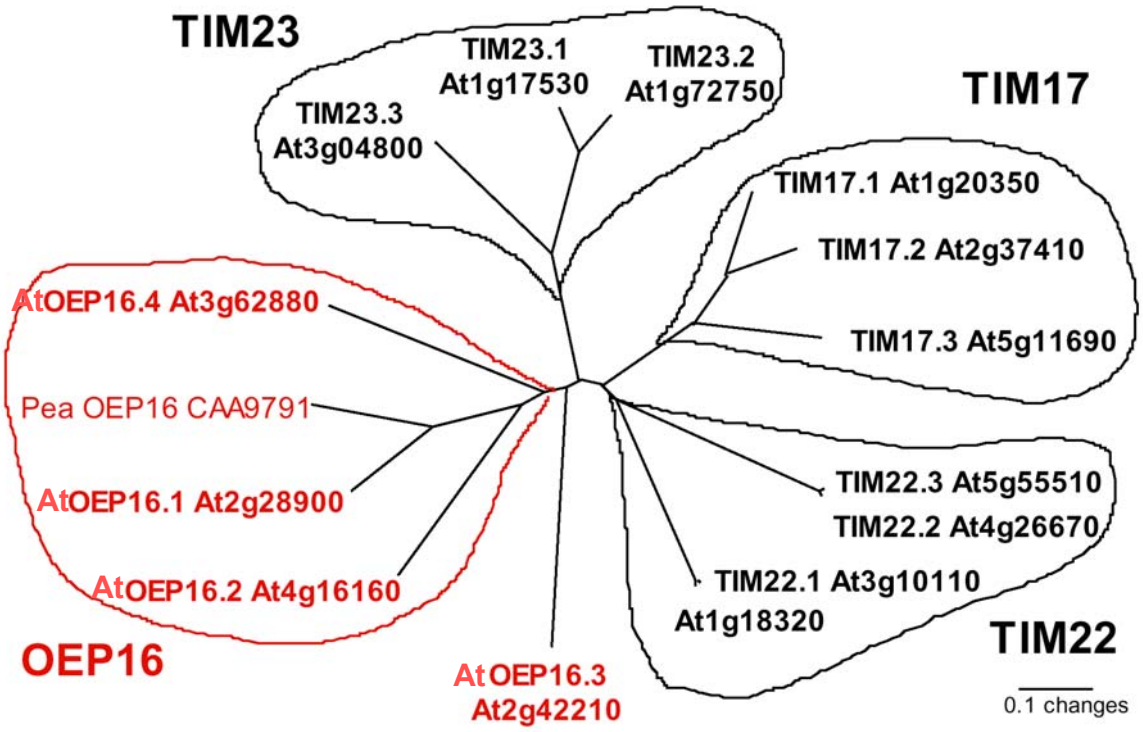

Fig. 3.4 Phylogenetic tree of OEP16 and TIM 17, TIM 22 and TIM 23 proteins from *Arabidopsis.*

Analysis was done using the Vector NTI program with the Kimura correction, ignoring positions with gaps, and blosum62mt2 score matrix. Accession numbers for proteins are given.

3.1.2.2 Isolation of *AtOEP16.1, AtOEP16.2, AtOEP16.3* and *AtOEP16.4*

As predicted by the *Arabidopsis* genome project (TAIR database), the genomic sequence of *AtOEP16.1* contains six exons and five introns, an exon-intron structure which is very similar to that of *AtOEP16.2*. *AtOEP16.4* consists of five exons and four introns. *AtOEP16.3* in contrast to the other *AtOEP16*s contains only two exons and one intron (Fig. 3.5).

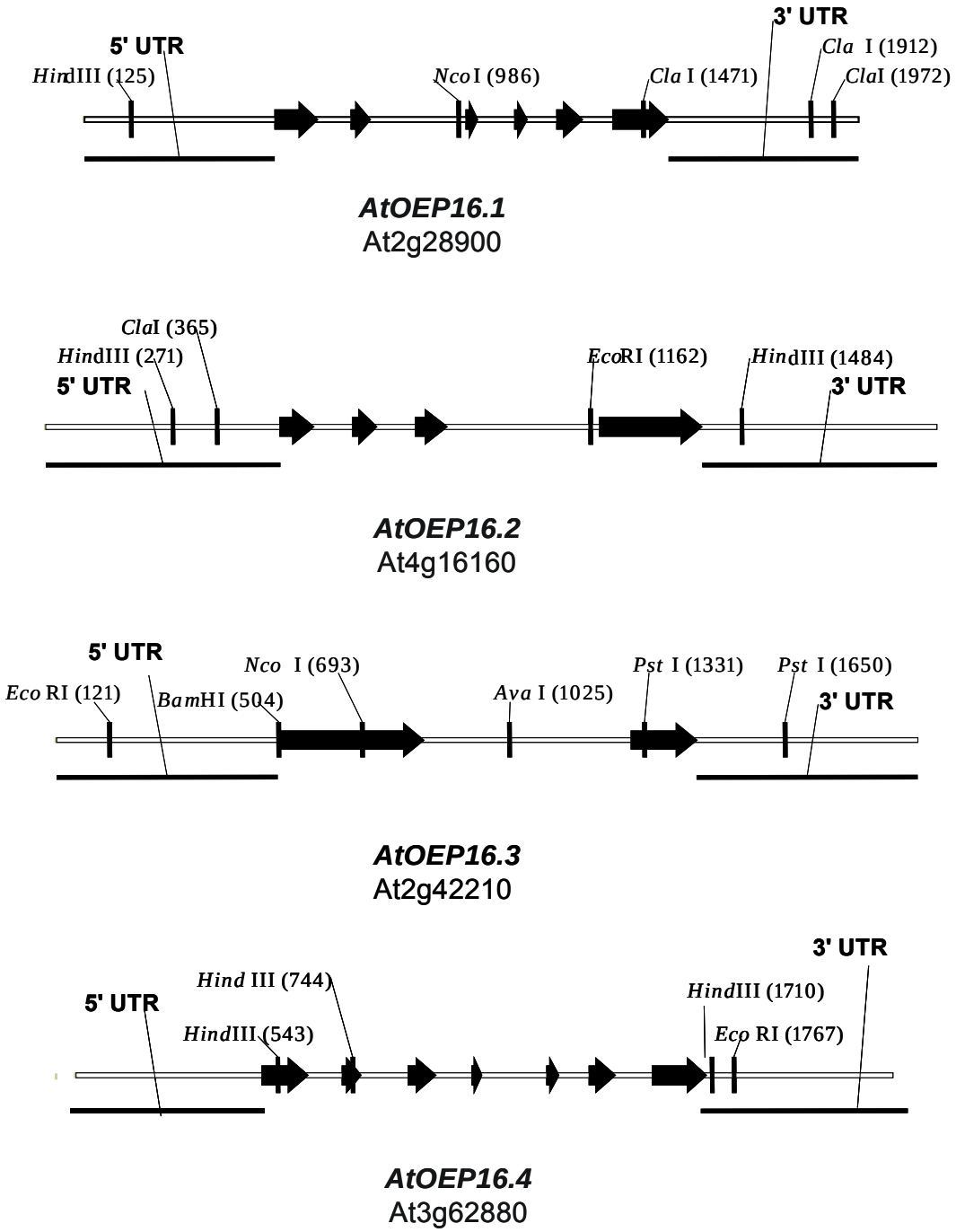

Fig. 3.5 Genomic organisation of *AtOEP16.1, AtOEP16.2, AtOEP16.3 and AtOEP16.4*.

The 5' and 3' untranslated regions (5' UTR and 3' UTR, respectively) and several sites for restriction enzymes are illustrated. Exons are shown as black arrows, introns in grey lines.

The coding regions for *AtOEP16.1*, *AtOEP16.3* and *AtOEP16.4* were amplified by PCR from cDNA synthesized using reverse transcription of total RNA from whole 4-week old *Arabidopsis* plants. The PCR primers were designed to introduce appropriate sites for

restriction enzymes to facilitate the subsequent cloning into different plasmid vectors. *AtOEP16.2* was originally obtained from Dr. T. Kavanagh (Department of Genetics, University of Dublin, Dublin) as a full-length cDNA clone containing 5' and 3' untranslated regions cloned between *Eco*RI (5') and *Xho*I (3') sites in the pBluescript SK vector. *AtOEP16.2* was subsequently subcloned into the pET21d expression vector. The cloning strategy and destination vectors for *AtOEP16.1-4* are summarized in Table 3.2.

Table 3.2 Strategy for of cloning of *AtOEP16.1, AtOEP16.2, AtOEP16.3 and AtOEP16.4.*

The template for cloning, restriction sites for digestion of the inserts and destination vectors, the names of the PCR primers, which were used for the PCR amplification of the cDNA and, the names of destination vectors and constructs are presented.

Gene	*AtOEP16.1*	*AtOEP16.2*	*AtOEP16.3*	*AtOEP16.4*
Template	cDNA	AtOEP16/pBs	cDNA	cDNA
Restriction sites	*Eco*RI (5‘) *Sal*I (3‘)	*Eco*RI (5‘) *Xho*I (3‘)	*Hind*III (5‘) *Xho*I (3‘)	*Eco*RI (5‘) *Xho*I (3‘)
PCR primers	o16araEcoRIf oep16araSalIr	seedEcoRIf seedXhoIr	42210HindIIIf 42210XhoIr	62880EcoRIF 62880XhoIR
Vector	pCR II	pET21d	pET21b	pET21b
Name of construct	AtOEP16I.1/pCRII	AtOEP16.2/pET21d	AtOEP16.3/pET21b	AtOEP16.4/pET21b

The fidelity of the PCR amplifications was verified by sequencing. The *AtOEP16.1* cDNA is 447 bp in length with an open reading frame that codes for a protein with 148 amino acid residues, a calculated molecular mass of 15.5 kDa. *AtOEP16.2* has an open reading frame of 531 bp and encodes a protein of 160 amino acids with a predicted molecular mass of 16.9 kDa *AtOEP16.3* has an open reading frame of 480 bp and encodes a protein of 159 amino acids with a predicted molecular mass of 17 kDa. *AtOEP16.4* has an open reading frame of 411 bp and encodes a protein of 136 amino acids with a predicted molecular mass of 14 kDa. All AtOEP16s have a theoretical pI in the basic range (Table 3.3).

Table. 3.3 Characteristics of the AtOEP16 orthologue proteins.

Amino acid length (Amino acid), predicted molecular mass (kDa), theoretical isoelectric point (pI) are shown for AtOEP16.1, AtOEP16.2, AtOEP16.3 and AtOEP16.4 proteins.

	AtOEP16.1	AtOEP16.2	AtOEP16.3	AtOEP16.4
Amino acids	148	160	159	136
kDa	15.5	16.9	17	14
pI	9.16	8.08	7.93	9.01

3.1.2.3 Intracellular distribution of the AtOEP16 proteins

Within the last few years proteomic analysis of leaf chloroplasts and mitochondria have been performed in *Arabidopsis* (Ferro at al., 2003; Froehlich et al., 2003; Heazlewood et al., 2004). Here, the AtOEP16.1 protein has been detected in outer envelope membranes of chloroplasts, whereas AtOEP16.3 appeared in mitochondria. Neither AtOEP16.2 nor AtOEP16.4 have been identified in chloroplasts or mitochondria in these studies.

For *in silico* analysis of the intracellular localization of AtOEP16 proteins, the prediction programs TargetP (Emanuelsson et al., 2000), Predator, CloroP (Emanuelsson et al., 1999) and the Aramemnon database have been used. As a result, the AtOEP16 proteins, similar to PsOEP16 and other outer envelope channel proteins, were predicted to have no defined location within the cell, mostly because of the absence of a classical chloroplast transit signal in their sequences.

A) Intracellular localisation via GFP-protein fusion

In a first approach, plasmids encoding C-terminal GFP and RFP fusions to these four OEP16 proteins were constructed and gold particles coated with plasmid DNA were bombarded into 5-day-old pea roots. Simultaneously, a control for targeting into plastids, *pSSU-dsRED* and mitochondria, *VDAC-RFP,* was co-bombarded in the same sample.

In a second approach, *Arabidopsis* protoplasts were isolated from mesophyll tissue of leaves, and then transformed with AtOEP16.1-4 GFP fusion constructs via polyethylene glycol (PEG).

The co-bombardment of *AtOEP16.1-GFP* and *pSSU-dsRED* showed after 24 hours, bright green and red fluorescence in spots within several cells of the root tissues sample. Merging of the GFP and dsRED fluorescence images showed co-localization of AtOEP16.1 and pSSU (Fig. 3.6 A). Hence, another control experiment with the mitochondrial localised protein VDAC was done. The transient co-expression of *VDAC-RFP* and *AtOEP16.1-GFP* did not show any co-localisation (Fig. 3.6 B). Thus, the AtOEP16.1-GFP fusion protein, like SSU, is embedded in the plastids of the pea root.

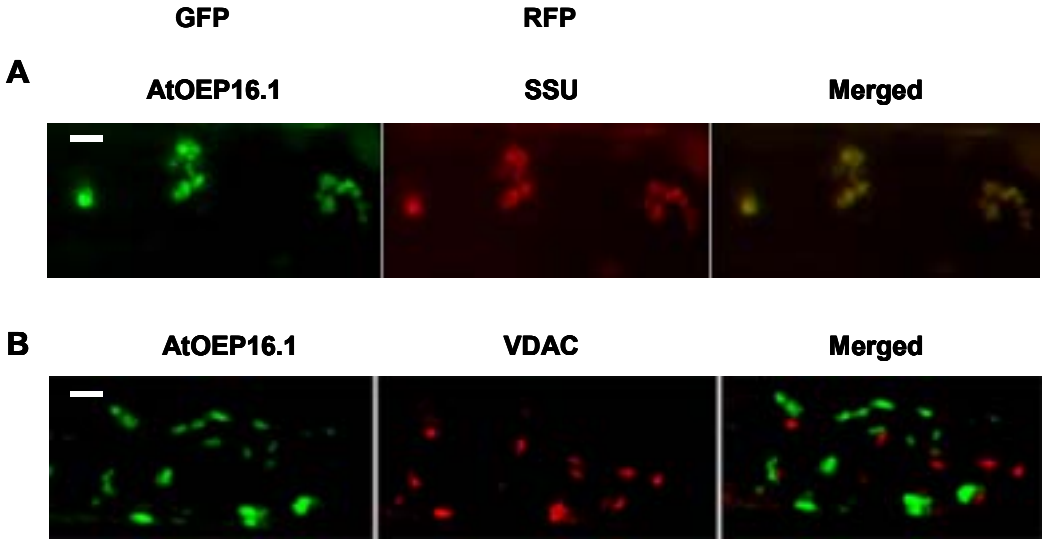

Fig 3.6 Transient expression of AtOEP16.1-GFP in pea root cells.

A. Fluorescence of biolistic co-bombarded *AtOEP16.1-GFP*, *pSSU-dsRED* and merged picture. Scale bar = 10 µm. **B.** Fluorescence of co-bombarded *AtOEP16.1-GFP*, *VDAC-RFP* and merged picture. Scale bar = 10 µm.

The co-bombarded of AtOEP16.2-GFP revealed co-localisation with the plastid marker protein SSU in pea root cells (Fig. 3.7 A). Surprisingly, co-bombardment of *AtOEP16.2-GFP* and *VDAC-RFP* showed fluorescence in the same spots as well (Fig. 3.7 B). To elucidate these controversial results, additional experiments by co-bombarding of *AtOEP16.1-RFP* with *AtOEP16.2-GFP* were done. About 24 hours after biolistic bombardment, emitted red and green fluorescence was detected. About 80% of the green fluorescence was found overlaid with red fluorescence and the residual 20% of green fluorescence, was localised in another region (Fig. 3.7 C). These results suggest that AtOEP16.1-GFP and AtOEP16.2-GFP are localised in plastids but that AtOEP16.2-GFP fusion protein is localised both in plastids and in mitochondria.

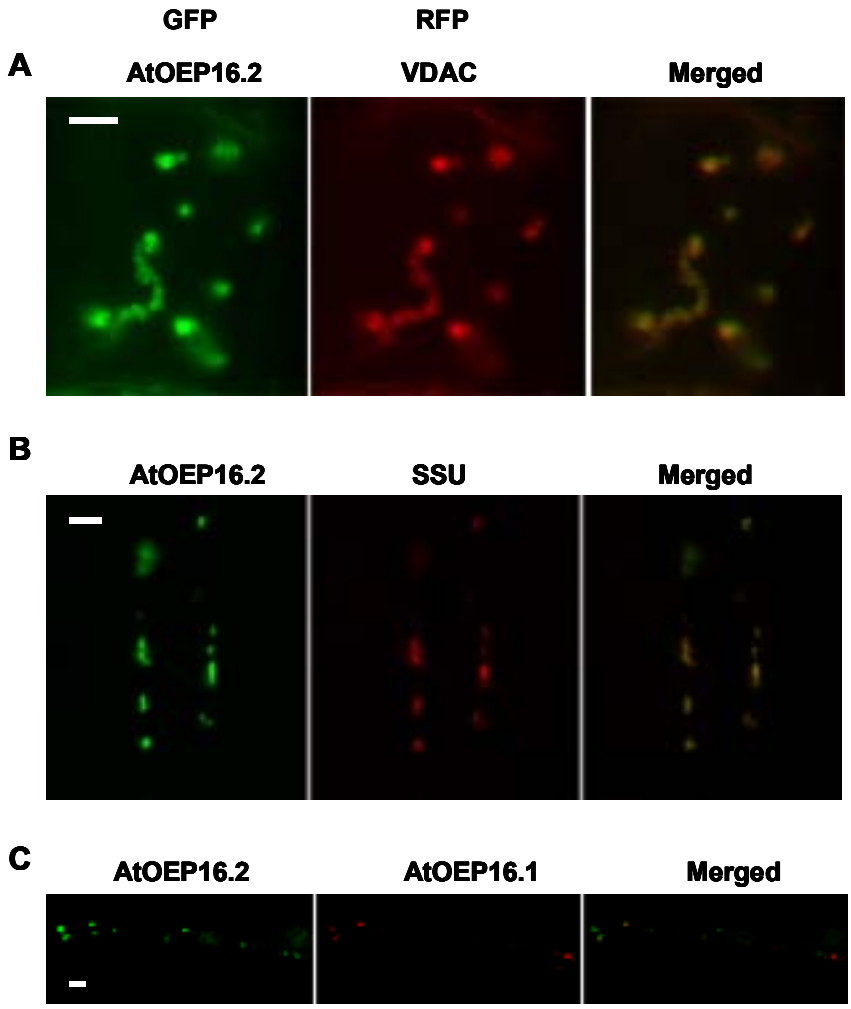

Fig. 3.7 Transient expression of AtOEP16.2-GFP in *Pisum sativum* root cells.

A. AtOEP16.2-GFP, pSSU-dsRED fluorescence and merged picture. Scale bar = 10 µm. **B.** AtOEP16.2-GFP, VDAC-RFP fluorescence and merged picture. Scale bar = 10 µm. **C.** AtOEP16.2-GFP, AtOEP16.1-RFP fluorescence and merged picture. Scale bar = 10 µm.

Fig. 3.8 shows the results of the fluorescence of AtOEP16.3 fused to the GFP reporter. In these experiments, two different tissue samples were used, (i) *Arabidopsis* protoplasts, and (ii) pea root tissue. The PEG-mediated transformation of *Arabidopsis* protoplasts with the *AtOEP16.3-GFP* plasmid revealed that AtOEP16.3-GFP fusion proteins are not associated with chlorophyll autofluorescence (Fig. 3.8 A). In the next experiments of co-bombardment of *AtOEP16.3-GFP* with the targeting control genes in pea root cells, the AtOEP16.3-GFP fusion protein was co-localised with VDAC-RFP but not with pSSU-dsRED (Fig. 3.8 B and C), suggesting that AtOEP16.3-GFP fusion is localised in the mitochondria.

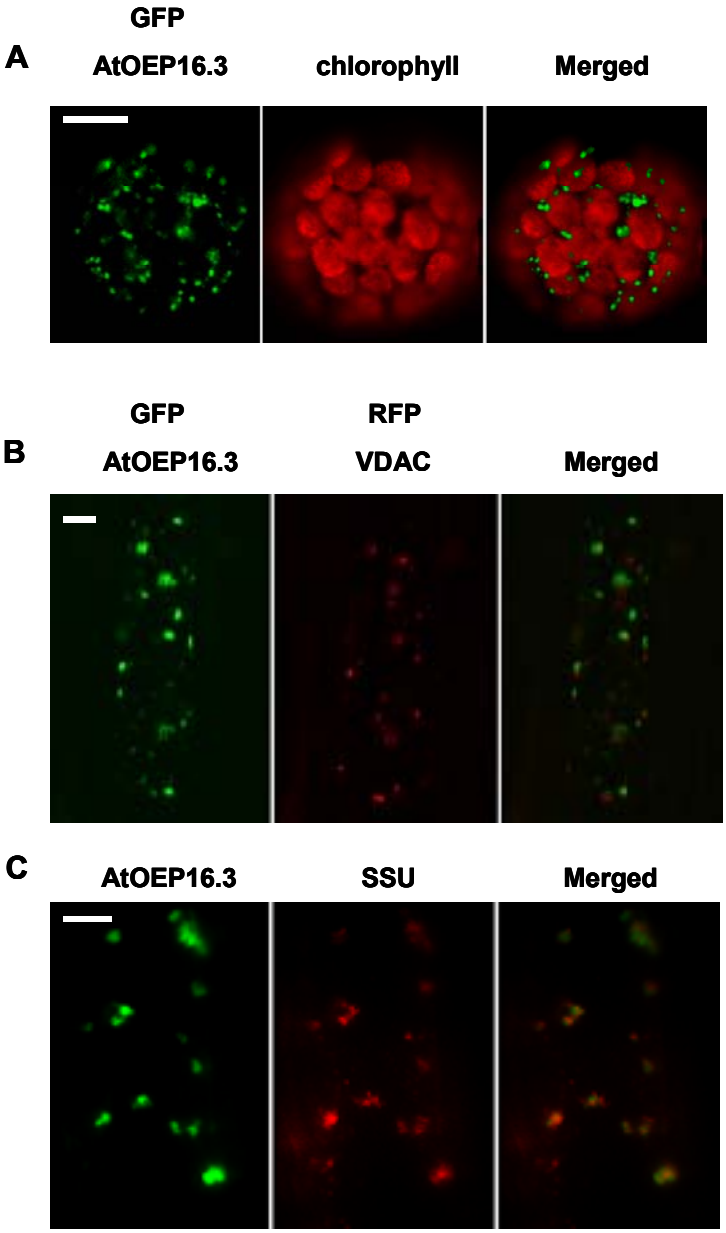

Fig. 3.8 Transient expression of AtOEP16.3-GFP.

A. AtOEP16.3-GFP fluorescence, chlorophyll autofluorescence and merged picture of PEG-transformed *Arabidopsis thaliana* protoplasts. Scale bar = 10 µm. **B-C.** *Pisum sativum* root cell. **B.** AtOEP16.3-GFP, VDAC-dsRED fluorescence and merged picture. Scale bar = 10 µm. **C.** AtOEP16.3-GFP, pSSU-dsRED fluorescence and merged picture. Scale bar = 10 µm.

The green fluorescence of the transiently expressed AtOEP16.4-GFP in *Arabidopsis* protoplasts had a punctuate shape surrounding the autofluorescence red light coming from the chlorophyll (Fig. 3.9 A). The co-bombardment of *AtOEP16.4-GFP* and *pSSU-dsRED* in the pea roots showed the overlap of green and red signal in the merged picture (Fig. 3.9 B). But

the co-bombardment of *AtOEP16.4-GFP* with the mitochondrial control also showed the same pattern (Fig. 3.9 C), suggesting a dual localization for AtOEP16.4.

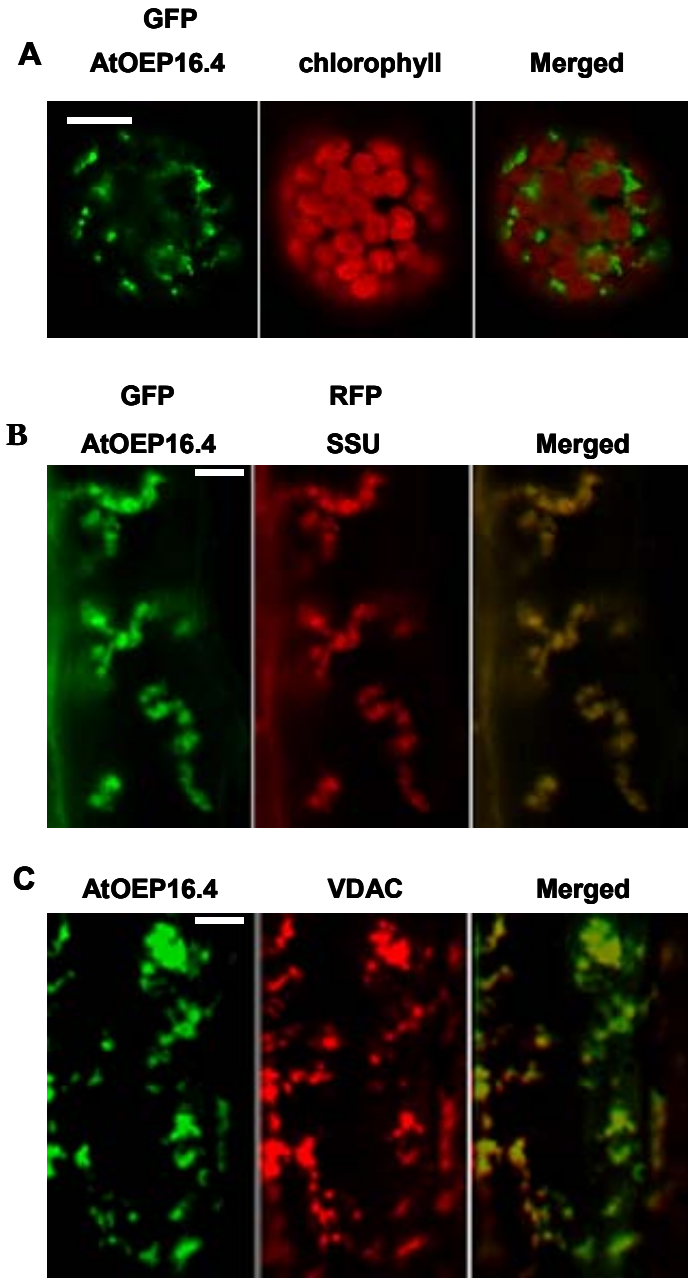

Fig. 3.9 Transient expression of AtOEP16.4-GFP.

A. AtOEP16.4-GFP fluorescence, chlorophyll autofluorescence and merged picture of PEG-transformed *Arabidopsis thaliana* protoplasts. Scale bar = 10 µm. **B-C.** *Pisum sativum* root cell. Scale bar = 10 µm. **B.** AtOEP16.4-GFP, pSSU-dsRED fluorescence and merged picture. **C**. AtOEP16.4-GFP, VDAC-dsRED fluorescence and merged picture.

B) Immunoblot analysis of subcellular localization of the AtOEP16 family

To obtain further insight into the subcellular localization of the *Arabidopsis* OEP16 orthologs, antisera were generated against these proteins, and immunoblot analysis of proteins of chloroplasts and mitochondria isolated from *Arabidopsis* leaves was performed.

As shown in Fig. 3.10 A, the anti-AtOEP16.1 antiserum detected a protein with an apparent molecular mass of 16 kDa in the chloroplast sample prepared from leaves of 6-week-old *Arabidopsis* plants, whereas the anti-AtOEP16.2 antiserum did not recognise any protein in chloroplasts or mitochondria. The AtOEP16.3 protein was present in mitochondria. The anti-AtOEP16.4 antibodies did not detect any band in the tested samples.

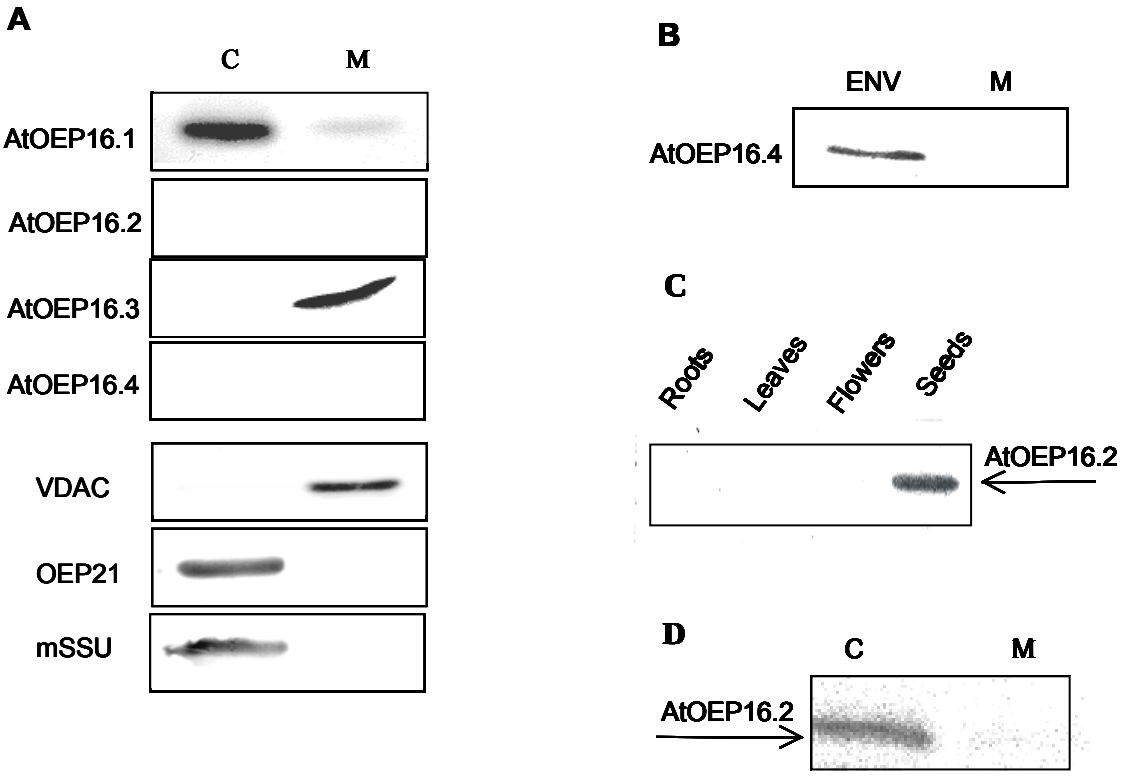

Fig. 3.10 Immunoblot analysis of the subcellular localization of members of AtOEP16 family in *Arabidopsis*.

A. 100 μg total protein from chloroplasts (line C) and mitochondria (line M) purified from leaves of 6-week-old *Arabidopsis* plants were separated on 12.5% SDS-Gel followed by immunoblotting. **B.** immunodetection of the AtOEP16.4 protein; ENV, envelope fraction of leaf chloroplasts (10 μg protein), M, leaf mitochondria (100 μg protein) purified from leaves of 6-week-old *Arabidopsis*. **C.** Localisation of the AtOEP16.2 protein in different tissues of Arabidopsis; 100 μg total protein was immunoblotted. Leaves and roots were harvested from 6-week-old plants. **D.** Localisation of the AtOEP16.2 protein in *Arabidopsis* plants possessing 2 cotyledons and 2 primary leaves in chloroplasts (C) and in mitochondria (M); 100 μg total protein was immunoblotted.

As control for the purity of isolated chloroplasts and mitochondria, immunodetection of chloroplastic proteins OEP21, mSSU and the mitochondrial protein, VDAC, was performed (Fig. 3.10 A).

Absence of the AtOEP16.2 and AtOEP16.4 proteins could be because of low levels of these proteins *in vivo*. Therefore, a fraction of envelope membrane proteins was purified from *Arabidopsis* chloroplasts derived from leaves of 6-week-old plants and used for immunoblot analysis. Subsequent immunoblotting showed that the AtOEP16.4 protein of apparent molecular mass of 14 kDa is located to the envelope of chloroplasts (Fig. 3.10 B). The AtOEP16.2 protein was not detected in this assay. Therefore, to elucidate an *Arabidopsis* tissue abundant for the AtOEP16.2 protein, fractions of total membrane proteins from leaves, roots, flowers and seeds were isolated and used for western blot analysis. Here, this protein with an apparent molecular mass of 17 kDa was found to be expressed in seeds only (Fig. 3.10 C). Unfortunately, chloroplasts and mitochondria cannot be prepared from these organs, therefore all tissues of *Arabidopsis* were analysed for presence of the *AtOEP16.2* RNA with Digital Northern (see Discussion). Since AtOEP16.2 is expressed in cotyledons, *Arabidopsis* plants at the cotyledon stage (2 cotyledons + 2 rosette leaves) were used for chloroplast and mitochondria isolation followed by immunoblot analysis. Western blot analysis with the anti-AtOEP16.2 antiserum revealed a band of apparent molecular mass of 17 kDa in the chloroplast sample, suggesting that AtOEP16.2 is localised in the chloroplasts (Fig. 3.10 D).

The summarized results of the analysis of the subcellular localization of OEP16 family in *Arabidopsis* are presented in Table 3.4.

Table 3.4 Summary of results focused on subcellular distribution of AtOEP16 orthologs.

Results of proteomic analysis, GFP protein fusion experiments and immunoblot analysis were summarized. Ch – chloroplasts; mit – mitochondria.

	Proteomics	GFP fusion	Immunoblot analysis
AtOEP16.1	ch	ch	ch
AtOEP16.2		ch/mit	ch
AtOEP16.3	mit	mit	mit
AtOEP16.4		ch/mit	ch

3.1.2.4 Gene expression patterns of the *AtOEP16* family

A) Affymetrix analysis of the *AtOEP16* family.

With the knowledge that the PsOEP16 protein is expressed in the whole pea plant in equal amounts (Pohlmeyer et al., 1997), the attention was first turned to the transcript content of the *Arabidopsis OEP16*s genes in photosynthetic (leaf) and non-photosynthetic (root) tissues. For this purpose, Affymetrix gene chip analysis on mRNA samples purified from 4-week old *Arabidopsis* leaves and roots was performed. Experiments were done by Dr. Rowena Thomson (Department Biologie I, Botanik LMU, München) within the DFG SPP-1108 project.

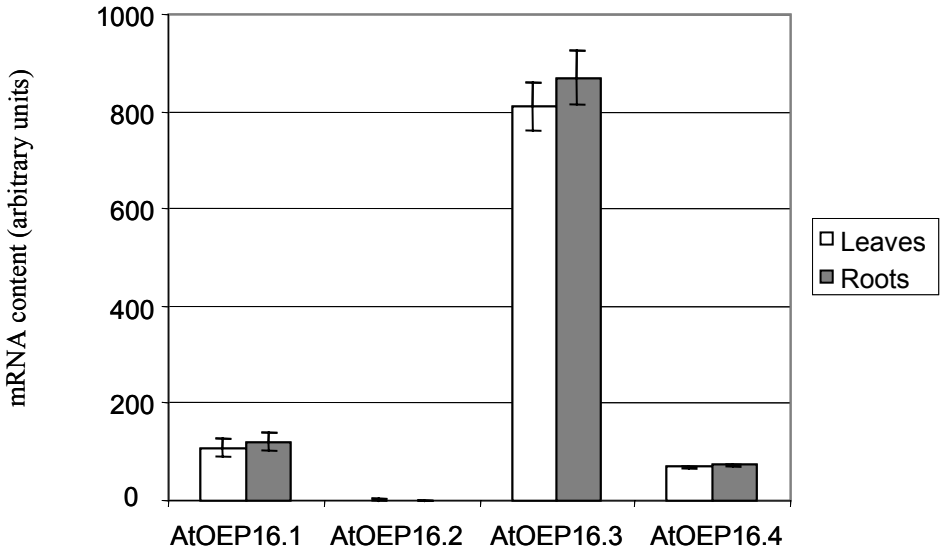

Fig. 3.11 Affymetrix *Arabidopsis* genome microarray analysis of the *AtOEP16.1*, *AtOEP16.2*, *AtOEP16.3* and *AtOEP16.4* mRNA levels in leaves and roots of 4-week-old *Arabidopsis* plants. mRNA levels are depicted in arbitrary units. Error bars denote standard deviation SD of n=3 biological replicas (Dr. Thomson, Dept. Biologie, LMU, München, DFG SPP-1108 project)

Under standard 16-h-photoperiod growth conditions, the *AtOEP16.1* and *AtOEP16.4* genes were expressed in relatively same levels in leaves and roots (Fig. 3.11). A signal for the transcript of the *AtOEP16.2* gene in the tested tissues could not be detected, suggesting that *AtOEP16.2* mRNA is absent in leaves and roots of 4-weeks old plants. These results are in line with immunoblot analysis results (Fig. 3.10). The amount of *AtOEP16.3* mRNA was about 8-10-fold higher than for the *AtOEP16.1* and *AtOEP16.4* transcript levels and was of 811 ± 50 signal level in leaves and 869.36 ± 56 signal level in roots.

B) RT-PCR analysis of the *AtOEP16.1*, *AtOEP16.2* and *AtOEP16.4* distribution in *Arabidopsis.*

Since the current study was aimed to investigate the chloroplast localised OEP16 genes, all following experiments concentrated on the *AtOEP16.1*, *AtOEP16.2* and *AtOEP16.4* genes and gene products. To confirm the results from Affymetrix microarray analysis, RT-PCR assays on total RNA, isolated from leaves and roots of 4-week-old plants and from flowers and siliques, was performed. RT-PCR results represent end-point PCR with the quantification not as exact as Affymetrix.

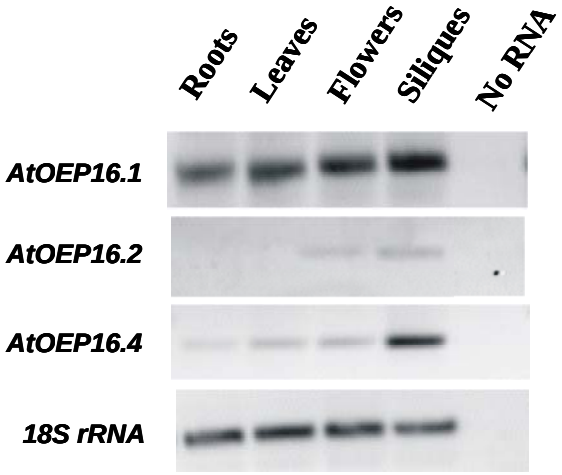

Fig. 3.12 RT-PCR analysis of the *AtOEP16.1*, *AtOEP16.2* and *AtOEP16.4* mRNA in *Arabidopsis*.

For one-step RT-PCR analysis, 20 ng of total RNA isolated from 4-week-old *Arabidopsis* was used. Primers for assay were next: o16araClaIa and o16araXhoIr (for *AtOEP16.1*), oep16SNBamH1-1 and oep16scPst1-2 (for *AtOEP16.2*), 62880XhoIR and 62880EcoRIF (for *AtOEP16.4*) and 18SF and 18SR (for 18S rRNA, house-keeping control).

The analysis showed the presence of specific PCR product bands of 400 bp size, corresponding to the *AtOEP16.1*, *AtOEP16.2* and *AtOEP16.4* mRNA (Fig. 3.12). The signal of the *AtOEP16.1* PCR products was strong in roots, leaves, flowers and siliques. The *AtOEP16.2* mRNA amplification gave weak signals in the flowers and siliques only. The presence of the *AtOEP16.4* PCR product was detected in all tissues. In roots, leaves and flowers the *AtOEP16.4* signals were weak, whereas in siliques it was strong. 18S rRNA was used as a house-keeping control in this assay. These results confirmed the Affymetrix results and revealed expression of *AtOEP16.2* in flowers and siliques.

C) Promoter-GUS analysis of *AtOEP16.1, AtOEP16.2* and *AtOEP16.4*

For further analysis, the expression patterns and functional role of the *AtOEP16*s promoters were examined. For this purpose the promoter regions of *AtOEP16.1, AtOEP16.2 and AtOEP16.4* were fused to the b-glucuronidase (*GUS*) reporter gene *uidA* in the pKGWFS7 vector (Karimi et al., 2005). Plasmid DNA was then transferred to *Arabidopsis* plants via floral dip infiltration, mediated by *Agrobacterium tumefaciens* to allow expression of the promoter::GUS fusion protein under control of the respective OEP16 promoters. Histochemical staining of 8 independent transgenic *Arabidopsis* lines of T1 and T2 progeny harboring the *AtOEP16.1 promoter::GUS* construct gave intensive blue staining in the different organs of the plant at different developmental stages (Fig. 3.13). In the flowers GUS expression was detected in the vegetative tissues, e.g. in the flower stalks of the flower buds (Fig. 3.13 A, B), in the filaments of the stamens (Fig. 3.13 C), in the carpels but not in the stigma (Fig. 3.13 D), in the siliques (Fig. 3.13 E, F) and in the abscission zone of the petals and sepals (base of the silique) (Fig. 3.13 E). In the developing and germinating seeds the GUS staining was observed in the cotyledons of the embryo (Fig. 3.13 G, H). No GUS activity was detected in the radicle. After germination for 3 days in the light, *Arabidopsis* seedlings showed GUS expression in the cotyledons and the primary root, but not in the root tip (Fig. 3.13 I, J). In older plants, the GUS staining was observed mostly in the hydatodes of leaves as shown in Fig. 3.13 K-N.

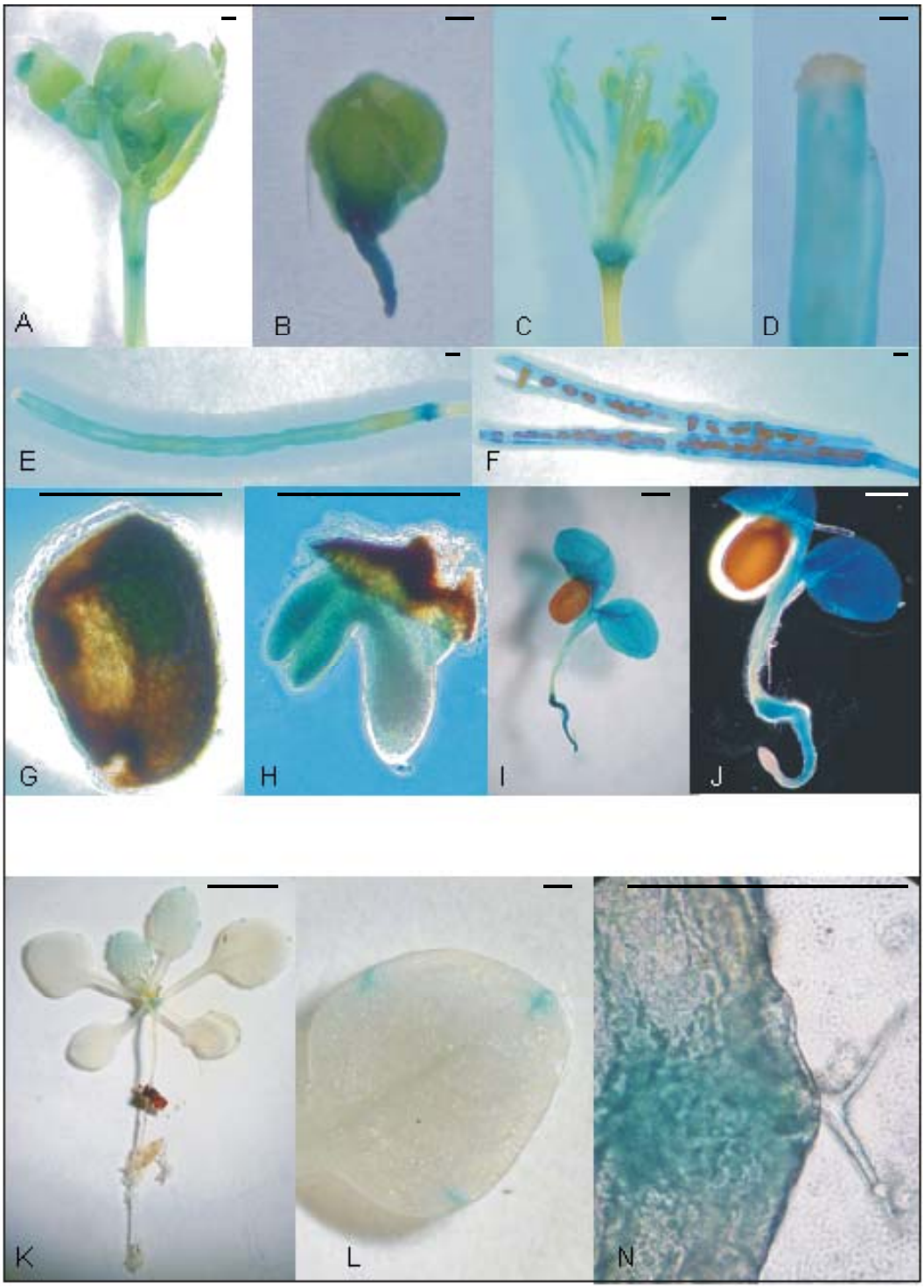

Fig. 3.13 β-glucuronidase staining of *Arabidopsis* transformants harboring *AtOEP16.1* promoter::GUS construct.

A, B, flower bud(s); C, flower with flower stalk; D, the part of pistil with stigma; E, silique; F, opened silique with seeds; G, seed with seed coat (stage 0.10), imbibition in water for 3 days; H, seed without seed coat (stage 0.10), imbibition in water for 3 days; I, J, seedling (stage 1.0), 3 days of imbibition in water + 3 days of growth in light; K, *Arabidopsis* plant, stage 1.04; L, leaf of plant in K; M, leaf, hydatode region. Growth stages are given according to Boyes et al., 2001. Scale bars for A-J and L, N = 1 mm, for K = 1 cm.

The GUS expression under control of the *AtOEP16.2* gene promoter region, monitored by histochemical GUS analysis of the several individual lines of T1 and T2 progeny, transformed with *AtOEP16.2 promoter::GUS* construct, showed blue staining in the flowers first when their stamens are developed (Fig. 3.14 A, B). Here signals were found in the anthers, this blue staining further could be specified to pollen grains. Observation by microscopy of the flower staining showed that GUS activity around the carpel stigmas in the flowers and the stigma in the siliques was due to pollen attached to the stigmas rather than to the stigmas themselves (Fig. 3.14 J). In the *in vitro* germinating pollen, *AtOEP16.2*-GUS expression was detected also in the emerging and pollen tube (Fig. 3.14 K-N).

The developing and germinating seeds of transgenic plants harboring *AtOEP16.2* promoter-GUS construct were tested for GUS activity. GUS staining was not detected during early embryogenesis (Fig. 3.14 O), i.e. before pattern formation was completed (Goldberg *et al.*, 1994). Transformants showed intense staining in maturing embryos or in desiccating seeds (Fig. 3.14 P, R). Germinating seeds showed the same embryo-staining patterns (Fig. 3.14 S, T). A significant level of GUS staining was detectable in seeds after imbibition on water medium at 4° C for 3 days. No staining was observed in the seed coat of developing or germinating seeds. After germination the 2-cotyledon-seedlings and plants of next developmental stages express GUS in the cotyledons and hypocotyl (Fig. 3.14 U-W). No GUS activity was detected and rosette or cauline leaves nor in roots (Fig. 3.14 V). Therefore, *AtOEP16.2* expression was regulated in a tissue- and time- dependent manner.

Several independent lines of *Arabidopsis* transformants harboring the 1500 bp promoter region of the *AtOEP16.4* gene, fused to GUS reporter gene, exhibited no GUS staining in all tissues (data not shown). An analysis of the 1500 bp upstream sequence of the *AtOEP16.4* gene revealed a putative TATA box in position of –1242 and several predicted *cis*-acting elements, but it seems likely that transcription of *AtOEP16.4* gene in *Arabidopsis* is too low to detect its with GUS-staining assay.

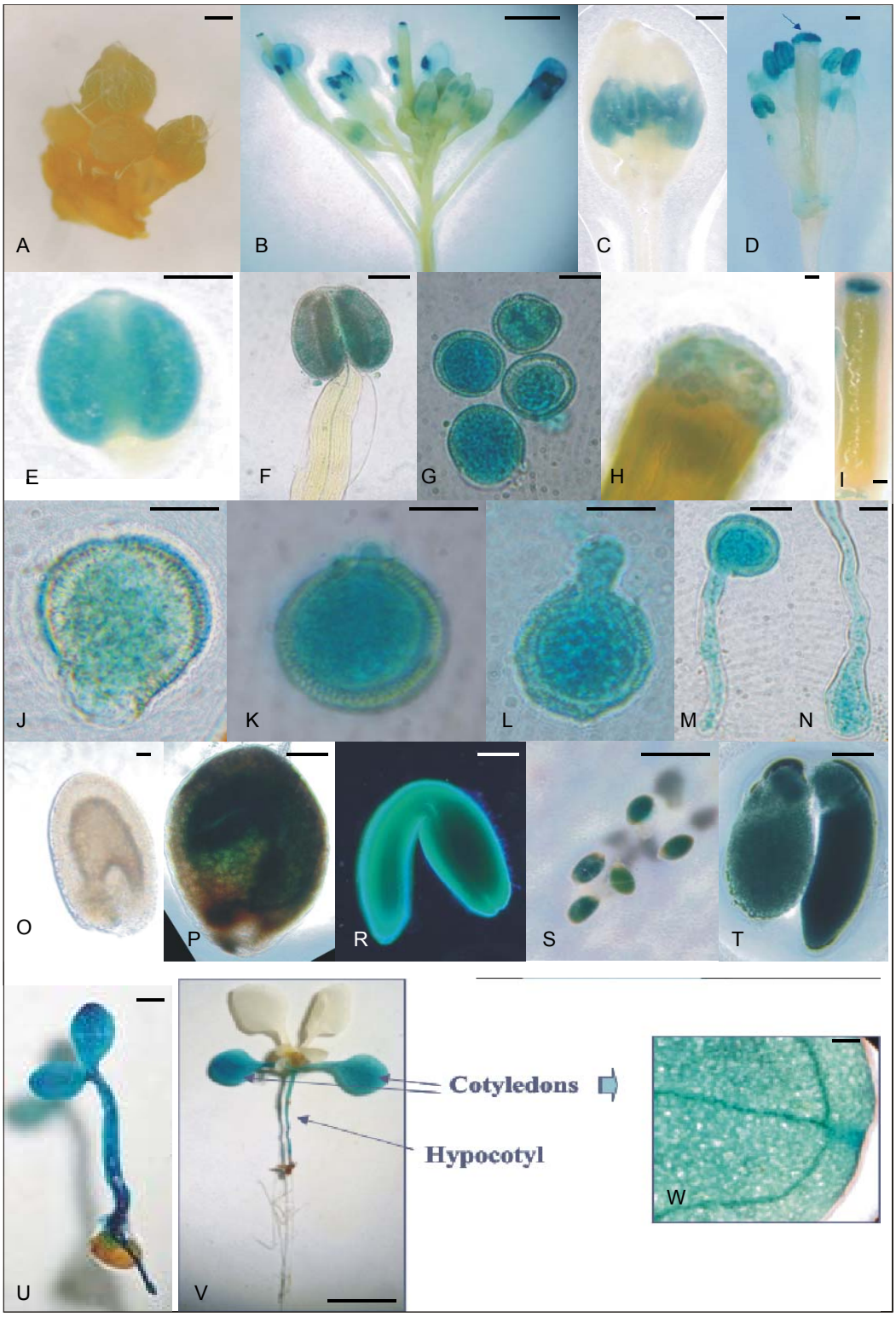

Fig. 3.14. Histochemical GUS staining of *Arabidopsis* transformants harboring *AtOEP16.2 promoter::GUS* construct.

A, flower buds; B, inflorescence; C, flower buds with developing anthers; D, flower; E, anther; F, stamen; G, pollens; H, stigma with pollens; I, silique; J-N, germinating pollen grains; N, pollen tube; O, P, developing seeds; R, developing embryo; S-T, seed imbibition in water for 3 days; S, seeds; T, seed without seed coat; U, 6-day-old seedling; V, *Arabidopsis*, stage 1.04; X, close-up of the section of the cotyledon. Scale bars for A, C, D, I, S, U = 1 mm, for B, V = 1 cm, for E-H and J-R, T, W = 0,1 mm.

3.1.2.4 T-DNA knockout mutants of *AtOEP16s*

To investigate the role of the AtOEP16 proteins in plant metabolism and development, a T-DNA insertion library and public available T-DNA insertion mutant databases were screened for *AtOEP16* knockout mutants.

A) Isolation and characterisation of *Arabidopsis OEP16.1* knockout mutants

A PCR-based reverse-genetics screen of a T-DNA collection, generated by Rick Amasino's lab (Gene Knockout Service Facility of the AFGC, the Biotechnology Center of the University of Wisconsin, USA), resulted in the isolation of one *Arabidopsis* mutant, harboring a T-DNA insertion in the *AtOEP16.1* gene (WS ecotype, see 2.11).

The PCR experiments on genomic DNA isolated from the *Atoep16.1* mutant line with T-DNA-specific and *AtOEP16.1*-specific primers showed that T-DNA is localized 68 bp upstream of the first methionine in the open reading frame of *AtOEP16.1* (Fig. 3.15 A). In the following this mutant line is designed *Atoep16.1-p* (p:- "in promoter").

A second knockout mutant (SALK_024018) of the *AtOEP16.1* locus was found in the T-DNA insertion mutant SALK database (Col-0 background). The PCR experiments on genomic DNA showed that the AtOEP16.1 locus in this line possessed a T-DNA insert within exon 2. Here the T-DNA element disrupts AtOEP16.1 protein synthesis after Asp-48. This mutant was named *Atoep16.1-e* (Fig. 3.15 A). To screen for homozygous *Atoep16.1-p* and *Atoep16.1-e* plants, selection for the mutated AtOEP16.1 alleles was performed by PCR analysis with two sets of primers: (i) T-DNA-specific and *AtOEP16.1*-specific, and (ii) two gene-specific primers. Genomic DNA extracted from wild-type *Arabidopsis* was used for control. The PCR results are shown in Fig. 3.15 B. In *Atoep16.1-p* line, the bands of 1200 bp (with first set of primers) and the absent product of 1550 bp (with second set of primers) were detected in contrast to wild-type plants and designate the homozygous line. In *Atoep16.1-e* line the band of 300 bp (with first set of primers) and absence of a band of 1550 bp (with second set of primers) were detected in contrast to wild-type plants and identified this line as homozygous.

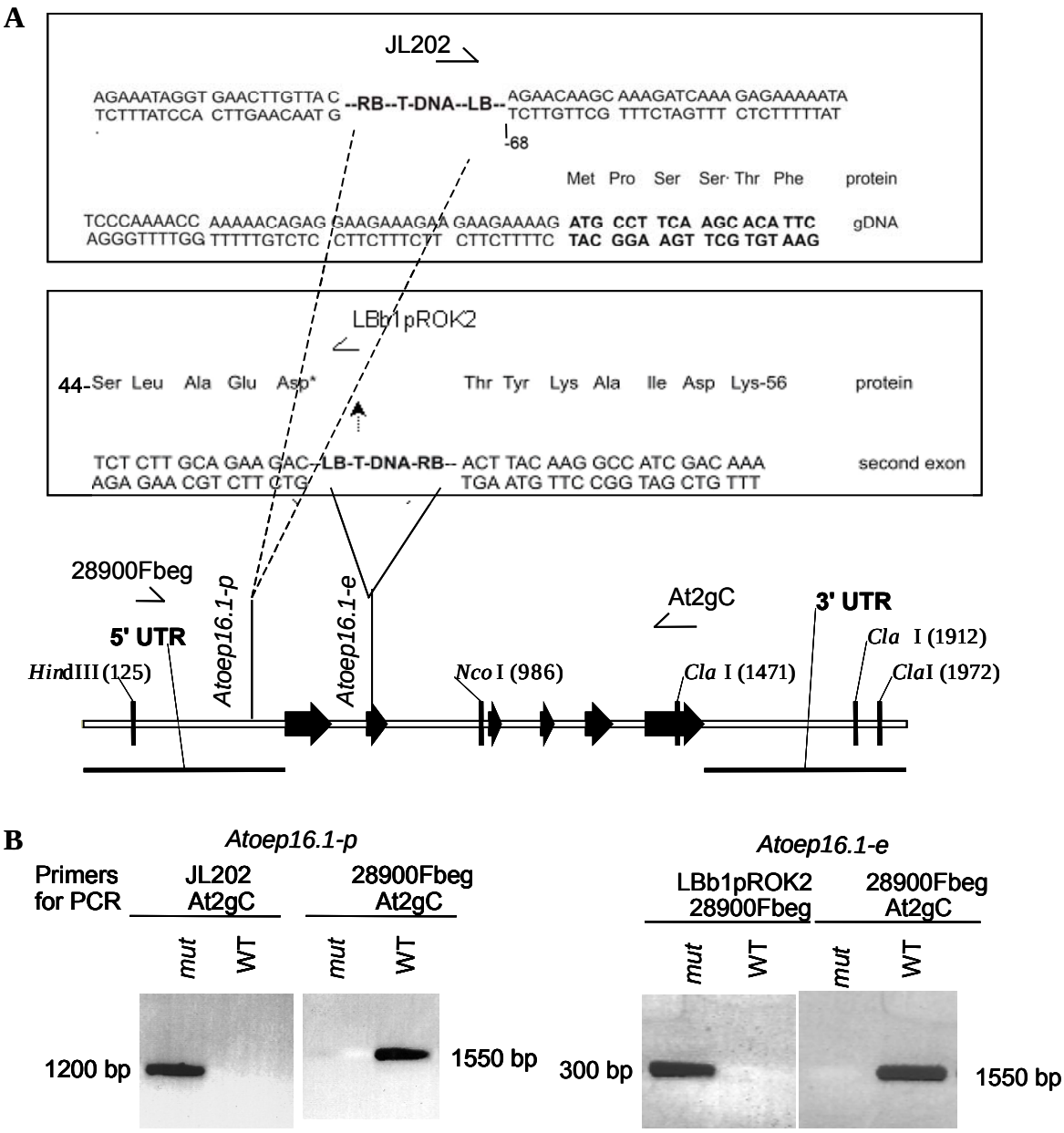

Fig. 3.15 The *Atoep16.1-p and Atoep16.1-e* knockout mutants identification and analysis.

A. Schematic diagram of the T-DNA insert localization (i) at position –68 upstream of the first putative start codon in the open reading frame of *AtOEP16.1* in *Atoep16.1-p* mutant and (ii) in the second exon of *AtOEP16.1* in *Atoep16.1-e* mutant. T-DNA disrupts ORF after Asp*48 in *Atoep16.1-e* mutant. For the T-DNA orientation, position of left (LB) and right (RB) borders is shown. The ORF for the *AtOEP16.1* gene is depicted in bold. Positions of JL202, At2gC, 28900Fbeg primers are shown. Exons are shown as black arrows. **B.** PCR analysis of wild-type and *Atoep16.1-p* and *Atoep16.1-e* individual homozygous lines using following primers pairs for *Atoep16.1-p* (i) T-DNA specific JL202 and gene-specific At2gC, and (ii) gene-specific 28900Fbeg and At2gC; and for *Atoep16.1-e* (i) T-DNA specific LBb1ROK2 and gene-specific 28900Fbeg, and (ii) gene-specific 28900Fbeg and At2gC. Mut, mutant; WT, wild-type.

RT-PCR analysis of the *Atoep16.1-p* and *Atoep16.1-e* homozygous lines was performed to check the influence of the promoter- and exon-inserted T-DNA element on the *AtOEP16.1* mRNA level in mutant plants compared with wild-type *Arabidopsis*. As shown in Fig. 3.16 A, leaves of the homozygous *Atoep16.1-p* line had no PCR-product band of 340 bp, which corresponds to the PCR product, amplified from wild-type *AtOEP16.1* mRNA.

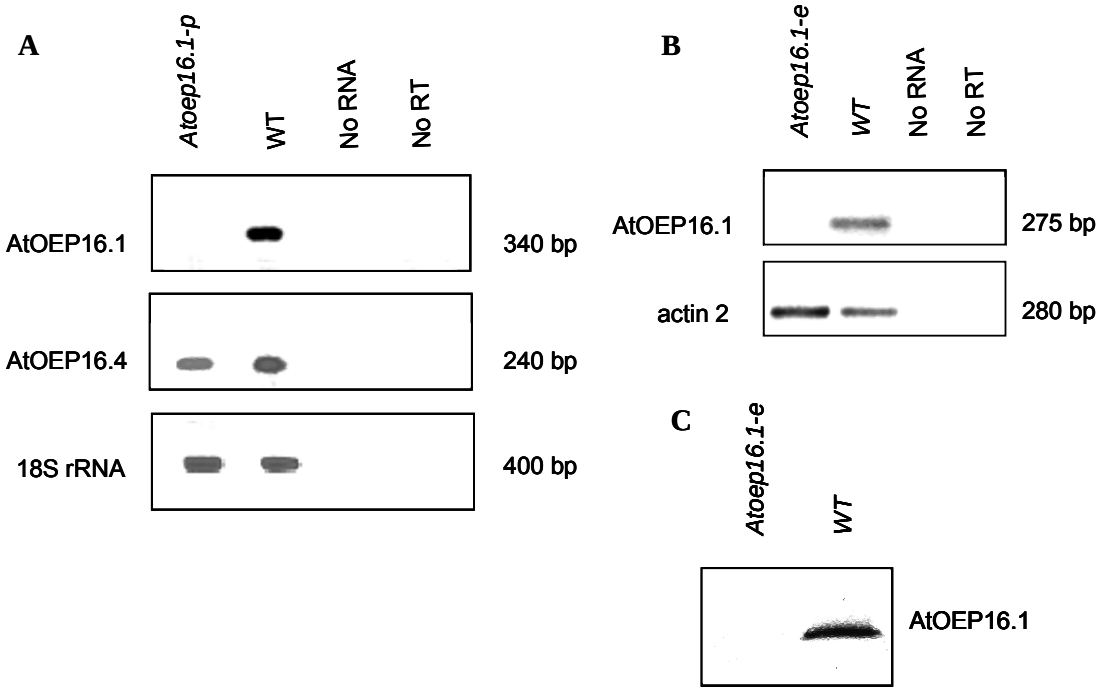

Fig. 3.16 RT-PCR and immunoblot analyses of the *Atoep16.1-p* and *Atoep16.1-e* knockout mutants.

A. 100 ng of total RNA from leaves of 4-week-old *Arabidopsis* plants was used as template for the one-step RT-PCR analysis of *Atoep16.1-p* T-DNA mutant. Primer pairs o16araEcoRIF and o16araXhoIr, 62880SF and 62880R, and 18SF and 18SR were used for amplification of *AtOEP16.1*, *AtOEP16.4*, *18S rRNA*, respectively. The 18S rRNA gene (At2g01010) was amplified as house-keeping control. As negative control for this assay, No RNA and No RT controls were used. **B**. 100 ng of total RNA from leaves of 4-week-old *Arabidopsis* plants was used as template for one-step RT-PCR analysis of *Atoep16.1-e* T-DNA mutant. Primer pairs 28900lcf and 28900lcr, and actin2lcf and actin2lcr were used for RT-PCR analysis of *AtOEP16.1* and *Actin 2* genes, respectively. The *Actin 2* gene (At3g18780) was amplified as a house-keeping control. As negative control for this assay, No RNA and No RT controls were used. **C.** Immunoblot analysis of AtOEP16.1 in leaves of 4 week old *Atoep16.1-e* and wild-type plants. 20 µg membrane fraction proteins were loaded on a 12% polyacrylamide gel. Proteins were blotted on a nitrocellulose membrane, and immunodetection was performed with antisera against AtOEP16.1.

To test whether the disruption of *AtOEP16.1* gene expression affects the mRNA level of the *AtOEP16.4* gene, the closest relative to *AtOEP16.1*, RT-PCR analysis of *AtOEP16.4* in the homozygous *Atoep16.1-p* line was performed. The RT-PCR analysis showed that the knockout line and wild-type plants possessed a 240 bp band of almost the same intensity, representing *AtOEP16.4* mRNA. RT-PCR of the *18S rRNA* gene was used as a house-keeping control in this assay.

As shown in Fig. 3.16 B, representing results of RT-PCR analysis of *Atoep16.1-e* knockout mutant, wild-type plants possessed a amplified PCR product band of 275 bp, which is the expected size of the *AtOEP16.1* PCR product with amplification with two *AtOEP16.1* gene-specific primers. The *Atoep16.1-e* homozygous plants possessed no detectable PCR product band of the same size. RT-PCR of the *Actin2* gene was used as a house-keeping control in this assay.

To analyze the effect of the T-DNA insertion on the production of the AtOEP16.1 polypeptide, proteins were extracted from leaves of 4-week-old plants of *Atoep16.1-e* homozygous as well as wild-type plants. These proteins were tested in an immunoblot with polyclonal antibodies raised against the AtOEP16.1 protein. As shown in Fig. 3.16 C, the antibodies recognized an intense AtOEP16.1 protein band in wild-type plants. Homozygous plants for the *AtOEP16.1* knock out possessed no detectable AtOEP16.1 polypeptide band.

The phenotype of the homozygous *Atoep16.1-p* and *Atoep16.1-e* knockout mutants was inspected and compared with wild-type under standard growth conditions. No detectable difference was observed at any growth stage, including seed germination, plant morphology and growth, flowering time, fertility, silique development, and seed dormancy (data not shown). Cold stress (4°C for 3 days) also did not influence the phenotype of the knock out mutants as well.

B) cDNA macroarray analysis of the *Atoep16.1-p* knockout mutant

To compare gene expression in leaves of 4-week-old *Atoep16.1-p* knockout mutant plants with gene expression in leaves in wild-type, cDNA macroarray analysis on membranes with spotted cDNAs, was conducted during my stay in the lab of Dr. Schäffner (GSF Forschungszentrum, München) within the DFG SPP 1108 project. This macroarray consists of 700 membrane transporter cDNAs (Clomibitza et al., 2004).

When hybridized to an array (Fig. 3.17 A, B), 16 genes showed changes in expression more than 2.5-fold higher or lower. Several channels were down-regulated in the *Atoep16.1-p* knockout mutant (Table 3.4). The mRNA level of LHT1 (At5g40780), amino acid permease,

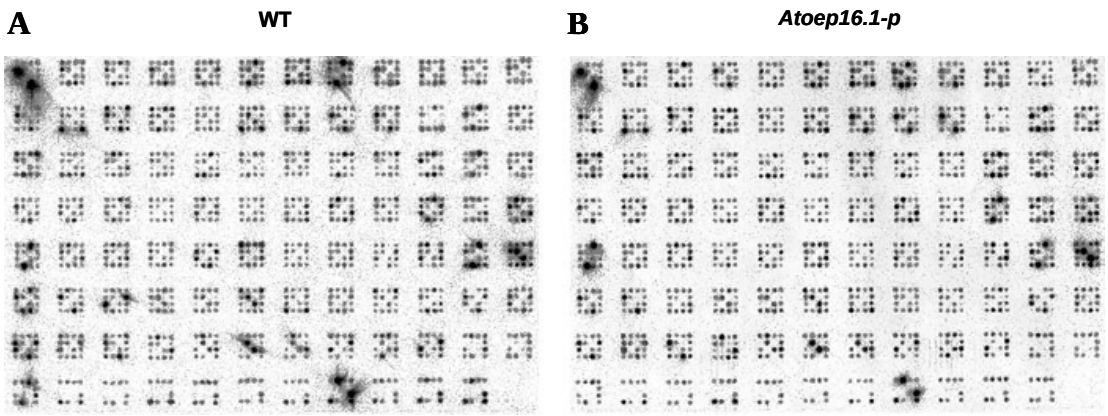

Fig. 3.17 Macroarray analysis of *Atoep16.1-p* knockout mutant.

A. Hybridization of mRNA extracted from leaves of 4-week-old wild-type *Arabidopsis* plants. **B.** Hybridisation of mRNA extracted from leaves of homozygous 4-week-old *Atoep16.1-p Arabidopsis* plants.

which transports lysine and arginine, was decreased 3.58-fold compared with wild-type. The transcript levels of a putative cyclic nucleotide-regulated cation channel (At2g46430, 3.57-fold), two putative sugar transporters At4g04750 (3.38-fold) and ERD6 (At1g08930, 3.27-fold), a putative ABC transporter (At1g59870, 3.1-fold) (Martinoia et al., 2002) and ALA11, a putative calcium-transporting ATPase (At1g13210, 2.74-fold) were down-regulated. The level of the chloroplast-localized ATP sulfurylase precursor (At5g43780) mRNA in leaves of the *Atoep16.1-p* knockout mutant was 3.55-fold lower than in wild-type. ATP sulfurylase precursor is an enzyme, which is involved in glutathione and cysteine synthesis. The mRNA level of a catalase (At1g20620) decreased 2.82-fold in contrast to wild-type. The mRNA content of acyl hydrolase SAG101 (At5g14930), which is involved in leaf senescence decreased 2.59-fold. The transcript amount of the extra-large G-protein AtXLG1 (At4g34390, Lee and Assmann, 1999) was 3.75-fold lower in knockout in contrast to the wild-type.

Three genes contributing to amino acid metabolism and transport were up-regulated in leaves of the 4-week-old *Atoep16.1-p* T-DNA mutant. The mRNA level of naringenin-chalcone synthase (At5g13930), an enzyme of biosynthesis of L-phenylalanine and L-tyrosine derivatives, increased 2.87-fold compared with wild-type. The transcript amounts of S-adenosylmethionine synthase 2 (At4g01850) and a putative proline transporter (At2g36590) increased as well (3.06 and 3.48-fold, respectively). The mRNA content of two aquaporins (At5g47450 and At1g80760) and a nodulin intrinsic, plasma membrane targeted protein (At5g37810) increased 2.91, 3.77 and 2.91-fold, respectively.

Table 3.4 Macroarray analysis of *Atoep16.1-p* knockout mutant

List of down- and up-regulated genes in leaves of homozygous 4-week-old *Atoep16.1-p* knockout mutant. AGI code of gene, changing of mRNA levels, encoded protein and comments (from TAIR web site) are listed.

	AGI code	-fold	Encoded protein	Comments
Down-regulation, WT/mutant ≥ 2,5				
1	At5g14930	2.59	SAG101, acyl hydrolase	Involved in leaf senescence
2	At1g13210	2.74	ALA11, putative calcium-transporting ATPase	P-type ATPase, targeted to mitochondria
3	At1g20620	2.82	catalase	Decomposition of hydrogen peroxide
4	At1g59870	3.1	putative ABC transporter	Targeted to chloroplasts
5	At1g08930	3.27	putative sugar transporter	Electrochemical potential dependent
6	At4g04750	3.38	putative sugar transporter	C-compound and carbohydrate transporter
7	At5g43780	3.55	ATP sulfurylase precursor	Targeted to chloroplasts. Glutathione and cysteine synthesis
8	At2g46430	3.57	putative cyclic nucleotide-regulated cation channel	Calmodulin regulated
9	At5g40780	3.58	LHT1, amino acid permease	Lysine and histidine transporter
10	At4g34390	3.75	extra-large G-protein – like	
Up regulation, mutant/WT ≥ 2,5				
1	At5g13930	2.87	naringenin-chalcone synthase	Biosynthesis of L-phenylalanine and L-tyrosine derivatives
2	At5g47450	2.91	aquaporin	Targeted to tonoplast
3	At5g37810	2.91	plasma membrane integral protein	Nodulin intrinsic protein
4	At4g01850	3.06	S-adenosylmethionine synthase 2	Amino-acid biosynthesis
5	At2g36590	3.48	putative proline transporter	
6	At1g80760	3.77	aquaporin	Tonoplast targeted

C) Isolation and characterisation of an *Arabidopsis OEP16.2* knockout mutant.

The *AtOEP16.2* knockout mutant (SAIL 1334_672_D04, Col-0 background) was found by the web search in the Syngenta's T-DNA insertion library. The PCR experiments on genomic DNA showed that the T-DNA element in this mutant is inserted in the 3-rd intron of the

AtOEP16.2 locus. A schematic diagram of the T-DNA insert location and orientation is shown in Fig. 3.18 A. The T-DNA junction was amplified with the left border T-DNA specific primer and with the gene-specific primer. Homozygous mutant lines were screened with the two gene-specific primers (Fig. 3.18 B).

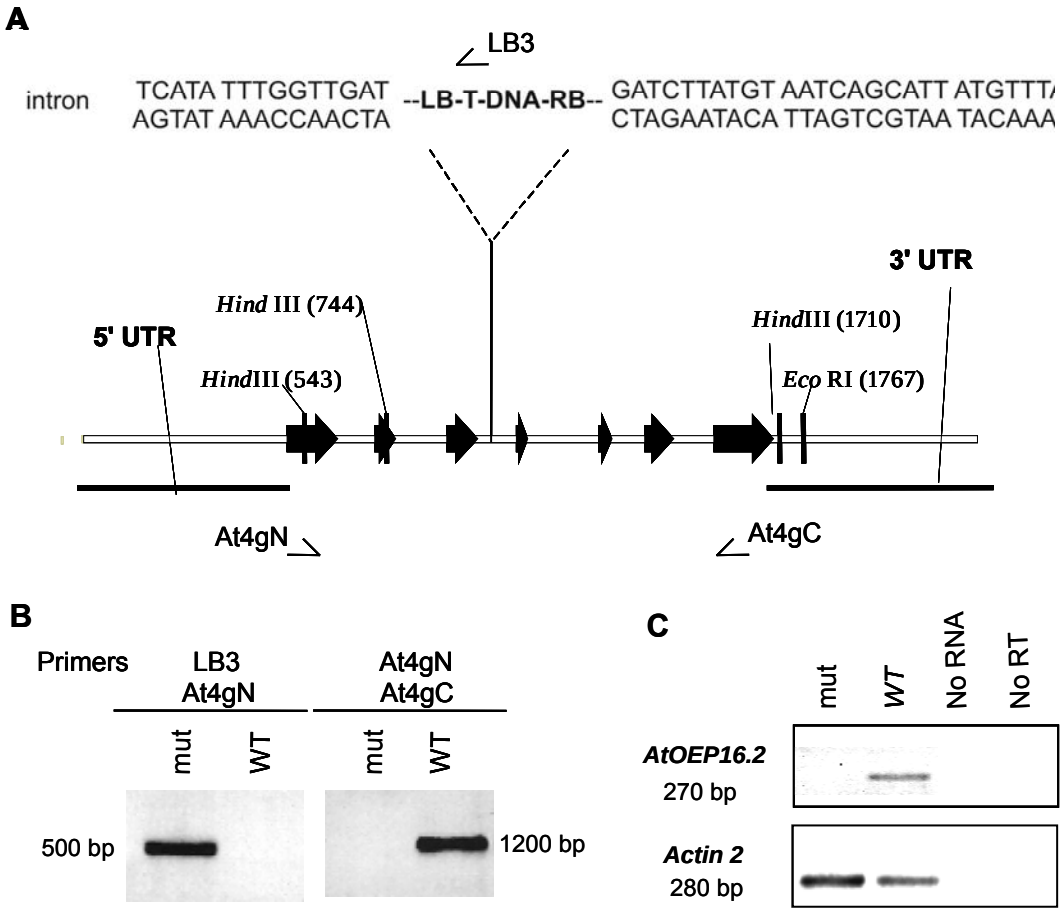

Fig. 3.18 Screening and analysis of the *Atoep16.2* T-DNA mutant.

A. Schematic diagram of the T-DNA element localization in the third intron of *AtOEP16.2* locus. For T-DNA the orientation of left and right borders are shown. Exons are shown as black arrows. **B.** PCR analysis of the individual homozygous lane of the *Atoep16.2* knockout mutant and wild-type (Col-0) using (i) T-DNA specific LB3 and gene-specific At4gN, and (ii) two gene-specific At4gN and At4gC primers. Mut, mutant; WT, wild-type. **C.** RT-PCR analysis of the *Atoep16.2* T-DNA mutant. 100 ng of total RNA from siliques from *Atoep16.2* and wild-type (WT) *Arabidopsis* plants was used for one-step RT-PCR with primers 16160lcf and 16160lcr for *AtOEP16.2*, and actin2lcf and actin2lcr for *Actin 2* gene, which was used as a house-keeping control in this assay. As negative control for the assay, No RNA and No RT controls were used.

To test the effect of T-DNA insertion into intron 3 of the *AtOEP16.2* gene on the mRNA level, RT-PCR analysis of homozygous *Atoep16.2* plants compared with wild-type *Arabidopsis* was performed. Since expression of the AtOEP16.2 is seed specific (see 3.1.2.4 C), total RNA was isolated from developing siliques. As shown in Fig. 3.18 C, wild-type plants possessed a PCR product band of 270 bp. This band corresponds to *AtOEP16.2* mRNA. In contrast to wild-type, no band was detected in the *Atoep16.2* T-DNA mutant. As internal control, the amplification of *Actin 2* was used in this assay.

The phenotype of the homozygous *Atoep16.2* knockout mutant was observed under standard growth conditions and compared with wild-type. No detectable difference was found at any growth stage, including seed germination, plant morphology and growth, flowering time, fertility, silique development, and seed dormancy (data not shown).

D) Isolation and characterisation of *Arabidopsis OEP16.4* knockout mutants

To obtain an *Arabidopsis* OEP16.4 knockout mutant, we screened T-DNA insertion mutants of the SALK database. One candidate knockout line, SALK 109275, was found. The PCR experiments on genomic DNA with the left-border T-DNA specific and gene-specific primers were performed to characterize the genomic region of the *AtOEP16.4* mutant locus. The sequencing showed that the *AtOEP16.4* locus in this line possessed a T-DNA insert within intron 3. Therefore, this mutant was named *Atoep16.4-i*. A second *Atoeop16.4* knockout mutant (Garlic 769 E11) was found by the web search in the Syngenta's T-DNA insertion library. The PCR experiments on genomic DNA in this mutant line with the left border T-DNA specific and with gene-specific primers showed that the T-DNA element is inserted in the last exon of the *AtOEP16.4* locus, therefore this mutant line was named *Atoep16.4-e*. A schematic diagram of the T-DNA location and orientation in the *AtOEP16.4* gene of these T-DNA mutants is shown in Fig. 3.19 A.

To screen for homozygous *Atoep16.4-i* and *Atoep16.4-e* mutant plants, PCR analysis was performed. Two sets of primers were used (i) the T-DNA left border specific primer and gene-specific primer, and (ii) two gene-specific primers. The PCR results are shown in the Fig. 3.19 B and C, respectively. In the *Atoep16.4-i* line the band of 1200 bp (with first set of primers) and absence of the 800 bp band (with second set of primers) were detected in contrast to wild-type plants. In *Atoep16.4-e* line the band of 400 bp (with first set of primers) and absence of a band of 800 bp (with second set of primers) were detected in contrast to wild-type plants and identified this line as homozygous.

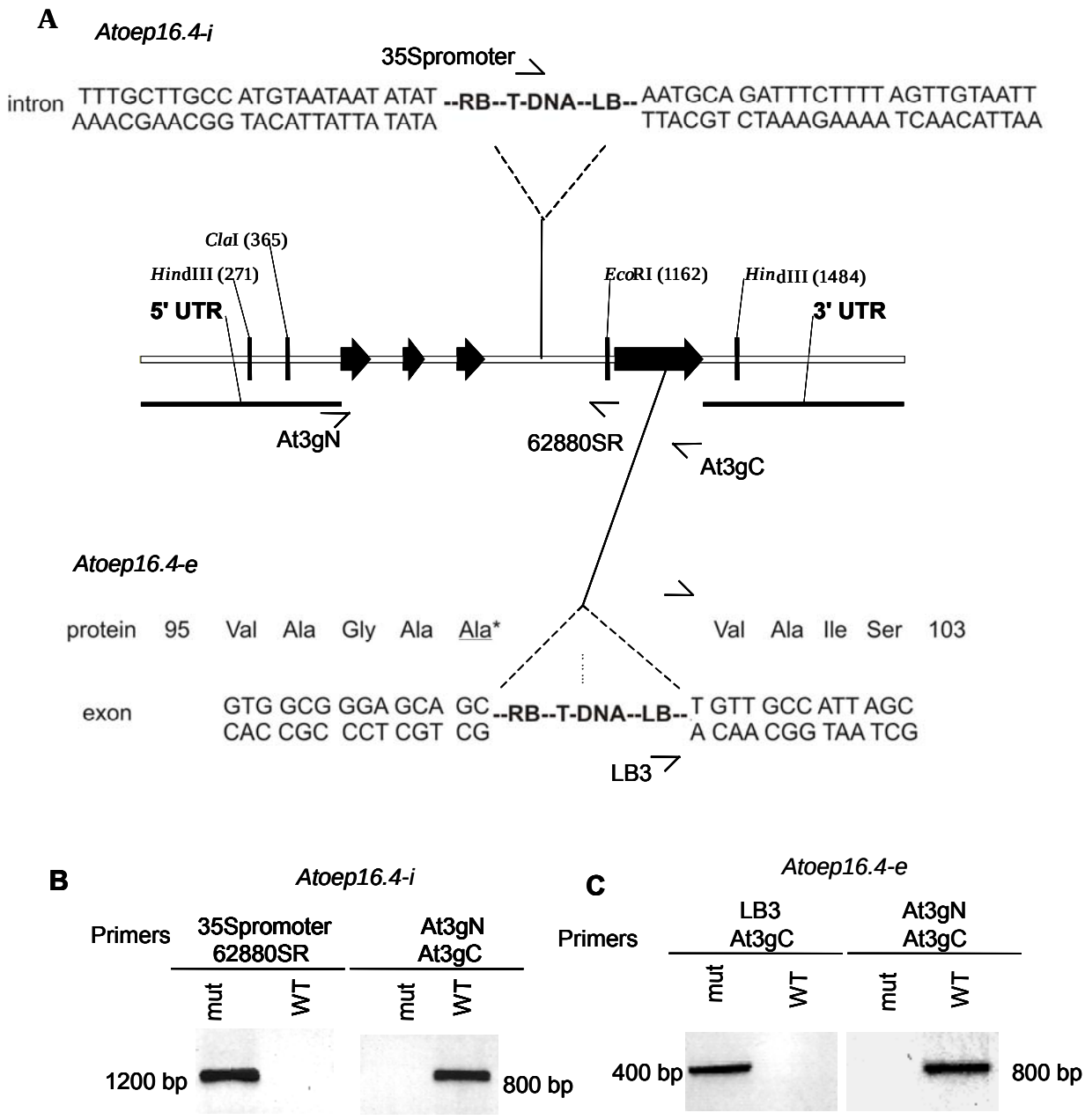

Fig. 3.19 Screening of the *Atoep16.4-i* and *Atoep16.4-e* T-DNA mutants.

A. Schematic diagram of the T-DNA insert localization in the third intron of *AtOEP16.4* locus in the *Atoep16.4-I* mutant and in the last exon of *AtOEP16.4* locus in the *Atoep16.4-e* mutant. For T-DNA the orientation of left (LB) and right (RB) borders are shown. Exons are shown as black arrows. Positions of primers for PCR are depicted. **B.** PCR analysis of the individual homozygous lane of the *Atoep16.4-i* knockout mutant and wild-type (Col-0) using (i) T-DNA specific '35Spromoter' and gene-specific 62880SR and (ii) two gene specific At3gN and At3gC primers. Mut, mutant; WT, wild-type. **C.** PCR analysis of the individual homozygous lane of the *Atoep16.4-e* knockout mutant and wild-type (Col-0) using (i) T-DNA specific LB3 and gene-specific At3gC and (ii) two gene specific At3gN and At3gC primers. Mut, mutant; WT, wild-type.

To test the effect of T-DNA insertion in AtOEP16.4 locus on mRNA level in *Atoep16.4-i* and *Atoep16.4-e* knockouts, one-step RT-PCR analysis was performed. Total RNA was extracted from leaves of 4-week-old mutant and wild-type plants. As shown in Fig. 3.20 A and B, leaves of *Atoep16.4-i* and *Atoep16.4-e* do not possess the *AtOEP16.4* bands in contrast to wild-type, suggesting absence of *AtOEP16.4* mRNA in these mutants.

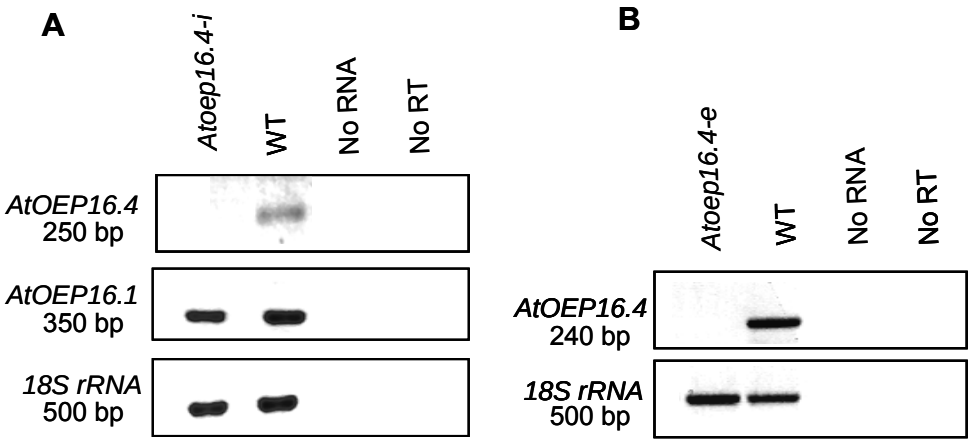

Fig. 3.20 RT-PCR analysis of the *Atoep16.4-i* and *Atoep16.4-e* T-DNA mutants.

A. 100 ng of total RNA from leaves from *Atoep16.4-i* and wild-type (WT) *Arabidopsis* plants was used for one-step RT-PCR with primers 62880lcf and 62880lcr for *AtOEP16.4*, and 18SF and 18SR for *18S rRNA* gene, which was used as a house-keeping control in this assay. As negative control for the assay, No RNA and No RT controls were used. **B**. 100 ng of total RNA from leaves from *Atoep16.4-e* and wild-type (WT) *Arabidopsis* plants were used for one-step RT-PCR with primers 62880SF and 62880R for *AtOEP16.4*, and 18SF and 18SR for *18S rRNA* gene, which was used as a house-keeping control in this assay. As negative control for the assay, No RNA and No RT controls were used.

To check whether the disruption of *AtOEP16.4* gene expression affects the mRNA level of the *AtOEP16.1* gene, the closest relative to *AtOEP16.4*, RT-PCR analysis of *AtOEP16.1* in the homozygous *Atoep16.4-i* line and wild-type plants was additionally performed. As shown in Fig. 3.20 A, intensity of the bands, corresponding to the *AtOEP16.1* mRNA, was not changed in the knockout mutant in comparison to the wild-type.

The RT-PCR of the *18S rRNA* gene was used as a house-keeping control in RT-PCR assays.

The phenotype of the homozygous *Atoep16.4-i* and *Atoep16.4-e* knockout mutants was inspected and compared with wild-type under standard growth conditions. No detectable difference was observed at any growth stage, including seed germination, plant morphology and growth, flowering time, fertility, silique development, and seed dormancy (data not shown).

E) Double knockout mutants

While the T-DNA knockout mutants on single *AtOEP16* genes have not exhibited any phenotype, several double knockout mutants were constructed. For this purpose two homozygous single mutants were crossed by applying pollen of one plant to the stigma surface of another. The following double mutants were produced: *Atoep16.4-i x Atoep16.1-e, Atoep16.4-e x Atoep16.1-p, Atoep16.4-i x Atoep16.2* and *Atoep16.4-e x Atoep16.2*. The presence of the T-DNA in both locuses in the F1 progeny was confirmed by PCR analysis. Plants of the F2 progeny were screened for homozygous and wild-type lines by PCR analysis. For the procedure and primers compare single mutants analysis 2.1.2.6 A), C) and D). Only the double *Atoep16.4-e x Atoep16.2* mutant had shorter siliques and less seeds per silique in contrast to wild-type plants. The double knockout mutants are under further detailed analysis.

3.1.2.4 Electrophysiological analysis of the recombinant AtOEP16.2 protein

To explore whether the AtOEP16.2 protein, sharing 50% similarity with the porin OEP16 from pea, forms a functional channel as well, electrophysiological studies on AtOEP16.2 were conducted. Therefore, AtOEP16.2 was overexpressed with a C-terminal 6-His-tag in *E. coli* cells, recovered from insoluble inclusion bodies, and purified to homogeneity by affinity chromatography (for details see 2.6). Electrophysiological measurements were carried out in lab of Prof. R. Wagner (Biophysik, Universität Osnabrück, FB Biologie/Chemie, Osnabrück). After fusion of AtOEP16.2 liposomes with planar bilayers, voltage-dependent single-channel currents were observed (Fig. 3.21 A). The AtOEP16.2 protein exhibited a conductivity with a reversal potential of V_{rev} = 43.7 ± 1.23 mV (V_{K^+} = 60 mV) (Fig. 3.21 B). This shows that the AtOEP16.2 is a channel with cation selectivity (P_{K+}/P_{Cl-} = 6.5). AtOEP16.2, similar to PsOEP16, was permeable to amino acids with the highest permeability to glutamate/glutamine and aspartate/asparagine (data not shown).

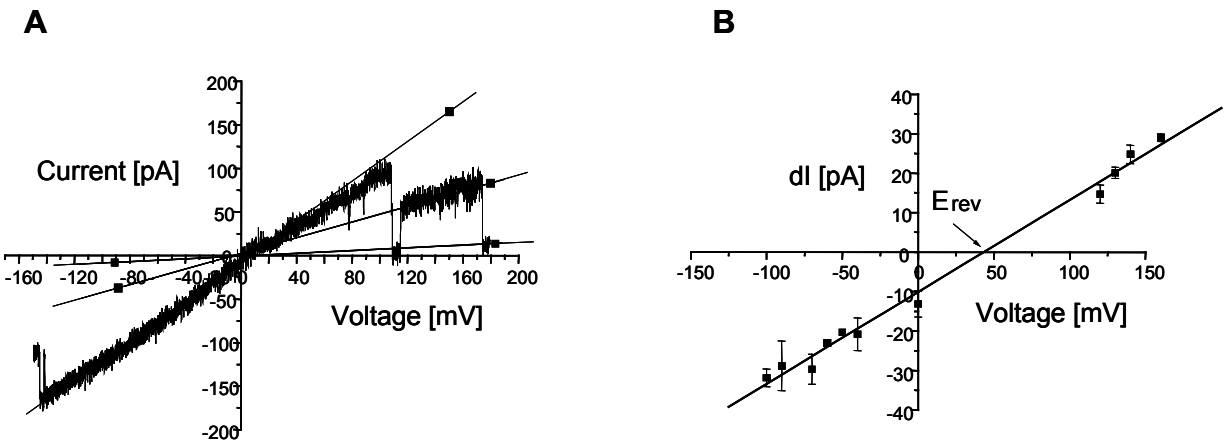

Fig. 3.21 Reconstituted AtOEP16.2 constitutes a voltage-sensitive, cation-selective pore.

A. Liposomes containing *E.coli*-overexpressed AtOEP16.2 were fused to black lipid membranes. The *cis* chamber contained 250 mM KCl and the *trans* chamber 20 mM KCl. A current from bilayer containing 3 active pores (3 solid lines) is shown. **B.** Current-voltage relationship from the data presented in A (n=3±SD). The electrophysiological experiments were carried out in lab of Prof. R. Wagner (Biophysik, Universität Osnabrück, FB Biologie/Chemie, Osnabrück).

3.2 OEP37 in *Pisum sativum* and in *Arabidopsis thaliana*

PsOEP37 (*Pisum sativum* outer envelope protein, 37 kDa) protein from pea chloroplast outer envelopes was described in Schleiff et al., 2003. The *PsOEP37* gene has an open reading frame of 990 bp encoding a protein comprising 329 amino acid residues with a predicted molecular mass of 37,5 kDa and a pI of 8.2.

3.2.1 Isolation of *OEP37* from *Arabidopsis*

A BLASTP search analysis in GenBank revealed only one orthologue of PsOEP37 in *Arabidopsis*. This protein is named AtOEP37, which is encoded by the *At2g43950* gene. The *AtOEP37* gene lies on chromosome 2 and has 6 exons and 5 introns. A schematic diagram of the gene organisation is given in Fig.3.22 A.

Total RNA from roots, leaves, flowers and siliques was isolated and analyzed by one-step RT-PCR with 20 ng of total RNA as a template. Fig. 3.22 B shows, that RT-PCR with primers specific for the *AtOEP37* gene gave a PCR product bands of 1200 bp in all tested organs with the highest level in leaves. This RT-PCR product was used for a full-length

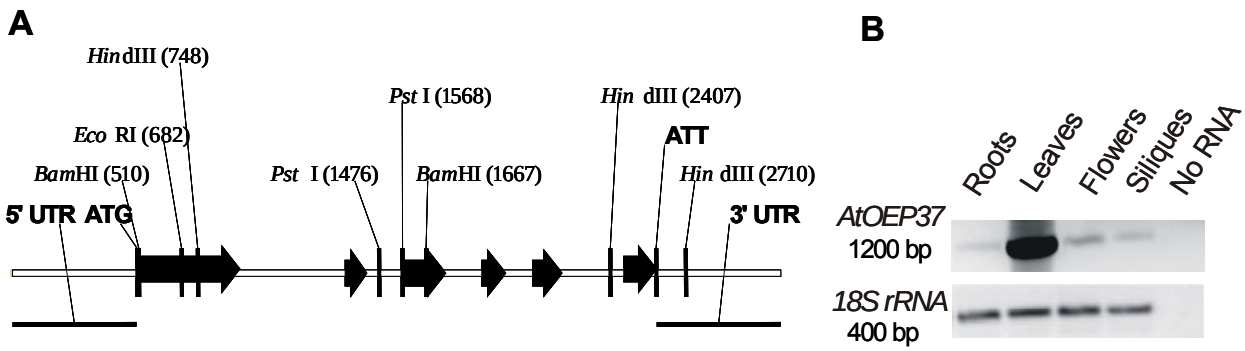

Fig. 3.22 *OEP37* in *Arabidopsis*.

A. Schematic diagram of the *AtOEP37* gene structure. The initiator ATG and terminator ATT codons, as well as 5' and 3' untranslated regions (5' UTR and 3' UTR, respectively) and several sites for restriction enzymes are illustrated. Exons are shown as black arrows, introns in grey lines. **B.** One-step RT-PCR analysis of AtOEP37 in different tissues of *Arabidopsis*. 20 ng of total RNA was used for reaction with the o37aXhoIr and o37araXbaIs primers for *AtOEP37*, and 18SF and 18SR for the house-keeping control, *18S rRNA*. As negative control for this assay, No RNA control was used.

cDNA cloning. The cDNA has a 1032 bp open reading frame for a protein of 343 amino acid residues with a deduced molecular mass of 38,8 kDa and a pI of 9,16. The protein sequence alignment showed that the PsOEP37 and the AtOEP37 proteins share 60% identity and 75% similarity over their entire sequence length (Fig. 3.23).

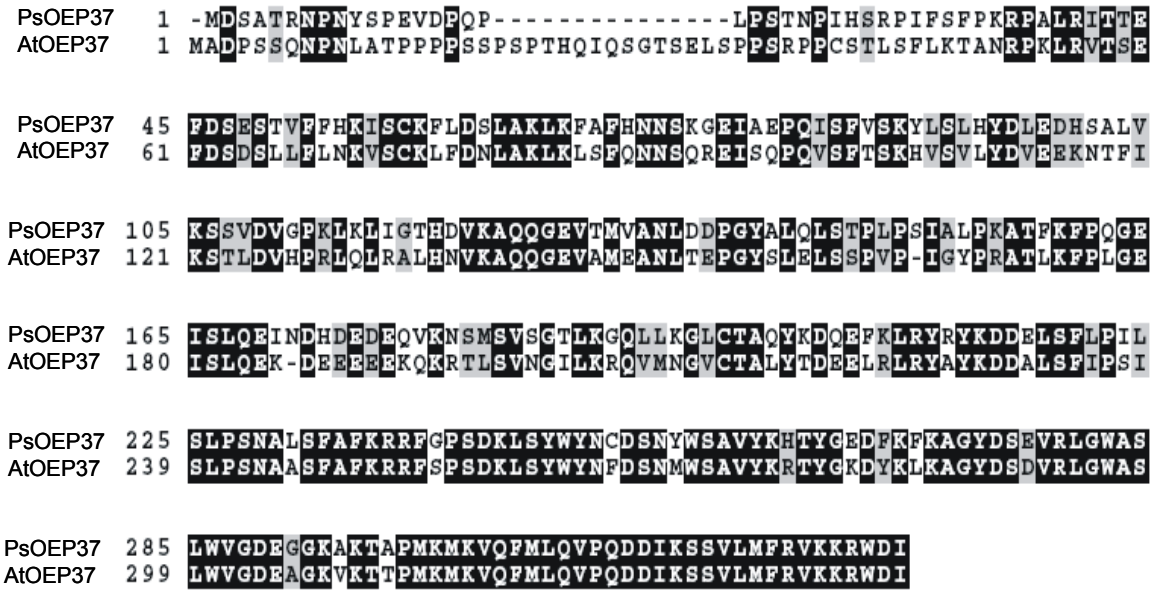

Fig. 3.23 Protein sequence alignment of PsOEP37 and AtOEP37

Identical amino acids are shown in black background, similar amino acids are indicated in gray background.

Modelling of the channel topology (Schleiff et al., 2003) revealed that the AtOEP37 and PsOEP37 proteins are transmembrane proteins composed of 12 β-sheets, which form a β-barrel within the membrane (Fig. 3.24). The proteins contain large soluble domains at both sides of the outer envelope membrane.

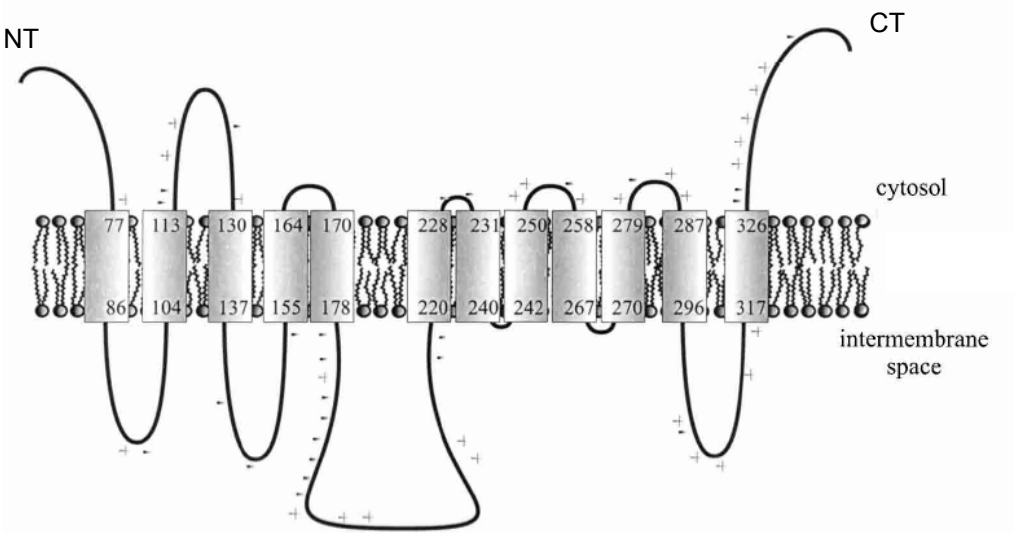

Fig. 3.24 The topological model of AtOEP37 (Schleiff et al., 2003).

The AtOEP37 protein represents a β-barrel channel-forming protein, and the proposed topology is shown. A black line presents the amino acid sequences connecting the transmembrane β-sheets (gray boxes). Cytosol and intermembrane space and N (NT) and C terminal (CT) of protein are indicated.

3.2.2 Subcellular and suborganellar localization of the AtOEP37 and PsOEP37 proteins

To identify the subcellular localization of the AtOEP37 protein, chloroplasts and mitochondria from 10-day-old *Arabidopsis* seedlings were isolated and immunodetection was performed. Fig. 3.25 shows that polyclonal antibodies against the AtOEP37 protein recognised a band of approximately 40 kDa in chloroplasts. For control of chloroplasts and mitochondria purity, immunodetection of VDAC, OEP21, and mSSU with corresponding antisera was performed.

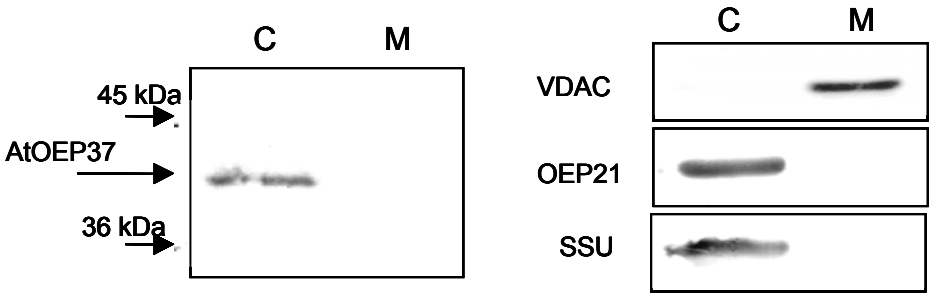

Fig. 3.25 Subcellular localization of AtOEP37.

Chloroplasts (C) or mitochondria (M) (60 µg protein) were loaded on a 12% polyacrylamide gel. Proteins were blotted on a nitrocellulose membrane, and immunodetection was performed with antisera against the AtOEP37, VDAC, OEP21, and SSU proteins.

Schleiff et al. (2003) showed, that PsOEP37 is localized in chloroplasts in pea. For investigation of the localization of PsOEP37 within chloroplasts, isolated pea chloroplasts were fractionated into outer, inner envelope membranes, thylakoids and stroma, followed by immunoblotting. Immunoblotting with the polyclonal antiserum, raised against the PsOEP37 protein, demonstrated the presence of approximately 37 kDa band in the outer envelope membrane fraction, suggesting that the PsOEP37 protein is localized to the outer envelope of chloroplasts (Fig. 3.26). No cross-reacting proteins were detected in the inner envelope membrane, thyladoids or stroma of chloroplasts.

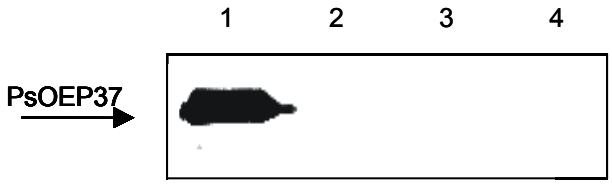

Fig. 3.26 Immunoblot analysis of the PsOEP37 protein in chloroplasts.

1, outer envelope; 2, inner envelope; 3, thylakodis; 4, stroma. 20 µg proteins were loaded on a 12% polyacrylamide gel. Proteins were blotted on a nitrocellulose membrane, and immunodetection was performed with antisera against PsOEP37.

To gain insight into the nature of the membrane association of PsOEP37, the outer envelope membrane vesicles were treated with 1 M NaCl, 4 M Urea or 0,1 M Na_2CO_3 (pH 11). The insoluble membrane and soluble fractions were assayed for the presence of PsOEP37 using the anti-PsOEP37 antibody. As shown in Fig. 3.27, the PsOEP37 protein remained in the

membrane fraction but not in the soluble fraction. Since these procedures are known to strip peripheral proteins from membranes, it is suggested that PsOEP37 is an integral membrane protein.

Fig. 3.27 Immunoblot analysis of chloroplastic outer envelope membrane vesicles. Outer envelope membrane vesicles (20 μg protein) were untreated (oe) or treated with NaCl, Urea or Na_2CO_3 and then separated into the membrane (M) and soluble (S) fractions. After blotting reacted with a polyclonal rabbit antiserum against the recombinant PsOEP37 protein.

3.2.3 OEP37 expression analysis

3.2.3.1 *AtOEP37* mRNA distribution within the *Arabidopsis* plant

To investigate the distribution of AtOEP37 within the *Arabidopsis* plant, monitoring of the *AtOEP37* mRNA content in various organs was done using several approaches. First, mRNA from leaves and roots of 4-week-old plants was extracted and Affymetrix genome array analysis was performed (Dr. Rowena Thomson, Dept. Biologie, LMU, München, DFG SPP-1108 project). As shown in Fig. 3.28, the *AtOEP37* transcript levels in Arabidopsis were low in the tested organs. The leaves possessed 153 ± 16 of the *AtOEP37* transcript, whereas the roots contained 91 ± 9 of mRNA (n=3).

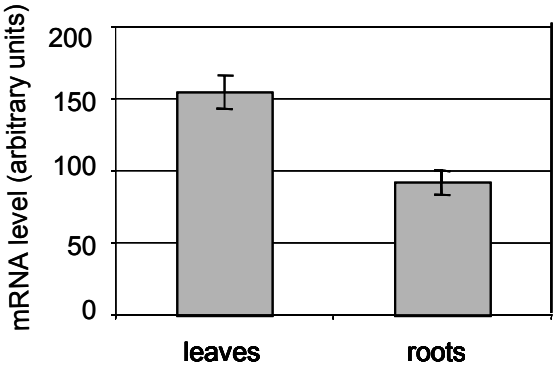

Fig. 3.28 Affymetrix *Arabidopsis* genome array analysis of *AtOEP37* mRNA levels in leaves and roots of 4 weeks old *Arabidopsis* plants. mRNA levels are depicted in arbitrary units. Error bars denote standard deviation SD of n=3 biological replicas (Dr. Rowena Thomson, Dept. Biologie, LMU, München, DFG SPP-1108 project).

3.2.3.2 The *AtOEP37* gene expression in leaves depending on plant age

To check the *AtOEP37* mRNA levels in leaves in dependence of plant age, total RNA from leaves of 1 to 7-week-old *Arabidopsis* plants (1 week step) was used for one-step RT-PCR analysis. As shown in Fig. 3.29, RT-PCR with the *AtOEP37* specific primers gave the PCR product bands of 550 bp in leaves of 1-7 week-old *Arabidopsis* in equal intensity. RT-PCR of *Actin 2/7* was used as a house-keeping control in this assay. The RNA levels did not change significantly within the first to seven weeks of development.

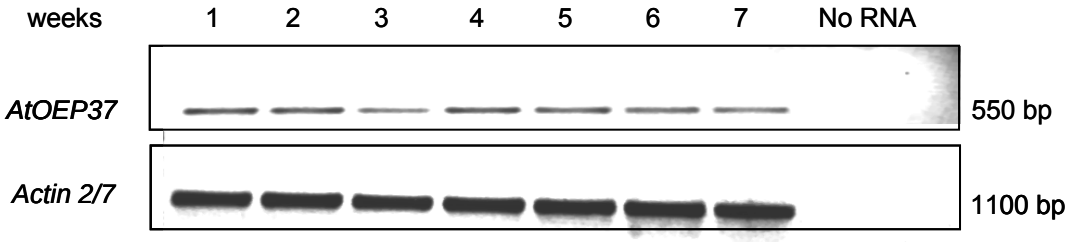

Fig. 3.29 One-step RT-PCR analysis of 1-7-week-old *Arabidopsis* plants.

50 ng total RNA was used for RT-PCR. Primers for *AtOEP37* were 037araSR and o37araXbaIs; for *Actin 2/7* were Actin2/7F and Actin2/7R. As negative control for this assay, No RNA control was used.

3.2.3.3 *AtOEP37* promoter::GUS analysis

The expression pattern of *AtOEP37* with respect to specific tissues and developmental stages was examined by fusing 1.5 kb of the *AtOEP37* upstream promoter region with GUS and transformation in *Arabidopsis* plants as described in Methods (see 2.4.3 and 2.8). Two positive independent plants of T1 and T2 progeny were analysed for GUS activity by staining various organs of the plants (Fig. 3.30).

In the seeds, which were imbibed before germination, GUS staining was observed in the hilum, attaching seed to placenta in the siliques (Fig. 3.30 A). No blue staining was detected in embryos (Fig. 3.30 B). In 3- and 7-day-old seedlings, GUS staining was detected in cotyledons, roots, including meristematic, vascular, cortical cell types the transition zone (Fig. 3.30 G- I) and epidermally derived hair roots (Fig. 3.30 C-F). No staining was observed in the root cap (Fig. 3.30 G). In the etiolated 7 day-old seedlings, GUS staining was observed only in cotyledons (Fig. 3.30 J). In 2 to 3-week old juvenile plants, weak level of staining was observed only in aerial portions: in cotyledons, rosette leaf primordium in the subepidermal and cortical cells (shoot apex), and expanded rosette leaves (Fig. 3.30 K-M). No GUS

expression in roots was detected with that method in contrast to more sensitive RT-PCR and Affymetrix analyses. In inflorescence, blue staining was observed in flower stalks and petals (Fig. 3.30 N and O, respectively).

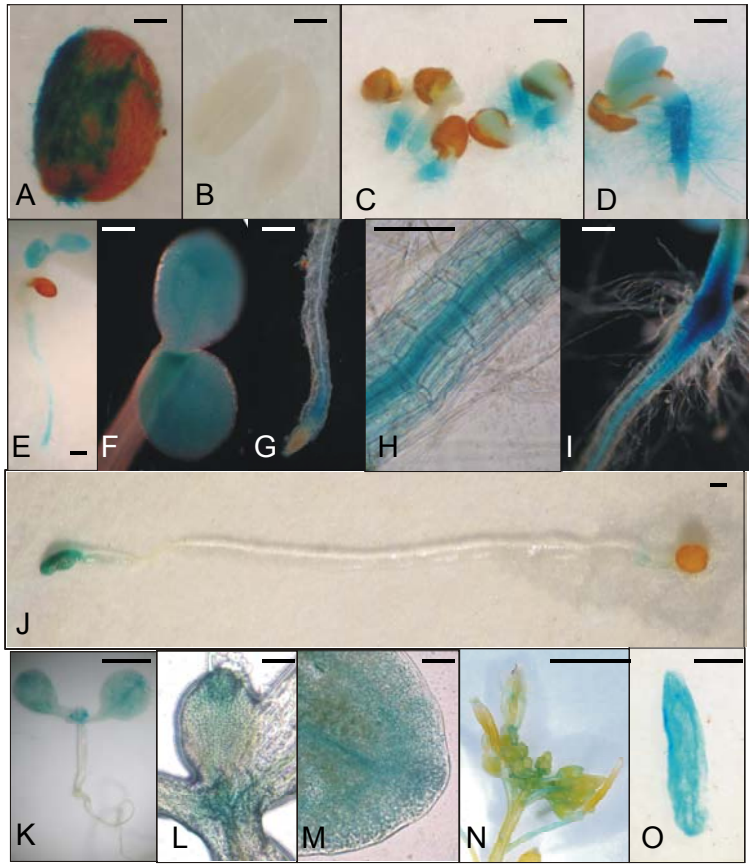

Fig. 3.30 GUS staining of the various organs/tissues of the *Arabidopsis* plants expressing *AtOEP37::GUS* construct.

A, seed imbibed at 4°C for 3 days. B, embryo prepared from seeds in A. C, D, 3-day old seedlings. E-I, 7-day-old light-grown seedlings: E, seedling; F, cotyledons of E; G, root with root cap; H, middle portion of root; I, transition zone of root. J, 7-day-old etiolated seedling. K-O 2- to 6-week-old *Arabidopsis*. K, seedling; L, shoot apex; M, portion of rosette leaf; N, inflorescence; O, petal. Scale bars for A, B, L, M = 0,1 mm, for C-J = 0,5 mm, for K, N = 0,5 cm, for O = 1 mm.

3.2.3.4 Tissue-specific expression of the PsOEP37 protein

To investigate the distribution of the PsOEP37 protein in *Pisum sativum* plants, membrane fractions of proteins were isolated from roots, rosette and cauline leaves, flowers, siliques and seeds of pea. Western blot analysis was performed with these protein fractions.

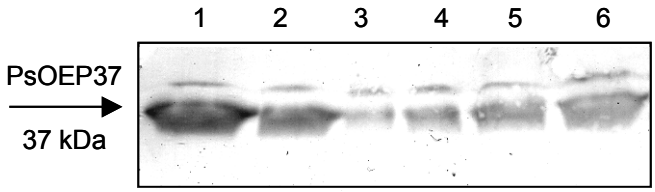

Fig. 3.31 Immunoblotting of PsOEP37 localization in *Pisum sativum* plants.

60 μg of membrane fraction proteins isolated from roots (1), rosette (2) and cauline (3) leaves, flowers (4), siliques (5) and seeds (6) were loaded on a 12% polyacrylamide gel and blotted against the anti-PsOEP37 antibodies.

Immunoblotting with the polyclonal antiserum against the PsOEP37 protein demonstrated the presence of a 37 kDa protein in all tested organs, with the highest level in roots, rosette leaves, siliques and seeds (Fig.3.31). The lowest levels of PsOEP37 were detected in cauline leaves and flowers.

3.2.4 Isolation and characterization of an *AtOEP37* knockout mutant

A search in the GABI T-DNA insertion library revealed one candidate line GABI 722C01 (GABI-Kat, Rosso et al., 2003) for a knockout mutant in the *AtOEP37* locus (Col-0 background). Amplification of the T-DNA flanking genomic fragment with the left border T-DNA specific and the *AtOEP37* gene-specific primers gave a 1000 bp PCR product, which was sequenced. Sequencing showed that the T-DNA insert is localized in the end of exon 2, interrupting the ORF at the last amino acid of exon 2. A schematic diagram of T-DNA element localisation and orientation in the *AtOEP37* gene is shown in Fig. 3.32.

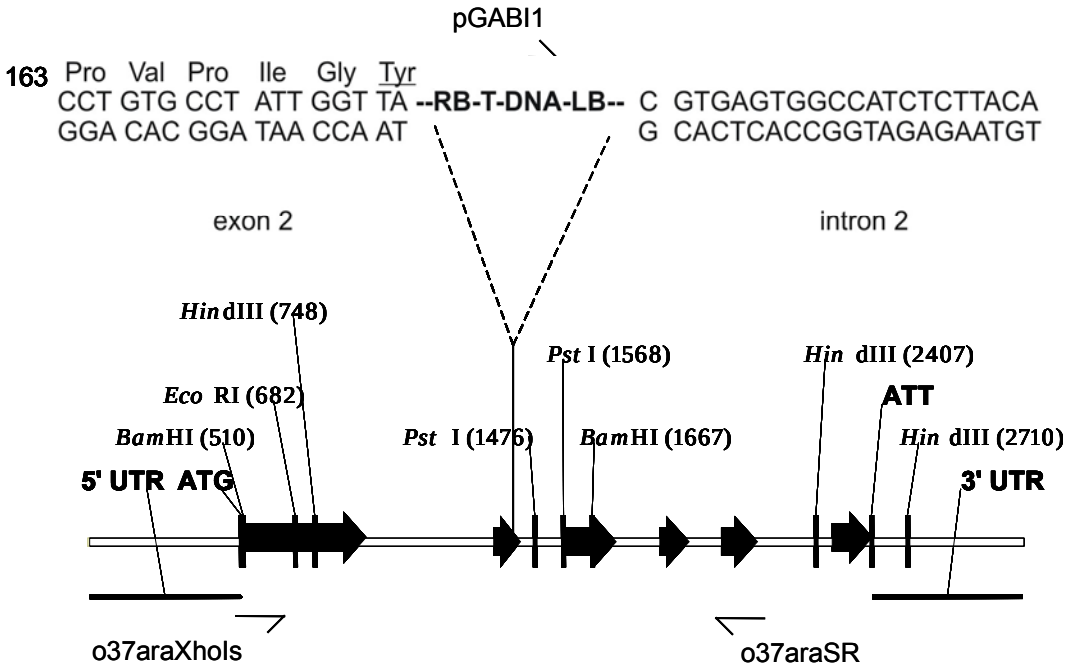

Fig. 3.32 The *Atoep37* T-DNA insertion knockout mutant.

Schematic diagram of T-DNA insert localization in the *AtOEP37* locus. T-DNA disrupts ORF after Tyr*168. For T-DNA element, the orientation of left (LB) and right (RB) borders is shown. Primer annealing positions are depicted.

A homozygous *Atoep37* line was identified by PCR analysis with two sets of primers: (i) T-DNA specific and the *AtOEP37* gene-specific primers, and (ii) two *AtOEP37* gene-specific

primers (Fig. 3.33). The phenotype of the homozygous *Atoep37* knockout mutant was inspected and compared with wild-type under standard growth conditions. No detectable difference was observed.

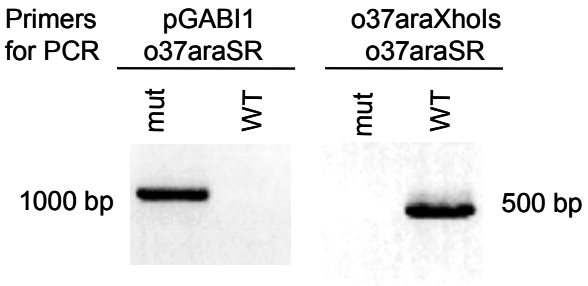

Fig. 3.33 PCR analysis of individual homozygous line *Atoep37* and wild-type (Col).

For PCR next primers were used: (i) T-DNA specific pGABI1 and gene-specific o37araSR, and (ii) two gene-specific o37araXhoIs and o37araSR. Mut, mutant; WT, wild-type.

3.2.5 Electrophysiological analysis of the recombinant PsOEP37 protein

Overexpression of the PsOEP37 protein was performed in *E. coli* BL21(DH3) cells after IPTG-induction of T7 promoter in the *PsOEP37/pET14b* plasmid (see 2.6). To check protein overexpression, the *E. coli* cells, harvested before and 3 hours after IPTG induction were lysed and proteins were separated on PAGE. Fig. 3.34 A shows that the IPTG-induced *E. coli* lysat contained a 37 kDa band corresponding to the overexpressed PsOEP37. The *E. coli* cells, harvested before IPTG induction, did not possess this band. The recombinant PsOEP37 protein was purified in form of inclusion bodies and Ni-affinity chromatography of the urea-

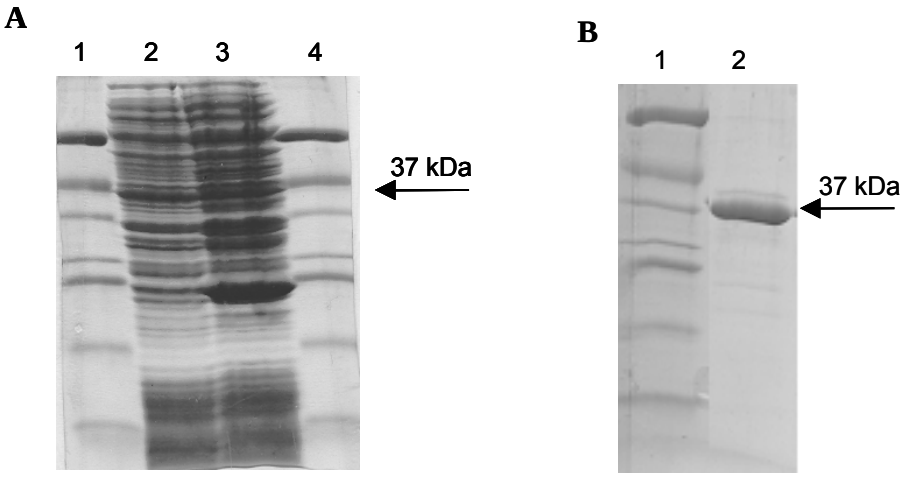

Fig. 3.34 PAGE analysis of overexpressed and purified of the PsOEP37 protein.

A. Overexpression of PsOEP37 in *E. coli* cells BL21(DH3). 1 and 4, protein marker; 2, *E. coli* lysat before induction; 3, *E. coli* lysat after IPTG induction. **B.** Purification of the recombinant PsOEP37 protein using affinity chromatography. 1, protein marker; 2, eluted recombinant PsOEP37 protein.

denaturated protein (see 2.6 and Fig. 3.34 B). To explore the PsOEP37 channel activity, electrophysiological studies were conducted on the purified recombinant protein. All electrophysiological measurements were curried out by Tom Götze in lab of Prof. R. Wagner (Biophysik, Universität Osnabrück, FB Biologie/Chemie, Osnabrück).

Recombinant AtOEP37 was solubilized in MEGA-9 and reconstituted into lipid vesicles. After fusion of AtOEP37 liposomes with planar bilayers, voltage-dependent single-channel currents were observed (Fig. 3.35 A). Multiple channel copies were detectable in the bilayer, which opened or closed in voltage-dependent manner. In asymmetric KCl solutions (250:20 mM KCl) the PsOEP37 protein exhibited conductivity with a reversal potential of V_{rev} = + 49 mV (V_{K^+} = 60 mV, Fig. 3.35 B). This shows that the PsOEP37 is a channel selective for monovalent cations (P_{K+}/P_{Cl-} = 14:1, Fig. 3.35 C). As obvious from Fig. 3.35 C, the PsOEP37

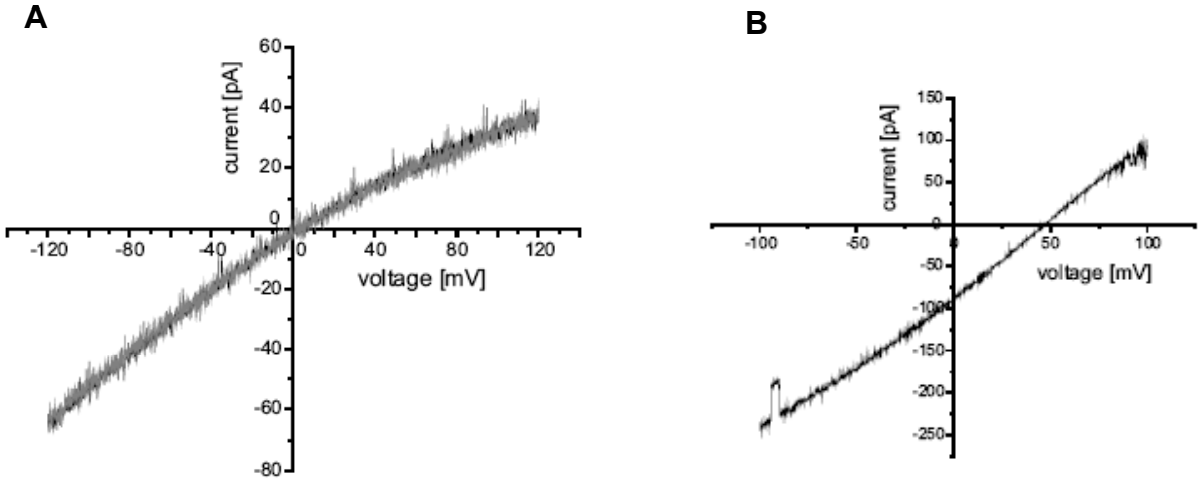

C

Electrolyte	Gradient [mM]	E_{rev} [mV]		P [+] : P [-]
KCl	250 : 20	+ 48.5	± 4.7	14 : 1
$CaCl_2$	125 : 10	- 1.9	± 7.6	0.9 : 1
$MgCl_2$	125 : 10	- 3.2	± 6.0	0.8 : 1

Fig. 3.35 Conductance properties of the PsOEP37 channel.

A. Current voltage relation of the PsOEP37 channel deduced from the fully open channel in 250 mM KCl, 10 mM Mops/Tris pH 7 (symmetrical cis/trans). **B**. Current recording in response to an applied voltage ramp from V_m=0 to + 100 mM and V_m=0 to – 100 mV from bilayers containing a single PsOEP37 channel. The bath solution contained 250/20 mM KCl, 10 mM Mops/Tris pH 7 (cis/trans). Zero current crossing at V_{rev} = 49 mV. **C.** Selectivity of the PsOEP37 channel. Zero current potentials V_{rev} were measured for the given ionic gradients and the permeability ratios were calculated according to the GHK constant field approach. Measurements and analysis were done in lab of Prof. R. Wagner (Biophysik, Universität Osnabrück, FB Biologie/Chemie, Osnabrück).

channel is permeable to monovalent cations but does not show any remarkable selectivity for divalent cations at all.

3.3 VDAC in *Pisum sativum* and *Arabidopsis thaliana*

3.3.1 Pea and *Arabidopsis* VDAC orthologous proteins

During a screen of a cDNA library derived from leaves of 5-day-old light-grown pea seedlings, a cDNA that encoded for a VDAC-like protein (voltage-dependent anion channel) was isolated (Clausen et al., 2004). Comparison of the deduced sequence with sequences in the database showed that it was identical to a cDNA (Gen Bank Acc. No. Z25540) isolated from a library prepared from the envelope of non-green plastids of pea root (Fischer et al. 1994). Pea root VDAC was thought to be present only in non-green plastids but absent in chloroplasts. However, the presence of a cDNA in a library that contained only mRNA from green tissue suggested that VDAC might also be present in chloroplasts. Therefore in this thesis subcellular localization and expression profile were analyzed in more details.

In *Arabidopsis*, five different VDAC isoforms are present, which are encoded by the genes At5g15090, At3g01280, At3g49920, At5g67500 and At5g57490. The alignment of the deduced amino acid sequences of pea and *Arabidopsis* VDACs indicated high levels of similarity, ranging from 85% to 50%, which are evenly distributed along the sequences (Fig.3.36 A, B).

The pea VDAC sequence together with five the *Arabidopsis* VDAC sequences were used to construct a phylogenetic tree. As shown in Fig. 3.36 C, the VDAC family splits in three different significantly separated branches of the tree. VDAC from pea, At5g15090 and At3g01280 fall in one group whereas two other *Arabidopsis* VDAC orthologs, At3g49920 and At5g67500 fall in a second subgroup. The At5g57490 VDAC isoform forms the third subgroup.

A

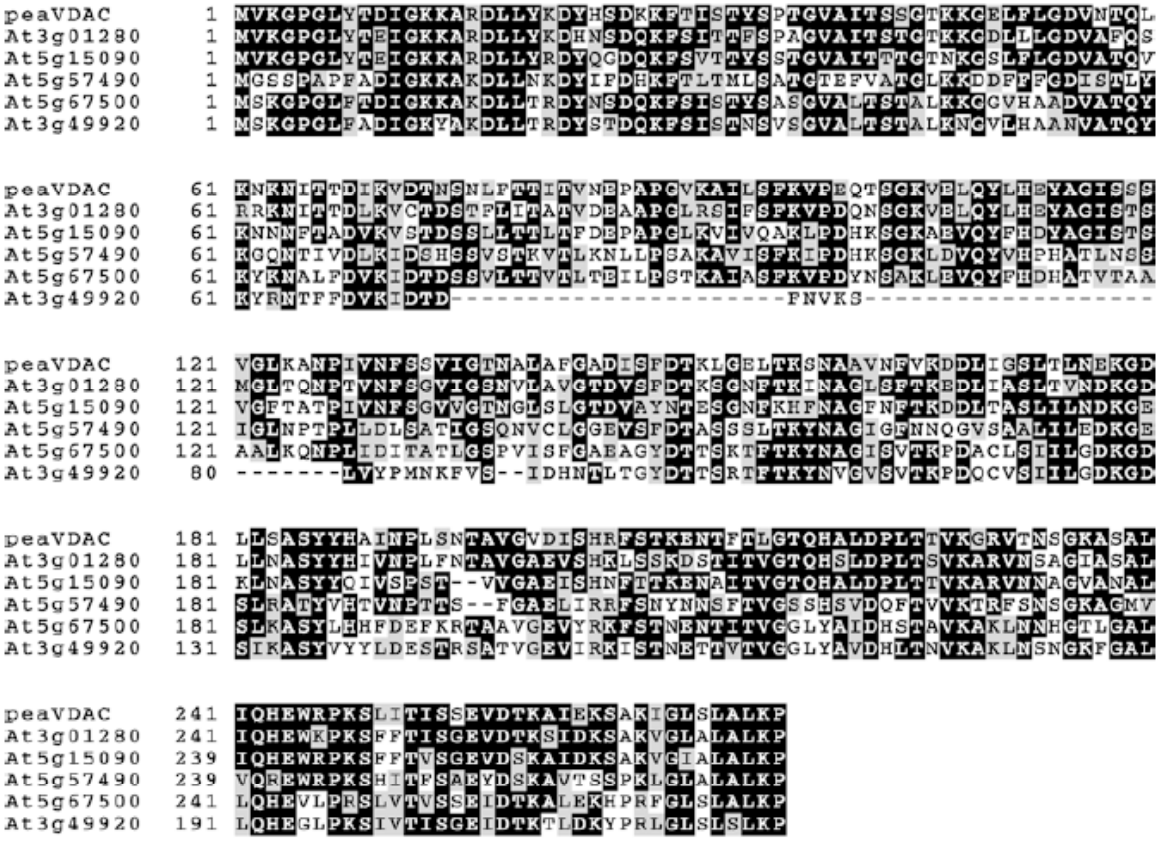

B

	Identity (%)	Similarity (%)
At3g01280	69%	85%
At5g15090	64%	80%
At5g67500	49%	69%
At5g57490	44%	66%
At3g49920	31%	50%

C

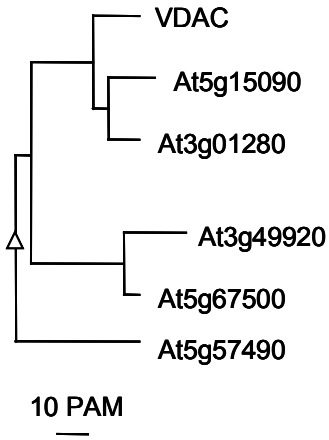

Fig. 3.36 VDAC orthologs in pea and *Arabidopsis*.

A. Amino acid alignment of VDAC from *Pisum sativum* with VDAC isoforms from *Arabidopsis*. Identical amino acids are boxed in black; similar exchanges are shaded in grey. **B**. Identity and similarity of the *Arabidopsis* VDAC proteins with pea VDAC. **C**. Phylogenetic tree of VDAC from *Pisum sativum* (VDAC) and five VDAC isoforms from *Arabidopsis* (Atg numbers from TAIR database are given). Tree was constructed using Multalin 5.4.1 program (blosum62, F.Corpet, 1988).

3.3.2 Subcellular localization of the VDAC protein

As described earlier, VDAC isoform might also be present in non-green plastids (Fischer et al. 1994). In order to test this, a construct with a C-terminal fusion of GFP to the open reading frame of the pea VDAC gene was generated. For transient expression, the GFP-fusion protein was bombarded in pea roots. The GFP-signal was monitored by fluorescence microscopy. Pea root cells were transformed either with a single plasmid expressing VDAC–GFP or were co-transformed with two different plasmids, one expressing VDAC–GFP and a positive control of the chloroplast-targeted ps-ds-Red (Jach et al. 2001). As shown in Fig. 3.37 A, the VDAC–GFP fusion protein localized only to mitochondria, which were visualized by staining with Mitotracker. In contrast to this the ps-ds-Red fusion protein was targeted into a compartment that is clearly distinct from mitochondria, i.e. no overlap between VDAC–GFP and ps-ds-Red fluorescence occurred (Fig. 3.37 B). The ps-ds-Red-labeled compartments are most likely non-green plastids.

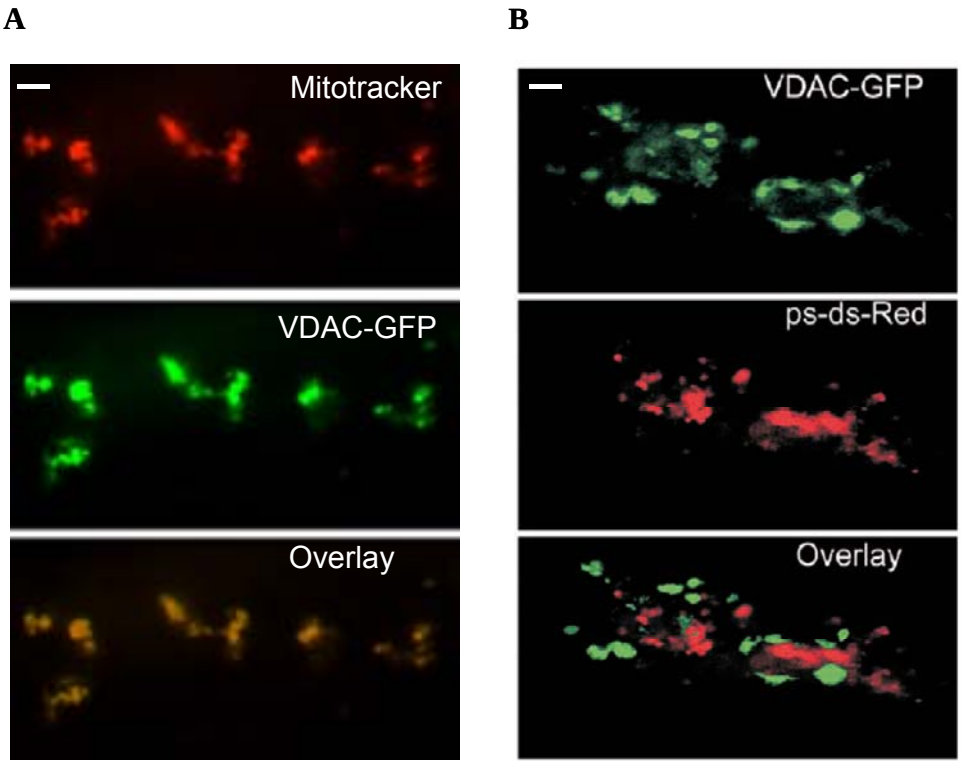

Fig. 3.37 Subcellular localization of VDAC–GFP and ps-ds-Red in pea root cells.

Segments of 5-day-old pea roots were bombarded either with VDAC–GFP alone (**A**) or co-bombarded simultaneously with ps-ds-Red (**B**). Localization of mitochondria was visualized by staining with Mitotracker. Scale bar = 10 µm.

Since the VDAC orthologs from pea and *Arabidopsis* share a high homology in protein sequence, antibodies raised against pea VDAC were used in immunoblot analysis with *Arabidopsis* samples, fractionated to chloroplasts and mitochondria. In attempt to find a VDAC isoform, which is located in chloroplasts of *Arabidopsis*.

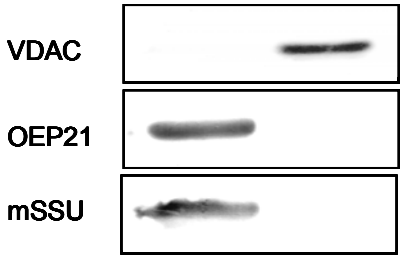

Fig. 3.38 Localization of VDAC in *Arabidopsis*.

100 μg total protein from chloroplasts (line C) and mitochondria (line M) purified from leaves of 6-week-old *Arabidopsis* plants were separated on 12.5% SDS-Gel followed by immunoblotting.

As shown in Fig. 3.38, in *Arabidopsis* mitochondria a single band of apparent molecular weight of 29 kDa was identified, suggesting that, are located to mitochondria, but not to the chloroplasts. At3g49920 is predicted to have a lower molecular weight than other four AtVDACs and one could expect additional band on immunoblot in mitochondria or chloroplasts fraction. The absence of this band is probably due to the very low levels of At3g49920 protein or due to the wrong prediction of the ORF.

3.3.3 The VDACs mRNA levels in leaves and roots in *Arabidopsis*

The distribution of the VDAC mRNA between green (leaf) and non-green (root) tissues in Arabidopsis was investigated using two approaches. First, to examine tested tissues for expression of the *Arabidopsis* VDAC genes, RT-PCR analysis was performed using cDNA from leaves and roots of 4-week-old plants.

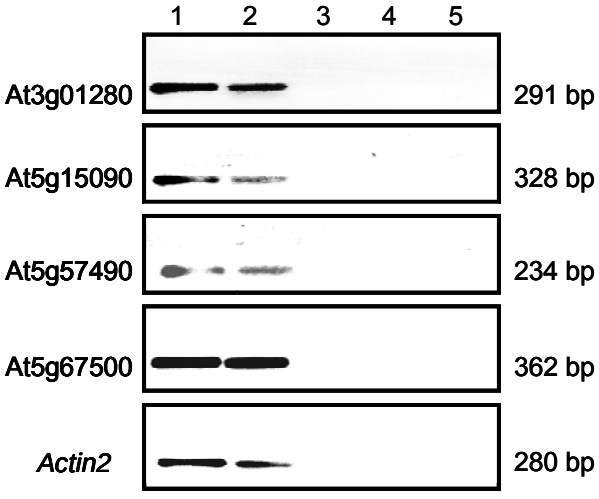

Fig. 3.39 RT-PCR analysis of the *Arabidopsis* VDAC genes in leaves and roots.

100 ng total RNA was used for RT-PCR. 1, leaves; 2, roots; 3, No RNA; 4, No RT leaves; 5, No RT roots. *Actin 2* was used as a house-keeping control. As negative control, No RNA and No RT controls were used. Next primers were used for RT-PCR: At3g01280 LCfw and At3g01280 Lcrev; At5g15090 LCfw and At5g15090 Lcrev; At5g57490 LCfw and At5g57490 Lcrev; At5g67500 LCfw and At5g67500 Lcrev. Band corresponding to At3g49920 was not detected.

As shown in Fig. 3.39, the RT-PCR resulted in the single PCR product bands for the VDAC genes both in leaves and roots, while one gene, At3g49920, was absent (not shown).

As a second approach, Affymetrix full genome microarray for leaves and roots was performed by Dr. Rowena Thomson (Department Biologie I, Botanik LMU, München) within DFG SPP-1108 project.

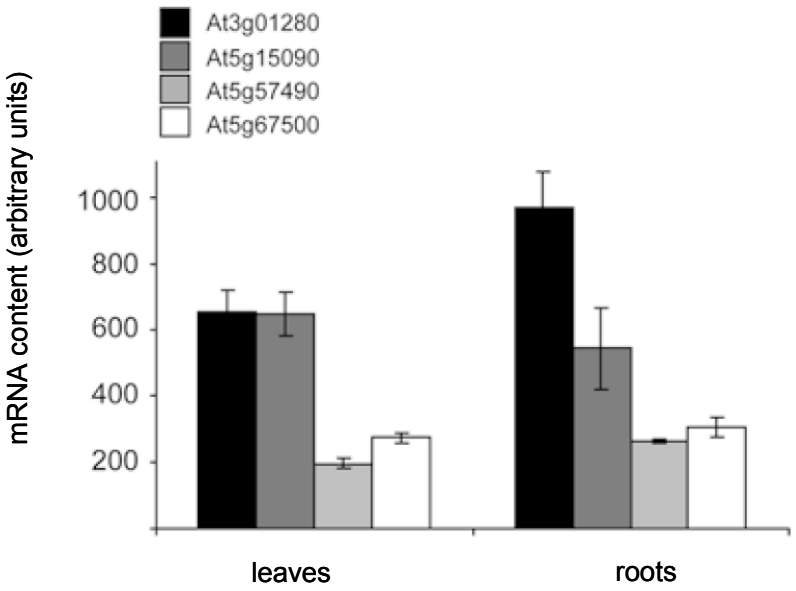

Fig. 3.40 Genome expression profiles for VDAC isoforms in roots and leaves. mRNA levels are depicted in arbitrary units. Error bars denote standard deviation SD of n=3 biological replicas (Dr. Thomson, Dept. Biologie, LMU, München, DFG SPP-1108 project)

The results in Fig. 3.40 show that four VDAC genes are expressed to different degrees in leaves and roots of *Arabidopsis*, while the At3g49920 gene was not present on the Affymetrix chip. In general, these results confirm the results of the RT-PCR analysis.

Results of subcellular localization and gene-expression experiments suggest that VDAC in pea and *Arabidopsis* are localized to mitochondria of leaves and roots.

4 Discussion

Chloroplasts and mitochondria are semiautonomous organelles that are involved in different metabolic pathways essential for the whole plant cell. Two membranes, outer and inner envelopes, which separate the chloroplasts stroma and mitochondria matrix from the cytoplasm, surround these organelles.

4.1 The OEP16 family in pea and *Arabidopsis thaliana*

Pea chloroplasts so far contain one identified channel isoform protein PsOEP16 located in the outer envelope membrane (Pohlmeyer et al., 1997), whereas *Arabidopsis* possesses four orthologs: AtOEP16.1, AtOEP16.2, AtOEP16.3 and AtOEP16.4. The *Arabidopsis* OEP16 isoforms share 79-46% homology in protein sequence with PsOEP16 and have a theoretical pI in the basic range suggesting chloroplast outer envelope or at least membrane location of all AtOEP16s. The domain structure and phylogenetic analyses revealed that the OEP16 proteins belong to the TIM17/TIM22/TIM23 family, which facilitates pre-protein translocation from the cytosol into mitochondria (Rassow et al., 1999), and form a new family of pre-protein and amino acid transporters, called PRAT. Although all AtOEP16 proteins of Arabidopsis are similar to mitochondrial TIMs, it could be shown that AtOEP16.1, AtOEP16.2 and AtOEP16.4 are located in chloroplasts and only AtOEP16.3 is in mitochondria (see below).

4.1.1 Structure and topology of the OEP16 proteins

All topology and structure analyses have been done on PsOEP16. Due to the high similarity, the same topology and structure are suggested for *Arabidopsis* orthologs. Based on site-directed mutagenesis and spectrometric analyses of recombinant PsOEP16 (Linke et al., 2004) the topology model for OEP16 with four α-helical domains was developed (see Fig. 3.2). The α-helical structure is known for several membrane proteins, *e.g.* for the mitochondrial TIM17/22/23 proteins and for LivH, an amino acid transporter of the *E. coli* (Milisav et al., 2001; Folsch et al., 1998; Meier et al., 2005; Nazos et al., 1986). The transmembrane α-helices of the OEP16 proteins are encoded by a 16-22 stretch of predominantly hydrophobic residues.

The transmembrane α-helix I of the OEP16 orthologs is responsible for substrate specifity and, together with helix II, for pore formation (Pohlmeyer et al., 1997; Steinkamp et al.,

2000). It is amphiphilic due to its partial exposure to the water-filled pore, containing two charged residues in the middle of the membrane.

Pohlmeyer et al. (1997) showed that the N-terminal part of PsOEP16 is exposed to the cytoplasm, therefore the hydrophilic loop domain connecting the transmembrane domains I and II is faced to the chloroplast interior or packed in the water-filled pore formed by the transmembrane regions. Similarly to PsOEP16, the AtOEP16s channels contain this soluble loop domain I with 28 amino acid residues in PsOEP16, AtOEP16.1 and AtOEP16.4, 29 amino acid residues in AtOEP16.3 and 36 amino acid residues in AtOEP16.2. This loop region contains a high proportion of small polar residues like Ala, Ser, Gly and Thr and charged amino acid residues like Lys, Arg, Asp and Glu. The soluble loop domain I has no strong sequence similarity among the AtOEP16s and may form part of the selectivity filter or facilitate the gating of the OEP16 proteins. Such long soluble loop domain is common for the porin proteins from Gram-negative bacteria (Conlan et. al., 2000).

In the position just before the start of the first α-helix spanning the membrane, all OEP16s share a conservative proline residue, which has a very rigid cyclic ring and therefore, presence of proline in protein sequence allows the disruption of the a-helical turn and the creation of a fixed kink in the beginning of the first transmembrane domain.

The AtOEP16.1 protein contains a cysteine residue at position 71, in the beginning of the second transmembrane domain. This cysteine residue, having a reactive sulfhydryl group could be responsible for forming a disulfide bridge, which might trigger the correct folding of the AtOEP16.1 channel in a dimeric form in the membrane. At the same position of the PsOEP16 there is also cysteine residue, which was shown to form homodimers in cross-link experiments (Pohlmeyer et al., 1997). In contrast, AtOEP16.2 and AtOEP16.3 do not possess any cysteine residues. Interestingly, AtOEP16.4 contains five cysteine residues, one in the first and fourth transmembrane region, one in the first soluble loop and two cysteines in the second transmembrane segment.

The PsOEP16 and AtOEP16.1 proteins possess histidine residues at different positions of their soluble loop I, whereas AtOEP16.2 has histidine residues in all the soluble parts of the protein sequence. The imidazole side chain of histidine has a pK_a of 6.8 at the pH of cytoplasm. Small shifts of cellular pH change the charge of histidine side chain. Histidine is frequently found in protein active sites and can play a role in binding to specific amino acids, such as proline or other amino acids possessing an aromatic ring (Macias et al., 2002). Ability of the histidine residues in the soluble loop I of the AtOEP16.2 protein as well as the longest

length (36 residues) of this loop in contrast to other AtOEP16s might determine the selectivity of AtOEP16.2 protein.

PsOEP16, AtOEP16.1 and AtOEP16.2 contain aspartate residue in transmembrane domain I and Lys and Glu residues in transmembrane region II. These amino acid residues might facilitate the selective transport of charged solutes, e.g. charged amino acids or other compounds with primary amino groups like it was shown for PsOEP16.

4.1.2 Subcellular localization of the AtOEP16.1-4 proteins

A combination of strategies is usually required for the determination of the subcellular localization of membrane proteins. *In silico* prediction analysis did not show any target organelle for the AtOEP16.1-4 proteins, since a classical N-terminal cleavable transit signal sequence defining a destiny organelle was not identified.

Transient expression of the AtOEP16.1-4 proteins fused to fluorescent reporter proteins in pea roots and *Arabidopsis* protoplasts as well as immunoblot analysis revealed that AtOEP16.1, AtOEP16.2 and AtOEP16.4 are located in plastids, whereas AtOEP16.3 was found in mitochondria.

Several mass spectrometry-based proteomic studies of *Arabidopsis* leaf chloroplasts and mitochondria have been done (Wijk et al., 2000; Millar et al., 2005; Bardel et al., 2002; Ferro et al., 2003; Froehlich et al., 2003) and localization of a lot of proteins was elucidated. Thus, AtOEP16.1 has been found in the outer membrane of plastids, whereas AtOEP16.3 was shown to be in mitochondria. The AtOEP16.2 and AtOEP16.4 proteins have not been detected, probably because of the specific (AtOEP16.2) or the low level of expression (AtOEP16.4) in leaf tissue (compare 4.1.4) and limitations of the above-mentioned proteomic studies. These results are in line with our findings.

In summary, these results point to localization of the AtOEP16.1, AtOEP16.2 and AtOEP16.4 proteins in plastids, while AtOEP16.3 is in mitochondria.

4.1.3 *AtOEP16.1-4* gene expression

To obtain evidence about the tissue-specific distribution of the members of the OEP16 family in *Arabidopsis*, several approaches were used, namely immunoblot analysis, RT-PCR analysis, Affymetrix microarray analysis and analysis of *Arabidopsis* plants transformed with promoter-GUS transcriptional fusions from each gene. The data derived from these approaches were complemented by a sequence-based analysis of the promoter regions in an

attempt to identify putative *cis*-elements that might account for the observed expression patterns.

A search in public Affymetrix microarray gene expression databases (the AtGene Express Project) showed that the transcript levels of the AtOEP16 orthologs are present in different tissues of *Arabidopsis* (Fig. 4.1). The *AtOEP16.1* mRNA is found in all tissues throughout plant development with the highest levels in leaves and flowers. Expression of the *AtOEP16.2* gene was observed only in stamens of flowers, seeds and siliques with seeds at the different developmental stages. The highest level of *AtOEP16.2* mRNA is present at the late stages of the seed development.

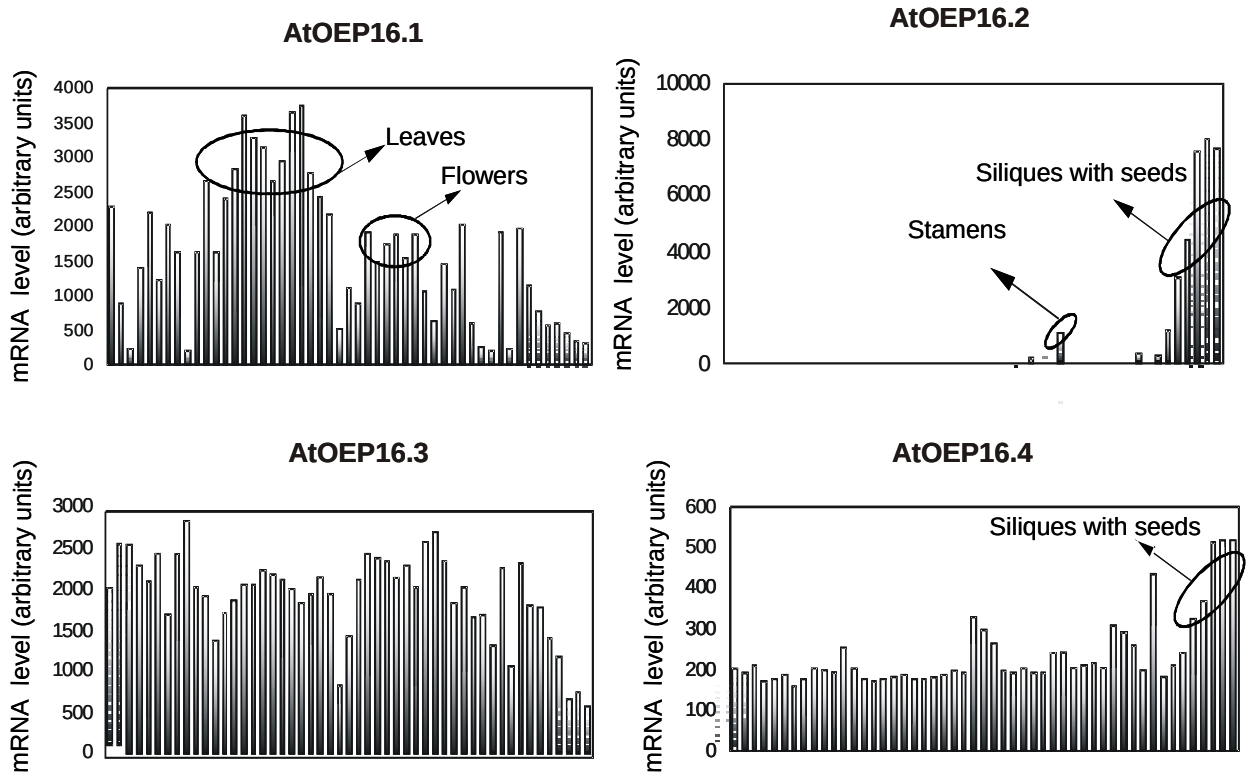

Fig. 4.1 Overview of transcription levels of AtOEP16 orthologues in *Arabidopsis* according to Affymetrix microarray results of AtGene Express Project.

The transcript content is given in arbitrary units (n=3). See table for x-axis legends and link to the web page of the data Affymetrix microarray results in Appendix.

The *AtOEP16.3* and *AtOEP16.4* transcripts were detected in all tested tissues. While *AtOEP16.1-3* are expressed at high levels, AtOEP16.4 is in general 10 fold lower. These *in silico* data are consistent with the experimental results obtained (compare 3.1.2.4).

Affymetrix microarray analysis data (NASC database: Honys) revealed that the *AtOEP16.2* is transcribed at high levels in pollen of all developmental stages: in the unicellulate

microspores, the bicellular and tricellular pollen (Fig. 4.2 A). In the mature pollen the levels of the *AtOEP16.2* gene transcript decreases. The data of the Affymetrix microarray analysis of the transcript levels in *Arabidopsis* seeds (NASC database: Bergua) showed that developed seeds, which were harvested from no-open yellow siliques, contain high levels of the *AtOEP16.2* transcript (Fig. 4.2 B). The mRNA level is decreasing 3-fold with seed maturation.

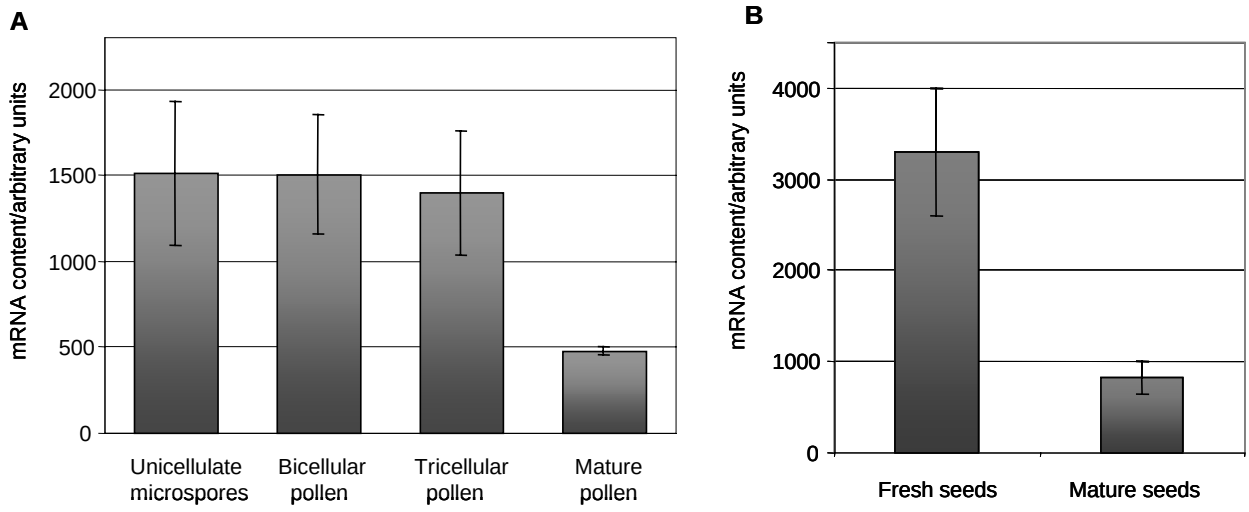

Fig. 4.2 Affymetrix microarray analysis of the *AtOEP16.2* transcript levels in *Arabidopsis*.
A, *AtOEP16.2* transcript levels in microspores and pollen (NASC database: Honys). **B**, *AtOEP16.2* transcript levels in fresh (from no-open yellow siliques) and mature (2 months after harvesting) seeds (NASC database: Bergua). The transcript content is given in arbitrary units (n=2±SD).

Considering that *Arabidopsis* expresses four OEP16 genes encoding proteins targeted to chloroplasts and mitochondria it seems likely that these orthologs carry out diverse physiological functions. If this is the case, one would expect to observe differences in the regulated expression of these proteins and their mRNAs in response to environmental stimuli. One such environmental stimulus tested is light, which influences expression of a multitude of plant genes, for example chloroplast genes, such as the small subunit of ribulose bisphosphate carboxylase *(rbcS)* (Pilgrim et al., 1993)**,** proteins of ELIP proteins (Grimm et al., 1987; Hutin et al., 2003), CAB, chlorophyll a/b binding protein (Beator and Kloppstech, 1993) and POR proteins (Su et al., 2001). Therefore, available online data of Affymetrix microarrays analysis of *Arabidopsis* throughout the diurnal cycle were checked.

As shown in Fig. 4.3, only the *AtOEP16.1* mRNA showed a diurnal oscillation. The leaf *AtOEP16.1* mRNA level was high in onset of dark, followed by the progressive transcript degradation during a 12-hours dark period and within the next two hours of the light-onset (13

and 14 hours time points on the plot). After following 2 hours of light, a re-accumulation of the *AtOEP16.1* transcript started and reached a maximum at the 12-hours of light-onset. In contrast to *AtOEP16.1*, transcripts encoding *AtOEP16.3* and *AtOEP16.4* did not change over the time-course of the experiment.

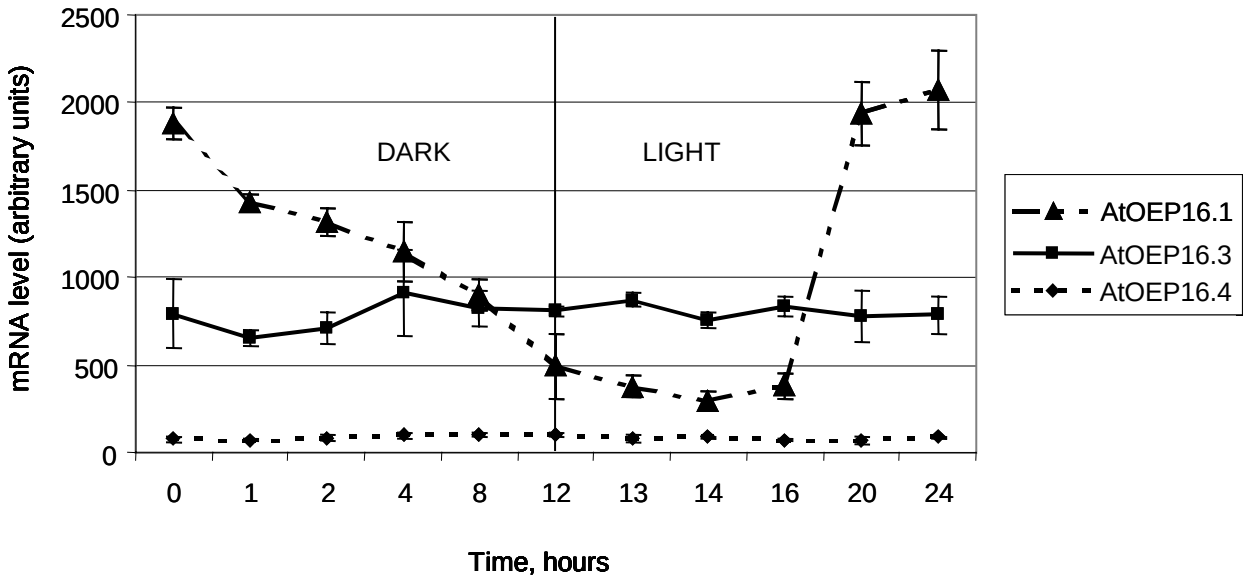

Fig. 4.3 Affymetrix microarray analysis of diurnal dependence of the *AtOEP16.1*, *AtOEP16.3* and *AtOEP16.4* transcript levels in leaves of *Arabidopsis.*

Leaves were harvested from *Arabidopsis* plants (Col-0) at growth stage 3.90 (Boyes et al., 2001) grown under a diurnal cycle of 12 hours dark - 12 hours light. Within this cycle, leaves were harvested at 0 (end of day), 1, 2, 4, 8, 12 (end of night), 13, 14, 16, 20 and 24 hours. The transcript content is given in arbitrary units (n=2±SD). The dark and light periods are indicated (NASC database: Smith).

Another environmental stimulus, which was tested, was a cold stress. Cold temperatures trigger the transcription of many cold-responsive genes, which encode a diverse array of proteins such as enzymes involved in respiration and metabolism of carbohydrates, lipids, phenylpropanoids and antioxidants; molecular chaperones, antifreeze proteins (Guy 1999; Liu 2002; Jang et al. 2004; Teige et al., 2004). Therefore, attempts to explore whether the transcription of the AtOEP16.1-4 genes is changed in answer to cold stress, corresponding Affymetrix microarray results were checked.

As shown in Fig. 4.4, the transcript levels of *AtOEP16.1* in shoots increased 2-fold after 3 hours and drastically after 6-24 hours of cold stress. Transcript levels of *AtOEP16.3* and *AtOEP16.4* were not changed. Interestingly, that mRNA levels of cold responsive protein

Cor15b (At2g42530, Chinnusamy et al., 2003) and cold acclimation protein FL3-5A3 (At2g15970, Seki et al., 2001) showed the same response patterns as well as *AtOEP16.1*.

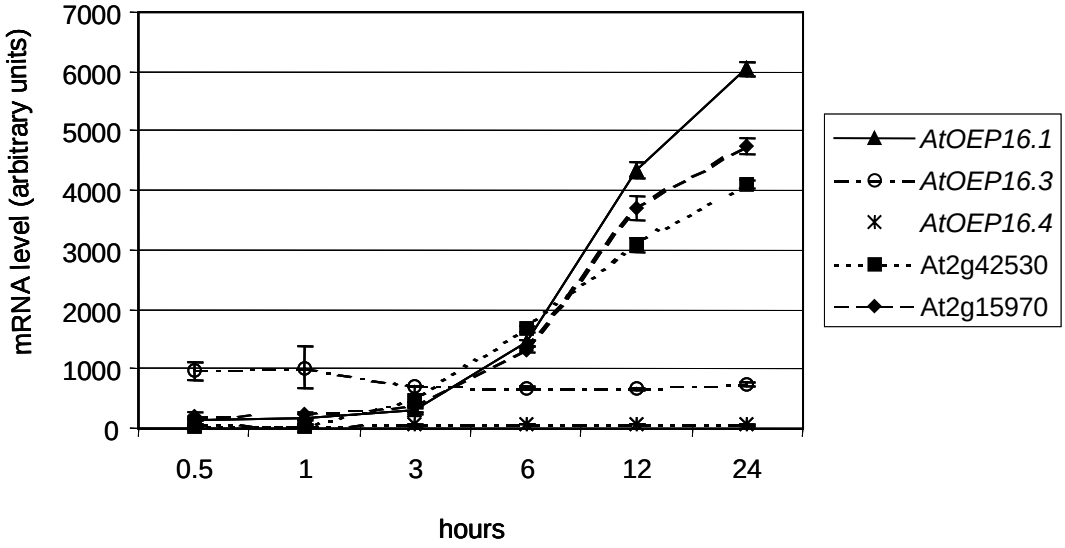

Fig. 4.4 Affymetrix microarray analysis of influence of cold stress (4°C) in *Arabidopsis.*
The mRNA levels of *AtOEP16.1*, *AtOEP16.3*, *AtOEP16.4*, At2g42530 and At2g15970 in shoots after 0.5, 1, 3, 6, 12 and 24 hours of cold stress. The transcript content is given in arbitrary units (n=2±SD). (NASC database: Nover).

A search for *cis*-acting elements using the NSITE-PL program revealed the presence of various binding sites in the *AtOEP16.1*, *AtOEP16.2* promoter regions, underlining the RT-PCR, Affymetrix microarray and promoter::GUS analysis results.

The sequence region of 1500 bp, chosen for promoter-GUS analysis of *AtOEP16.1,* possesses several putative regulatory elements (Fig. 4.5 A) involved in responses to (i) light - GT-1/16 JJ1 (Yukio Nagano et al**.,** 2001) and GATA box (Gilmartin et al., 1990; Reyes et al., 2004) and (ii) cold - DRE/CRT (Yamaguchi-Shinozaki et al., 1994) and MYC (Chinnusamy et al., 2003).

The sequence of the *AtOEP16.2* promoter region (728 bp upstream from ATG start codon) contains several putative *cis*-acting elements (Fig. 4.5 B) responsible for (i) embryogenesis and seed germination - box d motif (Mena, 2002; Isabel-LaMoneda, 2003), ABRE A and ABRE6/2 (Bensmihen, 2002; Lopez-Molina, 2003) and (ii) pollen development - Pollen1LELAT52 (Bate el al., 1989) and GTGANTG10 (Rogers et al., 2001).

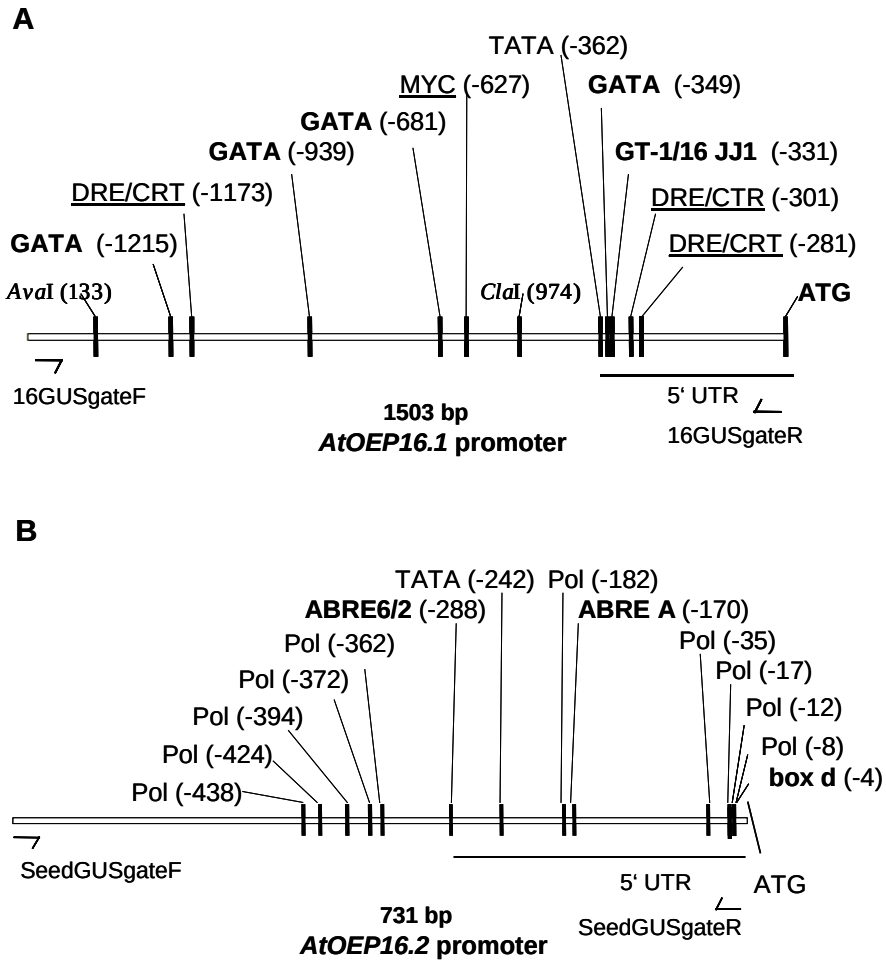

Fig. 4.5 Schematic representation of the *AtOEP16.1* and *AtOEP16.2* promoter region.

0 position is depicted for A in ATG codon. Several sites for restriction enzymes, annealing position of primers 16GUSgateF and 16GUSgateR (for *AtOEP16.1*) and SeedGUSgateF and SeedGUSgateR (for *AtOEP16.2*), TATA boxes, as well as 5' UTR are indicated. **A.** *AtOEP16.1* promoter region. Putative cis-acting elements involved (i) in light response (GT-1/16 JJ1 and GATA box) are shown in bold, (ii) in cold stress (DRE/CRT and MYC) are underlined. **B.** *AtOEP16.2* promoter region. Putative cis-acting elements involved in (i) embryogenesis and seed germination (box d motif, ABRE A and ABRE6/2) are in bold, (ii) pollen development (Pollen1LELAT52 and GTGANTG10) are depicted as Pol.

4.1.4 *Arabidopsis OEP16* knockout mutants

The homozygous knockout mutants *Atoep16.1-p, Atoep16.1-e, Atoep16.2, Atoep16.4-i* and *AtOEP16.4-e* were isolated. No phenotype, compared with wild-type, was observed at normal growth conditions. Cold stress did not cause any remarkable changes in homozygous *Atoep16.1-p* and *Atoep16.1-e Arabidopsis* plants. Thus, several double knockout mutants were produced to switch off at least two genes and to avoid possible substitution of a

disrupted gene with another, still functional in a single knockout mutant. The following double mutants were produced: *Atoep16.4-i x Atoep16.1-e, Atoep16.4-e x Atoep16.1-p, Atoep16.4-i x Atoep16.2, Atoep16.4-e x Atoep16.2*. Only the double *Atoep16.4-e x Atoep16.2* mutant had shorter siliques and less seeds per silique in contrast to wild-type plants. The double mutants are currently under investigation.

To analyse the changes in gene expression in leaves of the homozygous *Atoep16.1-p* knockout plants, cDNA macroarrays have been carried out. Three genes playing a role in amino acid metabolism and transport were up-regulated in leaves of the 4-week-old *Atoep16.1-p* T-DNA mutant, namely (i) naringenin-chalcone synthase, an enzyme for biosynthesis of L-phenylalanine and L-tyrosine derivatives, (ii) S-adenosylmethionine synthase 2 and (iii) a putative proline transporter. Several genes were found with reduced expression levels, namely LHT1, an amino acid permease, which transports lysine and arginine; a chloroplast-localized ATP sulfurylase precursor, involved in glutathione and cysteine synthesis; two putative sucrose transporters.

4.1.5 Proposed function of the *Arabidopsis* OEP16 proteins

AtOEP16.1-4 encode α-helical pore-forming membrane proteins. Similar to PsOEP16, it is proposed that the AtOEP16.1 channel transports amino acids and compounds with primary amino groups via the outer envelope of chloroplasts. Thus, the AtOEP16.1 channel is involved in nitrogen assimilation and amino acid metabolism. In non-legume plants, nitrogen assimilation begins with the uptake of inorganic nitrogen, nitrate or ammonium, from the soil. Nitrate is subsequently reduced to ammonium (NH_4^+) and then assimilated into an organic form as glutamate and glutamine. These amino acids are the nitrogen donors in the biosynthesis of essentially all other amino acids and other important nitrogen-containing compounds such as nucleic acids, chlorophyll, hormones and products of secondary metabolism (Oliveira et al., 2002).

AtOEP16.1 is a highly expressed ubiquitous protein. Transcriptome analysis, using Affymetrix ATH1 arrays, revealed that expression of the *AtOEP16.1* gene in leaves is light inducible and the *AtOEP16.1* mRNA content is reduced in dark (Fig. 4.3).

Additionally, Affymetrix ATH1 array analysis revealed that *AtOEP16.1* expression is induced by cold (Fig. 4.4), therefore it is suggested that AtOEP16.1 allows the adaptation of plant to the cold stress, as well as cold responsive protein *Cor15b* (At2g42530; Chinnusamy et al.,

2003) and cold acclimation protein *FL3-5A3* (At2g15970), showing the same mRNA level response patterns.

Electrophysiological studies of a second member of the AtOEP16 family, chloroplast localized AtOEP16.2, showed that, in lipid bilayer, AtOEP16.2 form a channel transporting amino acids. Structure analysis revealed that the AtOEP16.2 protein possesses a long intermembrane space loop connecting the first and second transmembrane domains of the pore. This loop is suggested to facilitate selective transport of amino acids through the channel, preferentially acidic amino acids, glutamate and glutamine and aspartate and asparagine, which make up to 64% of the total free amino acids found in leaf extracts in *Arabidopsis* (Lam et al., 1995; Schultz, 1994).

The AtOEP16.2 is highly abundant in seeds and pollen. In seeds, the AtOEP16.2 channel might transport amino acids or even small peptides necessary for seed storage proteins during seed development as well as for mobilization during germination. The high expression of the AtOEP16.2 channel at all stages of the pollen maturation could function as an amino acid supplying source for the vegetative and/or generative pollen cells. The expression of AtOEP16.2 during pollen tube germination indicates the transport activities of the AtOEP16.2 at this stage, when protein synthesis is very rapidly initiated. Interestingly, the AtOEP16.1 channel is highly expressed in the pistil of *Arabidopsis* flowers. Thus, these two amino acid transporting channels play an important role in fertilization.

Transcription of the AtOEP16.2 gene is directed by a divergent promoter region. 410 bp upstream of the ORF of the *AtOEP16.2* gene is situated in “head to head” orientation an adjacent ORF for a gene, which codes for a plastid targeted dihydrolipoamide dehydrogenase (DLD) (Taylor et al., 1993; Lutziger and Oliver; 2000). This enzyme catalyzes the reduction of the lipoamide group in the 2-oxoacid dehydrogenase and glycine decarboxylase multienzyme complex, allowing the production of acetyl coenzyme A for use in fatty acids biosynthesis. It is possible that AtOEP16.2 and DLD, simultaneously regulated by the same divergent promoter, play an important role in nitrogen assimilation and amino acid re-distribution within plant.

AtOEP16.3, in contrast to other AtOEP16s, is located in mitochondria and supposed to be a highly expressed ubiquitous channel transporting amino acids in/out of mitochondria, which accomplish the amino acids turnover, necessary for primary and secondary metabolism. Several enzymes, involved in amino acid biosynthesis, have been identified in *Arabidopsis* mitochondria, *e.g.* glutamate dehydrogenases At5g18170 (Melo-Oliveira et. al., 1996) and At5g07440 (Turano et al., 1997), and an aspartate aminotransferase At2g30970 (Schultz and

Coruzzi, 1995). Additionally, glycine and serine are inter-converted within mitochondria by glycine decarboxylase and serine hydroxymethyltransferase with production of large amounts of photorespiratory CO_2 (Bauwe and Kolukisaoglu, 2003).

AtOEP16.4 is low expressed ubiquitous protein, which is suggested to have a house-keeping function.

4.2 OEP37 proteins in pea and *Arabidopsis*

PsOEP37 and AtOEP37 channel proteins forms a selective β-barrel pore in outer envelope of chloroplasts. Immunoblot analysis showed expression of PsOEP37 in all tested pea organs, namely roots, rosette and cauline leaves, flowers, siliques and seeds.

AtOEP37, an orthologous protein to PsOEP37, was isolated in *Arabidopsis*. The AtOEP37 and PsoEP37 proteins share 60% identity and 75% similarity over their entire sequence length. The *AtOEP37* gene is encoded by At2g43950 and represents a single copy gene in *Arabidopsis* on chromosome 2. Immunoblot analysis showed that AtOEP37, similar to PsOEP37, is located in chloroplasts. Expression pattern analysis using RT-PCR and Affymetrix microarrays revealed that *AtOEP37* transcripts are ubiquitous. Abundance of low levels of *AtOEP37* in almost all tissues suggests that AtOEP37 is a stable, house-keeping protein throughout the various organs and developmental stages. Analysis of *Arabidopsis* plants transformed with promoter-GUS translational fusions revealed that the *AtOEP37* gene promoter region is active in cotyledons; meristematic, vascular, cortical tissues, the transition zone of roots and epidermis-derived hair roots in the 3- and 7-day-old seedlings. In 2 to 3-

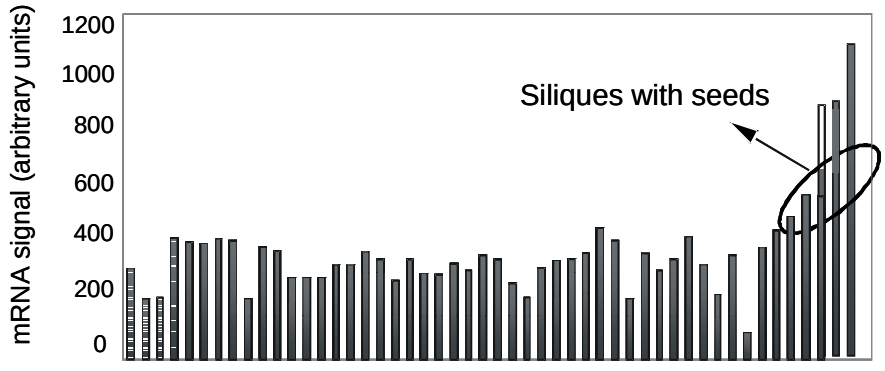

Fig. 4.6 Overview of transcription levels of the *AtOEP37* in *Arabidopsis* according to Affymetrix microarray results of AtGene Express Project.

The transcript content is given in arbitrary units (n=2). See table for x-axis legends and link to the web page of the data Affymetrix microarray results in Appendix.

week old juvenile plants, a weak level of staining was observed only in aerial portions: in cotyledons, rosette leaf primordium in the subepidermal and cortical cells (shoot apex), and expanded rosette leaves, flower stalks and petals. Additionally, a search in public Affymetrix gene expression databases (AtGene Express Project) showed that expression of *AtOEP37* was detected in all developmental stages and tissues of the *Arabidopsis* plant with relatively low levels and with high levels in developing seeds (Fig. 4.6).

4.3 VDAC proteins in pea and *Arabidopsis*

Voltage-dependent anion channels (VDAC), which are found in the outer membrane of mitochondria from all organisms studied so far (Zalman et al., 1980; Colombini, 1980), represent porins permeable for hydrophilic solutes. Each channel consists of a single polypeptide of about 30 kDa that forms an aqueous pore of about 3 nm in diameter (Thomas et al., 1991). VDAC proteins contain 46-50% hydrophilic amino acid residues and form the pore with anti-parallel amphiphilic β-strands (Benz, 1994).

A full length *VDAC* cDNA was derived from leaves of 5-day-old light-grown pea seedlings. Comparison of the deduced sequence with sequences in the database showed that it was identical to a cDNA (Gen Bank Acc. No. Z25540) isolated from a library prepared from the envelope of non-green plastids of pea root (Fischer et al. 1994). This protein had been shown to immunoreact with antibodies against mitochondrial porins. It was proposed that the VDAC-like porin is located in non-green plastids from roots only. However, isolation of the same cDNA from green seedlings suggested localization of that protein in both, green and non-green plastids. To test the localization of VDAC, a C-terminal fusion of VDAC to the reporter protein GFP was constructed and, after bombardment, transiently expressed in pea roots. Surprisingly, staining the pea roots, transfected by the VDAC-GFP fusion plasmid with a marker for mitochondria, Mitotracker, showed that the fluorescent signals detected from samples were co-localized, suggesting mitochondrial targeting of the VDAC protein. Additional experiments with a marker for plastids, ps-ds-RED, revealed that VDAC is not situated in plastids. In contrast to earlier results (Fischer et al., 1994) one could conclude that this is a classical VDAC protein located to the mitochondria but not to the plastids.

5 References

1 Aronsson H, Jarvis P. A simple method for isolating import-competent Arabidopsis chloroplasts. *FEBS Lett* 2002; 529(2-3):215-220.

2 Aseeva E, Ossenbuhl F, Eichacker LA, Wanner G, Soll J, Vothknecht UC. Complex Formation of Vipp1 Depends on Its {alpha}-Helical PspA-like Domain. *J Biol Chem* 2004; 279(34):35535-35541.

3 Bardel J, Louwagie M, Jaquinod M et al. A survey of the plant mitochondrial proteome in relation to development. *Proteomics* 2002; 2(7):880-898.

4 Bate N, Twell D. Functional architecture of a late pollen promoter: pollen-specific transcription is developmentally regulated by multiple stage-specific and co-dependent activator elements. *Plant Molecular Biology* 1998; 37(5):859-869.

5 Bauwe H, Kolukisaoglu U. Genetic manipulation of glycine decarboxylation. *J Exp Bot* 2003; 54(387):1523-1535.

6 Beator J, Kloppstech K. The Circadian Oscillator Coordinates the Synthesis of Apoproteins and Their Pigments during Chloroplast Development. *Plant Physiol* 1993; 103(1):191-196.

7 Bensmihen S, Rippa S, Lambert G et al. The homologous ABI5 and EEL transcription factors function antagonistically to fine-tune gene expression during late embryogenesis. *Plant Cell* 2002; 14(6):1391-1403.

8 Benz R. Porin from bacterial and mitochondrial outer membranes. *CRC Crit Rev Biochem* 1985; 19(2):145-190.

9 Benz R. Permeation of hydrophilic solutes through mitochondrial outer membranes: review on mitochondrial porins. *Biochim Biophys Acta* 1994; 1197(2):167-196.

10 Bhattacharjee H, Zhou T, Li J, Gatti DL, Walmsley AR, Rosen BP. Structure-function relationships in an anion-translocating ATPase. *Biochem Soc Trans* 2000; 28(4):520-526.

11 Bolter B, Soll J, Hill K, Hemmler R, Wagner R. A rectifying ATP-regulated solute channel in the chloroplastic outer envelope from pea. *EMBO J* 1999; 18(20):5505-5516.

12 Boyes DC, Zayed AM, Ascenzi R, McCaskill AJ, Hoffman NE, Davis KR, Gorlach J. Growth Stage-Based Phenotypic Analysis of Arabidopsis: A Model for High Throughput Functional Genomics in Plants. *Plant Cell* 2001; 13(7):1499-1510.

13 Bradford MM. A rapid and sensitive method for the quantitation of microgram quantities of protein utilizing the principle of protein-dye binding. *Anal Biochem* 1976; 72:248-254.

14 Chinnusamy V, Ohta M, Kanrar S et al. ICE1: a regulator of cold-induced transcriptome and freezing tolerance in Arabidopsis. *Genes Dev* 2003; 17(8):1043-1054.

15 Clausen C, Ilkavets I, Thomson R et al. Intracellular localization of VDAC proteins in plants. *Planta* 2004; 220(1):30-37.

16 Clough SJ, Bent AF. Floral dip: a simplified method forAgrobacterium-mediated transformation ofArabidopsis thaliana. *The Plant Journal* 1998; 16(6):735-743.

17 Colombini M. A candidate for the permeability pathway of the outer mitochondrial membrane. *Nature* 1979; 279(5714):643-645.

18 Colombini M. Structure and mode of action of a voltage dependent anion-selective channel (VDAC) located in the outer mitochondrial membrane. *Ann N Y Acad Sci* 1980; 341:552-563.

19 Conlan S, Zhang Y, Cheley S, Bayley H. Biochemical and biophysical characterization of OmpG: A monomeric porin. *Biochemistry* 2000; 39(39):11845-11854.

20 Davenport R. Glutamate Receptors in Plants. *Ann Bot* 2002; 90(5):549-557.

21 Day DA, Wiskich JT. Regulation of alternative oxidase activity in higher plants. *J Bioenerg Biomembr* 1995; 27(4):379-385.

22 De P, V, Prezioso G, Thinnes F, Link TA, Palmieri F. Peptide-specific antibodies and proteases as probes of the transmembrane topology of the bovine heart mitochondrial porin. *Biochemistry* 1991; 30(42):10191-10200.

23 Delcour AH. Solute uptake through general porins. *Front Biosci* 2003; 8:d1055-d1071.

24 Edwards K, Johnstone C, Thompson C. A simple and rapid method for the preparation of plant genomic DNA for PCR analysis. *Nucleic Acids Res* 1991; 19(6):1349.

25 Emanuelsson O, Nielsen H, von Heijne G. ChloroP, a neural network-based method for predicting chloroplast transit peptides and their cleavage sites. *Protein Sci* 1999; 8(5):978-984.

26 Emanuelsson O, Nielsen H, Brunak S, von Heijne G. Predicting subcellular localization of proteins based on their N-terminal amino acid sequence. *J Mol Biol* 2000; 300(4):1005-1016.

27 Ferro M, Salvi D, Brugiere S et al. Proteomics of the Chloroplast Envelope Membranes from Arabidopsis thaliana. *Mol Cell Proteomics* 2003; 2(5):325-345.

28 Fischer K, Weber A, Brink S et al. Porins from plants. Molecular cloning and functional characterization of two new members of the porin family. *J Biol Chem* 1994; 269(41):25754-25760.

29 Flugge UI. Metabolite transporters in plastids. *Curr Opin Plant Biol* 1998; 1(3):201-206.

30 Folsch H, Gaume B, Brunner M, Neupert W, Stuart RA. C- to N-terminal translocation of preproteins into mitochondria. *EMBO J* 1998; 17(22):6508-6515.

31 Forte M, Adelsberger-Mangan D, Colombini M. Purification and characterization of the voltage-dependent anion channel from the outer mitochondrial membrane of yeast. *J Membr Biol* 1987; 99(1):65-72.

32 Froehlich JE, Wilkerson CG, Ray WK et al. Proteomic study of the Arabidopsis thaliana chloroplastic envelope membrane utilizing alternatives to traditional two-dimensional electrophoresis. *J Proteome Res* 2003; 2(4):413-425.

33 Gier JW. Biogenesis of inner membrane proteins in Escherichia coli. *Annu Rev Microbiol* 2005; 59:329-355.

34 Gilmartin PM, Sarokin L, Memelink J, Chua NH. Molecular Light Switches for Plant Genes. *Plant Cell* 1990; 2(5):369-378.

35 Glombitza S, Dubuis Ph, Thulke O et al. Crosstalk and differential response to abiotic and biotic stressors reflected at the transcriptional level of effector genes from secondary metabolism. *Plant Molecular Biology* 2004; 54(6):817-835.

36 Grimm B, Kloppstech K. The early light-inducible proteins of barley. Characterization of two families of 2-h-specific nuclear-coded chloroplast proteins. *Eur J Biochem* 1987; 167(3):493-499.

37 Guy C. Molecular responses of plants to cold shock and cold acclimation. *J Mol Microbiol Biotechnol* 1999; 1(2):231-242.

38 Hancock RE, Siehnel R, Martin N. Outer membrane proteins of Pseudomonas. *Mol Microbiol* 1990; 4(7):1069-1075.

39 Heazlewood JL, Tonti-Filippini JS, Gout AM, Day DA, Whelan J, Millar AH. Experimental analysis of the Arabidopsis mitochondrial proteome highlights signalling and regulatory components, provides assessment of targeting prediction programs, and indicates plant-specific mitochondrial proteins. *Plant Cell* 2004; 16(1):241-256.

40 Hofmann K, Bucher P, Falquet L, Bairoch A. The PROSITE database, its status in 1999. *Nucl Acids Res* 1999; 27(1):215-219.

41 Hutin C, Nussaume L, Moise N, Moya I, Kloppstech K, Havaux M. Early light-induced proteins protect Arabidopsis from photooxidative stress. *PNAS* 2003; 100(8):4921-4926.

42 Isabel-LaMoneda I, Diaz I, Martinez M, Mena M, Carbonero P. SAD: a new DOF protein from barley that activates transcription of a cathepsin B-like thiol protease gene in the aleurone of germinating seeds. *Plant J* 2003; 33(2):329-340.

43 Jach G, Binot E, Frings S, Luxa K, Schell J. Use of red fluorescent protein from Discosoma sp. (dsRED) as a reporter for plant gene expression. *Plant J* 2001; 28(4):483-491.

44 Jang JY, Kim DG, Kim YO, Kim JS, Kang H. An expression analysis of a gene family encoding plasma membrane aquaporins in response to abiotic stresses in Arabidopsis thaliana. *Plant Mol Biol* 2004; 54(5):713-725.

45 Jeanteur D, Lakey JH, Pattus F. The bacterial porin superfamily: sequence alignment and structure prediction. *Mol Microbiol* 1991; 5(9):2153-2164.

46 Jiang X, Payne MA, Cao Z et al. Ligand-specific opening of a gated-porin channel in the outer membrane of living bacteria. *Science* 1997; 276(5316):1261-1264.

47 Karimi M, De Meyer B, Hilson P. Modular cloning in plant cells. *Trends Plant Sci* 2005; 10(3):103-105.

48 Koebnik R, Locher KP, Van Gelder P. Structure and function of bacterial outer membrane proteins: barrels in a nutshell. *Molecular Microbiology* 2000; 37(2):239-253.

49 Koop HU, Steinmuller K, Wagner H, Rossler C, Eibl C, Sacher L. Integration of foreign sequences into the tobacco plastome via polyethylene glycol-mediated protoplast transformation. *Planta* 1996; 199(2):193-201.

50 Kruft V, Eubel H, Jansch L, Werhahn W, Braun HP. Proteomic approach to identify novel mitochondrial proteins in Arabidopsis. *Plant Physiol* 2001; 127(4):1694-1710.

51 Kuhnen F, Barmettler K, Bhattacharjee S, Elimelech M, Kretzschmar R. Transport of Iron Oxide Colloids in Packed Quartz Sand Media: Monolayer and Multilayer Deposition. *J Colloid Interface Sci* 2000; 231(1):32-41.

52 Lam HM, Coschigano KT, Oliveira IC, Melo-Oliveira R, Coruzzi GM. The molecular genetics of nitrogen assimilation into amino acids in higher plants. *Annu Rev Plant Physiol Plant Mol Biol* 1996; 47:569-593.

53 Lam HM, Hsieh MH, Coruzzi G. Reciprocal regulation of distinct asparagine synthetase genes by light and metabolites in Arabidopsis thaliana. *Plant J* 1998; 16(3):345-353.

54 Lee YR, Assmann SM. Arabidopsis thaliana 'extra-large GTP-binding protein' (AtXLG1): a new class of G-protein. *Plant Mol Biol* 1999; 40(1):55-64.

55 Linke D, Frank J, Holzwarth JF, Soll J, Boettcher C, Fromme P. In vitro reconstitution and biophysical characterization of OEP16, an outer envelope pore protein of pea chloroplasts. *Biochemistry* 2000; 39(36):11050-11056.

56 Linke D, Frank J, Pope MS et al. Folding kinetics and structure of OEP16. *Biophys J* 2004; 86(3):1479-1487.

57 Liu J, Gilmour SJ, Thomashow MF, Van Nocker S. Cold signalling associated with vernalization in Arabidopsis thaliana does not involve CBF1 or abscisic acid. *Physiol Plant* 2002; 114(1):125-134.

58 Lopez-Molina L, Mongrand S, Kinoshita N, Chua NH. AFP is a novel negative regulator of ABA signalling that promotes ABI5 protein degradation. *Genes Dev* 2003; 17(3):410-418.

59 Ludwig O, Krause J, Hay R, Benz R. Purification and characterization of the pore forming protein of yeast mitochondrial outer membrane. *Eur Biophys J* 1988; 15(5):269-276.

60 Lutziger I, Oliver DJ. Molecular evidence of a unique lipoamide dehydrogenase in plastids: analysis of plastidic lipoamide dehydrogenase from Arabidopsis thaliana. *FEBS Lett* 2000; 484(1):12-16.

61 Macias MJ, Wiesner S, Sudol M. WW and SH3 domains, two different scaffolds to recognize proline-rich ligands. *FEBS Lett* 2002; 513(1):30-37.

62 Martinoia E, Klein M, Geisler M et al. Multifunctionality of plant ABC transporters--more than just detoxifiers. *Planta* 2002; 214(3):345-355.

63 Mascarenhas JP. Microspore and microgametophyte development in relation to biological activity of environmental pollutants. *Environ Health Perspect* 1981; 37:9-12.

64 Meier S, Neupert W, Herrmann JM. Conserved N-terminal Negative Charges in the Tim17 Subunit of the TIM23 Translocase Play a Critical Role in the Import of Preproteins into Mitochondria. *J Biol Chem* 2005; 280(9):7777-7785.

65 Melo-Oliveira R, Oliveira IC, Coruzzi GM. Arabidopsis mutant analysis and gene regulation define a nonredundant role for glutamate dehydrogenase in nitrogen assimilation. *Proc Natl Acad Sci U S A* 1996; 93(10):4718-4723.

66 Mena M, Cejudo FJ, Isabel-Lamoneda I, Carbonero P. A Role for the DOF Transcription Factor BPBF in the Regulation of Gibberellin-Responsive Genes in Barley Aleurone. *Plant Physiol* 2002; 130(1):111-119.

67 Milisav I, Moro F, Neupert W, Brunner M. Modular Structure of the TIM23 Preprotein Translocase of Mitochondria. *J Biol Chem* 2001; 276(28):25856-25861.

68 Millar AH, Heazlewood JL, Kristensen BK, Braun HP, Moller IM. The plant mitochondrial proteome. *Trends Plant Sci* 2005; 10(1):36-43.

69 Nakae T. Outer membrane of Salmonella. Isolation of protein complex that produces transmembrane channels. *J Biol Chem* 1976; 251(7):2176-2178.

70 Nazos PM, Antonucci TK, Landick R, Oxender DL. Cloning and characterization of livH, the structural gene encoding a component of the leucine transport system in Escherichia coli. *J Bacteriol* 1986; 166(2):565-573.

71 Nestorovich EM, Rostovtseva TK, Bezrukov SM. Residue Ionization and Ion Transport through OmpF Channels. *Biophys J* 2003; 85(6):3718-3729.

72 Nikaido H. Molecular Basis of Bacterial Outer Membrane Permeability Revisited. *Microbiol Mol Biol Rev* 2003; 67(4):593-656.

73 Oliveira IC, Brears T, Knight TJ, Clark A, Coruzzi GM. Overexpression of cytosolic glutamine synthetase. Relation to nitrogen, light, and photorespiration. *Plant Physiol* 2002; 129(3):1170-1180.

74 Osteryoung KW. Organelle fission in eukaryotes. *Curr Opin Microbiol* 2001; 4(6):639-646.

75 Philippsen A, Im W, Engel A, Schirmer T, Roux B, Muller DJ. Imaging the Electrostatic Potential of Transmembrane Channels: Atomic Probe Microscopy of OmpF Porin. *Biophys J* 2002; 82(3):1667-1676.

76 Pilgrim ML, McClung CR. Differential Involvement of the Circadian Clock in the Expression of Genes Required for Ribulose-1,5-Bisphosphate Carboxylase/Oxygenase

Synthesis, Assembly, and Activation in Arabidopsis thaliana. *Plant Physiol* 1993; 103(2):553-564.

77 Pohlmeyer K, Soll J, Steinkamp T, Hinnah S, Wagner R. Isolation and characterization of an amino acid-selective channel protein present in the chloroplastic outer envelope membrane. *PNAS* 1997; 94(17):9504-9509.

78 Pohlmeyer K, Soll J, Grimm R, Hill K, Wagner R. A High-Conductance Solute Channel in the Chloroplastic Outer Envelope from Pea. *Plant Cell* 1998; 10(7):1207-1216.

79 Reyes JC, Muro-Pastor MI, Florencio FJ. The GATA Family of Transcription Factors in Arabidopsis and Rice. *Plant Physiol* 2004; 134(4):1718-1732.

80 Robertson KM, Tieleman DP. Orientation and interactions of dipolar molecules during transport through OmpF porin. *FEBS Lett* 2002; 528(1-3):53-57.

81 Rogers HJ, Bate N, Combe J et al. Functional analysis of cis-regulatory elements within the promoter of the tobacco late pollen gene g10. *Plant Molecular Biology* 2001; 45(5):577-585.

82 Rohl T, Motzkus M, Soll J. The outer envelope protein OEP24 from pea chloroplasts can functionally replace the mitochondrial VDAC in yeast. *FEBS Lett* 1999; 460(3):491-494.

83 Rosso MG, Li Y, Strizhov N, Reiss B, Dekker K, Weisshaar B. An Arabidopsis thaliana T-DNA mutagenized population (GABI-Kat) for flanking sequence tag-based reverse genetics. *Plant Mol Biol* 2003; 53(1-2):247-259.

84 Sambrook JFEF&MT, Hrsg. Molecular Cloning - A Laboratory Manual, 2**nd** Edition. 1989. New York., Cold Spring Habour Laboratory Press. Ref Type: Generic

85 Schein SJ, Colombini M, Finkelstein A. Reconstitution in planar lipid bilayers of a voltage-dependent anion-selective channel obtained from paramecium mitochondria. *J Membr Biol* 1976; 30(2):99-120.

86 Schleiff E, Eichacker LA, Eckart K et al. Prediction of the plant {beta}-barrel proteome: A case study of the chloroplast outer envelope. *Protein Sci* 2003; 12(4):748-759.

87 Schmid A, Kromer S, Heldt HW, Benz R. Identification of two general diffusion channels in the outer membrane of pea mitochondria. *Biochim Biophys Acta* 1992; 1112(2):174-180.

88 Schultz CJ, Coruzzi GM. The aspartate aminotransferase gene family of Arabidopsis encodes isoenzymes localized to three distinct subcellular compartments. *Plant J* 1995; 7(1):61-75.

89 Seki M, Narusaka M, Abe H et al. Monitoring the expression pattern of 1300 Arabidopsis genes under drought and cold stresses by using a full-length cDNA microarray. *Plant Cell* 2001; 13(1):61-72.

90 Steinkamp T, Hill K, Hinnah SC et al. Identification of the Pore-forming Region of the Outer Chloroplast Envelope Protein OEP16. *J Biol Chem* 2000; 275(16):11758-11764.

91 Su Q, Frick G, Armstrong G, Apel K. POR C of Arabidopsis thaliana: a third light- and NADPH-dependent protochlorophyllide oxidoreductase that is differentially regulated by light. *Plant Mol Biol* 2001; 47(6):805-813.

92 Sukharev SI, Blount P, Martinac B, Kung C. Mechanosensitive channels of Escherichia coli: the MscL gene, protein, and activities. *Annu Rev Physiol* 1997; 59:633-657.

93 Sussman MR, Amasino RM, Young JC, Krysan PJ, Austin-Phillips S. The Arabidopsis Knockout Facility at the University of Wisconsin-Madison. *Plant Physiol* 2000; 124(4):1465-1467.

94 Taylor AE, Millar RE, Carmichael A, Cogdell RJ, Lindsay JG. Dihydrolipoamide dehydrogenase in plants: differences in the mitochondrial and chloroplastic forms. *Biochem Soc Trans* 1993; 21(1):38S.

95 Teige M, Scheikl E, Eulgem T et al. The MKK2 pathway mediates cold and salt stress signalling in Arabidopsis. *Mol Cell* 2004; 15(1):141-152.

96 Thomas L, Kocsis E, Colombini M, Erbe E, Trus BL, Steven AC. Surface topography and molecular stoichiometry of the mitochondrial channel, VDAC, in crystalline arrays. *J Struct Biol* 1991; 106(2):161-171.

97 Turano FJ, Thakkar SS, Fang T, Weisemann JM. Characterization and expression of NAD(H)-dependent glutamate dehydrogenase genes in Arabidopsis. *Plant Physiol* 1997; 113(4):1329-1341.

98 Tusher VG, Tibshirani R, Chu G. Significance analysis of microarrays applied to the ionizing radiation response. *PNAS* 2001; 98(9):5116-5121.

99 van Wijk KJ. Challenges and prospects of plant proteomics. *Plant Physiol* 2001; 126(2):501-508.

100 Watanabe Y, Inoko Y. Physicochemical characterization of the reassembled dimer of an integral membrane protein OmpF porin. *Protein J* 2005; 24(3):167-174.

101 Yamaguchi-Shinozaki K, Shinozaki K. A novel cis-acting element in an Arabidopsis gene is involved in responsiveness to drought, low-temperature, or high-salt stress. *Plant Cell* 1994; 6(2):251-264.

102 Zalman LS, Nikaido H, Kagawa Y. Mitochondrial outer membrane contains a protein producing nonspecific diffusion channels. *J Biol Chem* 1980; 255(5):1771-1774.

6 Appendix

6.1 The primers, used for PCR

	Name of primer	SEQUENCE (5'-3')
1	At2gN	GCCTTCAAGCACTTCTCCGGGACTGTTA
2	At2gC	AAAGGAATCCACACCATATGAACCAAATT
3	OEP16W77/FN	GCCGGCTATAGCTCCGAAGTATGCACCTTC
4	OEP16W77/FC	GAAGGTGCATACTTCGGAGCTATAGCCGGC
5	OEP16W100/FN	CATGGCATTCTTGAACTCCCTGGTGCCACG
6	OEP16W100/FC	CGTGGCACCAGGGACTTCAAGAATGCCATG
7	oep16araSpeIf	GGACTAGTATGCCTTCAAGCACATTC
8	oep16araSalIr	ACGCGTCGACGTAGAAATAATGATTG
9	attB1adapter	GGGGACAAGTTTGTACAAAAAAGCAGGCT
10	attB2 adapter	GGGGACCACTTTGTACAAGAAAGCTGGGT
11	16seedGATf	AAAAAGCAGGCTTAGAAGGAGATAGAACCATGGAGAAGAGTGGAGGAAG
12	16seedGAT-stopR	AGAAAGCTGGGTCGAAAACGCTAGAAAGGAG
13	62880GATf	AAAAAGCAGGCTTAGAAGGAGATAGAACCATGGAGGAAGAATTGCTCTCC
14	62880GAT-stopR	AGAAAGCTGGGTCATTAGTGTTGTTTGGGTTTTCTCTCC
15	42210SpeIf	GGACTAGTATGGATCCAGCTGAAATG
16	42210SalIr	ACGCGTCGACGGGAATCAGCTTCAGCTC
17	VDACSpeIf	GGACTAGTATGGTGAAGGGTCCTGG
18	VDACSalIr	ACGCGTCGACAGGTTTGAGAGCC
19	42210HindIIIf	CCCAAGCTTATGGATCCAGCTGAAATGAG
20	42210XhoIr	CCGCTCGAGGGAATCAGCTTCAGCTCTTTTCTC
21	62880EcoRIF	CCGGAATTCATGGAGGAAGAATTGCTCTC
22	62880XhoIR	CCGCTCGAGATTAGTGTTGTTTGGGTTTTC
23	oep16araSalIr-2	ACGCGTCGACGGTAGAAATAATGATTG
24	o16araClaIa	GGTAGCTAAATAGTGTCTTTGCCTTTCTTAC
25	16GUSgateF	AAAAAGCAGGCTTAGAAGGAGATAGAACCCCGCAAACAATCGGGTGC
26	16GUSgateR	AGAAAGCTGGGTCCTTTTCTTCTTCTTTCTTCC
27	SeedGUSgateF	AAAAAGCAGGCTTAGAAGGAGATAGAACCCTTCTCGACGGCGTGCAATG
28	SeedGUSgateR	AGAAAGCTGGGTCTTTTTTCTTTCTTTCTTCACTTGTTGC
29	62GUSgateF	AAAAAGCAGGCTTAGAAGGAGATAGAACCTTAAGAAAAGAGTTGGAAAAG
30	62GUSgateR	AGAAAGCTGGGTCCTCTGCAAAATTGAATTAGGAC
31	37GUSgateF	AAAAAGCAGGCTTAGAAGGAGATAGAACCTAGTGGACAAGATTAAGAC
32	37GUSgateR	AGAAAGCTGGGTCTGGAATTGGATTTGAGAGAATC
33	oep16SNBamH1-1	GAAAGAAAGGGATCCATGGAGAAG
34	oep16sPst1-2	AACTGCAGTTAGTAGACCTTTAGCGAATT
35	28900Fbeg	CACTCTCCATACTCTGGTTTG
36	JL202	CATTTTATAACGCTGCGGACATCTAC
37	o16araEcoRIF	CCGGAATTCATGCCTTCAAGCACATTCTC
38	o16araXhoIr	CCGCTCGAGGCCTTTCTTACCAACCGCTGAG
39	62880SF	ATAGGTTTAAGCGGCGTTTCTCAGGC
40	62880SR	ATATCGTTGAAGCCCACAATGTGTC
41	62880R	TTAATTAGTGTTGTTTGGGTTTTC
42	18SF	TTGTGTTGGCTTCGGGATCGGAGTAAT
43	18SR	TGCACCACCACCCATAGAATCAAGAA
44	LBb1pROK2	GCGTGGACCGCTTGCTGCAACT
45	28900lcf	ATCGGAGCTGTTGGAGTCA
46	28900lcr	CCTTTCTTACCAACCGCTGA
47	actin2lcf	TGGTCGTACAACCGGTATTGT
48	actin2lcr	TTCTCGATGGAAGAGCTGGT
49	At4gN	GTAATGGATGAGATAAGAAGCTTTGAGAA
50	At4gC	CTAGAAAGGAGATTAGCAGCGGTGGAAAT
51	LB3	TAGCATCTGAATTTCATAACCAATCTCGATACAC
52	16160lcf	GGAGCTTTACAAGCCGTGTC
53	16160lcr	CTGTTCCGCCAATCATGA
54	35Spromoter	TTGGAGAGAACACGGGGGACT
55	At3gN	TGCTCTTCCCTAACCGTCGAGTCAGTTCT
56	At3gC	CTGTCCTGGTGCAATTAGCCAAAACACTA
57	LBb1ROK2	GCGTGGACCGCTTGCTGCAAC
58	62880lcf	TTTCAATGCGGTCTTGTAAGTG
59	62880lcr	TGGTGCAATTAGCCAAAACA
60	37peaNdeIf	GGAATTCCATATGGATTCTGCTACGCGAAAC
61	37peaBamHIr	CGCGGATCCTTAAATGTCCCATCTCTTCTTAAC

	Name of primer	SEQUENCE (5'-3')
62	o37araXhoIs	CCGCTCGAGATGGCGGATCCATCTTCTCA
63	o37aXhoIr	CCGCTCGAGAATGTCCCATCTTTTCTTG
64	o37araXbaIs	GCTCTAGAATGGCGGATCCATCTTCTCA
65	O37araNcoIr	CATGCCATGGTCAAATGTCCCATCTTTTC
66	18SF	TTGTGTTGGCTTCGGGATCGGAGTAAT
67	18SR	TGCACCACCACCCATAGAATCAAGAA
68	O37araSF	TTACCCAAGAGCAACTCTTAAATTCCCAC
69	037araSR	GACGTTTGAGGATCCCATTAACAGATTC
70	Actin2/7F	GTCGTACAACCGGTATTGTGCT
71	Actin2/7R	GCTCGTAGTCAAGAGCGACAT
72	pGABI1	CCCATTTGGAGGTGAATGTAGACAC
73	pGABI2	ATATTGACCATCATACTCATTGC
74	At3g01280 LCfw	CTCTGTGAAGGCTCGT
75	At3g01280 LCrev	CTACAAATCCGGCAGG
76	At5g15090 LCfw	TGTCGGAACTCAACACG
77	At5g15090 LCrev	TACAAATCCCAACACCG
78	At5g57490 LCfw	GGATGGTGGTCCAGAG
79	At5g57490 LCrev	AAGTGATTCAATAACCCTACAAA
80	At5g67500 LCfw	CTCGACAAATGAAAACACG
81	At5g67500 LCrev	GCGGAACTATTTATTGATTCCA

6.2 Legend for x-axis of Fig.4.1 and Fig. 4.10

	Tissue
1.	cotyledons
2.	hypocotyl
3.	roots
4.	shoot apex, vegetative + young leaves
5.	leaves
6.	shoot apex, vegetative
7.	seedling, green parts
8.	shoot apex, transition (before bolting)
9.	roots
10.	rosette leaf #4, 1cm long
11.	rosette leaf #4, 1cm long
12.	rosette leaf # 2
13.	rosette leaf # 4
14.	rosette leaf # 6
15.	rosette leaf # 8
16.	rosette leaf # 10
17.	rosette leaf # 12
18.	rosette leaf # 12
19.	leaf 7, petiol
20.	leaf 7, proximal half
21.	leaf 7, distal half
22.	developmental drift; whole plant after transition, but before bolting
23.	developmental drift; whole plant after transition, but before bolting
24.	developmental drift; whole plant after transition, but before bolting

25.	senescing leaves
26.	cauline leaves
27.	stem, 2nd internode
28.	stem, 1st node
29.	shoot apex, inflorescence (after bolting)
30.	flowers stage 9
31.	flowers stage 10/11
32.	flowers stage 12
33.	flowers stage 12, sepals
34.	flowers stage 12, petals
35.	flowers stage 12, stamens
36.	flowers stage 12, carpels
37.	flowers stage 15
38.	flowers stage 15, pedicels
39.	flowers stage 15, sepals
40.	flowers stage 15, petals
41.	flowers stage 15, stamen
42.	flowers stage 15, carpels
43.	mature pollen
44.	siliques, w/ seeds stage 3
45.	siliques, w/ seeds stage 4
46.	siliques, w/ seeds stage 5
47.	siliques, w/o seeds stage 6
48.	siliques, w/o seeds stage 7
49.	siliques, w/o seeds stage 8
50.	siliques, w/o seeds stage 9
51.	siliques, w/o seeds stage 10

6.3 Constructs

Restr., restriction enzymes. Primers, primers for PCR (5'-3'). E.c. expression clone

	Insert	Vector	Template	Restr	Primers	Comments
1	PsOEP16	pET21b	(Pohlmeyer et al, 1997)			
2	PsOEP16	pET21b	PsOEP16/pET21b	NdeI (5') XhoI (3')	OEP16W77/FN OEP16W77/FC	W77F
3	PsOEP16	pET21b	PsOEP16/pET21b	NdeI (5')	OEP16W100/FN	W100F

	Insert	Vector	Template	Restr	Primers	Comments
				XhoI (3')	OEP16W100/FC	
4	AtOEP16.1	pCRII	cDNA	EcoRI (5') SalI (3')	o16araEcoRIf oep16araSalIr	
5	AtOEP16.2	pET21d	AtOEP16.2/pBs	EcoRI (5') XhoI (3')	seedEcoRIfseedXhoIr	
6	AtOEP16.3	pET21b	cDNA	HindIII (5') XhoI (3')	42210HindIIIf 42210XhoIr	
7	AtOEP16.4	pET21b	cDNA	EcoRI (5') XhoI (3')	62880EcoRIF 62880XhoIR	
8	AtOEP16.1	pOL-GFP	AtOEP16.1/pCRII	Spe I (5') Sal I (3')	oep16araSpeIf oep16araSalIr-2	C-terminal GFP fusin
9	AtOEP16.1	pOL-RFP	AtOEP16.1/pCRII	Spe I (5') Sal I (3')	oep16araSpeIf oep16araSalIr-2	C-terminal RFP fusion
10	AtOEP16.2	pDONR202	AtOEP16.2/pET21d		1. 16seedGATf 16seedGAT-stopR 2. attB1adapter attB2adapter	Adapter PCR Entry clone
11	AtOEP16.2	pK7FWG2	AtOEP16.2/pDONR202			E.c. GFP fusion
12	AtOEP16.3	pOL-GFP	cDNA	Spe I (5') Sal I (3')	422210SpeIf 42210SalIr	C-terminal GFP fusion
13	AtOEP16.4	pDONR202	AtOEP16.4/pET21b		1. 62880GATf 62880GAT-STOP 2. attB1adapter attB2adapter	Adapter PCR. Entry clone
14	AtOEP16.4	pK7FWG2	AtOEP16.4/pDONR202			E.c. GFP fusion
15	VDAC	pGFP2	Clausen et al, 2004			
16	VDAC	pOL-RFP	VDAC/pGFP2	Sal I (5') Spe I (3')		
17	pSSU	dsRED	Clausen et al, 2004			
18	AtOEP16.1	pET21b	cDNA	EcoRI (5') XhoI (3')	O16araEcoRIf O16araXhoIr	131 amino acids, for antibodies
19	AtOEP16.1 promoter	pDONR202	gDNA		1. 16GUSgateF 16GUSgateR 2. attB1adapter attB2adapter	Adapter PCR. Entry clone
20	AtOEP16.1 (promoter)	pKGWFS7	AtOEP16.1 promoter/ pDONR202			E.c. GUS fusion
21	AtOEP16.2 promoter	pDONR202	gDNA		1. 16seedGUSgateF 16seedGUSgateR 2. attB1adapter attB2adapter	Adapter PCR. Entry clone
22	AtOEP16.2 (promoter)	pKGWFS7	AtOEP16.2 promoter/ pDONR202			E.c. GUS fusion
23	AtOEP16.4 promoter	pDONR202	gDNA		1. 62GUSgateF 62GUSgateR 2. attB1adapter attB2adapter	Adapter PCR. Entry clone
24	AtOEP16.4 (promoter)	pKGWFS7	AtOEP16.4 promoter/ pDONR202			E.c. GUS fusion
25	AtOEP37 promoter	pDONR202	gDNA		1. 37GUSgateF 37GUSgateR 2. attB1adapter attB2adapter	Adapter PCR. Entry clone
26	AtOEP37 (promoter)	pKGWFS7	AtOEP37 promoter/ pDONR202			E.c. GUS fusion
27	PsOEP37	pET14b	PsOEP37/pBS (Schleiff et al., 222003)	NdeI BamHI	37peaNdeIf 37peaBamHIr	
28	AtOEP37	pRSETA	cDNA	XhoI NcoI	O37araXhoIs O37araNcoIr	

Curriculum vitae

Name	Iryna Ilkavets
Place of birth	Pinsk, Belarus
Date of birth	21.01.1972

Education

1991-1996	State University of Belarus, Minsk, Department of Biology Master of Science Degree Supervisor: Prof. Dr. N.M. Orel Research subject: Influence of SHF on metabolism in mouse brain
1996-2000	Photobiology Institute of National Academy of Sciences of Belarus, Minsk Research Scholar Supervisor Prof. Dr. I.D. Volotovski Research subject: Influence of phytochormons on cytosolic concentration of calcium in aequorin-expressing *Tobacco* and *Arabidopsis* plants
15.10.2000 – 13.12.2006	Department of Botany, Christian-Albrechts University of Kiel Department of Biology I, Ludwig Maximilians University, Munich Supervisor Prof. Dr. J. Soll Research subject: Membrane proteins in the outer membrane of plastids and mitochondria

Publications

- Götze T, Philippar K, **Ilkavets I**, J Soll, R. Wagner. OEP37 is a new member of the chloroplast outer membrane ion channels. Accepted in *JBC*.
- Clausen C[A], **Ilkavets I[A]**, Thomson R, Philippar K, Vojta A, Mohlmann T, Neuhaus E, Fulgosi H, Soll J. Intracellular localization of VDAC proteins in plants. *Planta*. 2004, 220:30-37.

  -[A] *authors contributed equally*
- Linke D, Frank J, Pope MS, Soll J, **Ilkavets I**, Fromme P, Burstein EA, Reshetnyak YK, Emelyanenko. Folding kinetics and structure of OEP16. *Biophys J*. 2004; 86(3):1479-87.

Selected talks and posters on meetings

- **Ilkavets I.** and J. Soll. Solute channels in chloroplasts. DFG SP-1108, Hirschberg, 2003.
- **Ilkavets I.**, Thomson R. and J. Soll. Outer membrane porins – evolution from bacteria to mitochondria and chloroplasts. Origin and Evolution of Mitochondria and Chloroplasts, FEBS Advanced Lecture Course, Hvar, Croatia, 2003.
- Philippar K., **Ilkavets I.**, Thomson R., Oster U. and J. Soll. Towards the function of membrane proteins in the outer envelope of *Arabidopsis* chloroplasts. 13th International Workshop on Plant Membrane Biology. Montpeller, 2004.
- Thomson R., **Ilkavets I.,** Soll J.. Die äußere Plastidenhüllmembran ist keine Sieb. 17. Tagung Molekularbiologie der Pflanzen, Dabringhausen, 2004.

Acknowledgements

I am particularly grateful to Prof. Dr. Jürgen Soll for giving me the opportunity to join his research group, for his supervision, guidance, helpful and stimulating discussions, for critical reading of the dissertation.

I am very grateful to Katrin for encouragement, guidance, valuable suggestions in the end of this work and for patience and critical reading of the dissertation.

I am thankful to Dr. Anton Schäffner, who introduced me to macroarray analysis and to Dr. Engstler for introduction in fluorescent microscopy. I am thankful to Rowena for her guidance and for the carrying out Affymetrix gene chip analysis.

I am thankful to Bettina, who introduced me to the project; to Ute and Enriko for helpful discussions.

I am grateful to Ulrike for the constant help, discussions and moral support. I am thankful to Karl and Ulrika for technical assistance and discussions. I am thankful to Gisela for growing and watering of *Arabidopsis* plants. I am thankful to Lars and Andi for help with computer. I am thankful to Lena for "russian" talks and to Fatima, Rita, Sonmia, Marko, Friderike, Ahmed, Ranja, Torsten, Claudia, Eva, Lea, Alexander, Sunchana, Mislav, Tina, Dani, Manu, Serena for nice conversations and moral support.

Ehrenwörtliche Versicherung

Die vorliegende Dissertation wurde von Dipl. Biol. Iryna Ilkavets selbständig und ohne unerlaubte Hilfe angefertigt. Der Verfasser hat zuvor nicht versucht, anderweitig eine Dissertation einzureichen oder sich einer Doktorprüfung zu unterziehen. Die Dissertation wurde keiner weiteren Prüfungskommision weder in Teilen noch als Ganzes vorgelegt.

19.12.2005
München